Machine Learning Technique Based Closed-loop Deep Brain Stimulation Controller Design

BY

PITAMBER SHUKLA
B.Tech., SASTRA University, India, 2009
M.S., University of Illinois at Chicago, Chicago, 2014

THESIS

Submitted as partial fulfillment of the requirements
for the degree of Doctor of Philosophy in Electrical and Computer Engineering
in the Graduate College of the
University of Illinois at Chicago, 2014

Chicago, Illinois

Dissertation Committee:

Daniela Tuninetti, Chair and Advisor
Rashid Ansari
Dan Schonfeld
Konstantin V Slavin, Neurosurgery
Ashfaq Khokhar, IIT

To my parents Dr Uma Shukla and Dr Anil Kumar Shukla, my brother Dr Munn Vinayak Shukla and sister-in-law Swati Shukla

ACKNOWLEDGMENTS

It is a great pleasure and proud privilege to express my deep sense of gratitude and everlasting indebtedness to my research supervisors Dr. Daniela Tuninetti and Dr. Daniel Graupe for their keen interest in research and for continuous guidance, suggestions and inspirations from the beginning of the study. I am obliged to them for sparing their valuable time in my endeavor.

I express my sincere thanks to Dr. Konstantin Slavin who has provided me necessary guidance and support whenever I needed without hesitation. I am obliged to him for providing me necessary umbrella to complete my research work. It is his support without which this work would have not been completed.

I am extremely grateful to Dr. Ishita Basu who supported me constantly throughout my research work. She helped me by explaining basics of this subject, collecting various data sets. She also helped me by discussing the problems at great details, analyzing results and providing critical comments and suggestions. Her contribution is invaluable for my research work.

I take this opportunity to thank all staffs specially Tina, Erica, Ala, Mona and Mihai in the ECE department for helping me with numerous administrative issues and making my stay comfortable. I would also like to thank all my friends and colleagues for their excellent support and help through out my research work.

I express gratitude and regards to my parents Dr. Uma Shukla and Dr. Anil Kumar Shukla, who saw this dream and provided great support to achieve it. Without their blessings it would have not been possible to complete this endeavor. I would like to thank my sister-in-law Swati Shukla for all her support and encouragement throughout this journey. Last but not least, I would like to bestow my deepest

regards and love to my brother Dr Munn Vinayak Shukla without whom I cannot imagine any of my achievements. He is always a great source of inspiration and support to me.

PS

CONTRIBUTION OF AUTHORS

Chapter 1 is the introduction chapter of this thesis which provides the literature review about the ET and PD diseases. This chapter highlights the treatments for the ET and PD diseases, in particularly about the DBS surgical procedure. Finally, this chapter provides the existing state of the art of DBS system and its shortcomings followed by the discussion about the significance of my research work to design an automated adaptive ON-OFF controlled closed-loop DBS system.

Some portions of Chapter 2 represents a published manuscript [1]: *Shukla, P., Basu, I., Graupe, D., Tuninetti, D., and Slavin, K. V.: A neural networkbased design of an on-off adaptive control for deep brain stimulation in movement disorders. In Engineering in Medicine and Biology Society (EMBC), 2012 Annual International Conference of the IEEE, 2012* for which I was the primary author and major driver of the research. Dr I. Basu guided in some of the data processing and also helped me in the manuscript writing. Dr K.V. Slavin, MD helped in recruiting the patients for this study and also guided me in manuscript writing. Dr. D. Tuninetti and Dr. D. Graupe were my research mentors provided their guidance for this work and contributed to the writing of the manuscript.

Parts of the Chapter 3 appeared in a published manuscripts [2]: *Shukla, P., Basu, I., and Tuninetti, D.: Towards closed-loop deep brain stimulation: Decision tree-based patients state classifier and tremor reappearance predictor. In Engineering in Medicine and Biology Society (EMBC), 2014 Annual International Conference of the IEEE, 2014* in which I was the first author and the major contributor for the research work. Dr I. Basu helped me in the manuscript writing. My research mentor Dr. D. Tuninetti provided her constant guidance for this work and contributed to the writing of the manuscript

CONTRIBUTION OF AUTHORS (Continued)

and [3]: *Shukla, P., Basu, I., Graupe, D., Tuninetti, D., Slavin, K. V., Metman, L. V., and Corcos, D. M.: A decision tree classifier for postural and movement conditions in essential tremor patients. In 6th International IEEE Engineering in Medicine and Biology Society (EMBC) Conference on Neural Engineering, accepted, 2013* for which I was the primary author and major contributor of the research work. Dr I. Basu helped me in the manuscript writing. Dr K. V. Slavin, MD and Dr L. V. Metman, MD helped in recruiting the patients for this work and provided their guidance in manuscript writing. Dr. D. M. Corcos provided his guidance in the sEMG/Acc data collection and also contributed in the manuscript writing. Dr. D. Tuninetti and Dr. D. Graupe were my research mentors provided their guidance for this work and contributed to the writing of the manuscript.

Chapter 4 represents a published manuscript [4]: *Shukla, P., Basu, I., Graupe, D., Tuninetti, D., and Slavin, K. V.: On modeling the neuronal activity in movement disorder patients by using the orntein uhlenbeck process. In Engineering in Medicine and Biology Society (EMBC), 2014 Annual International Conference of the IEEE, 2014.* and a unpublished manuscript [5]: *Shukla, P., Basu, I., Tuninetti, D., Graupe, D., and Slavin, K.: Stochastic modeling of neuronal activity in the thalamus of essential tremor and the subthalamic nucleus of parkinsons disease patients. Biological Cybernetics, submitted.* in which I was the first author and the major contributor to the work. Dr I. Basu helped me in undersanding the OUP process to model the neuronal activities in case of ET and PD patients. Dr K.V. Slavin, MD provided the MER data collected during DBS surgery and also helped me in manuscript writing. Dr. D. Tuninetti and Dr. D. Graupe were my research mentors provided their guidance for this work and contributed to the writing of the manuscript.

CONTRIBUTION OF AUTHORS (Continued)

In Chapter 5 represents the overall conclusions of my research. This chapter also discuss about the future directions to this research work.

TABLE OF CONTENTS

TABLE OF CONTENTS (Continued)

CHAPTER **PAGE**

TABLE OF CONTENTS (Continued)

CHAPTER **PAGE**

LIST OF TABLES

LIST OF TABLES (Continued)

LIST OF TABLES (Continued)

LIST OF FIGURES

LIST OF FIGURES (Continued)

LIST OF ABBREVIATIONS

ET	Essential Tremor
PD	Parkinson's Disease
DBS	Deep Brain Stimulation
VIM	Venteral Intermediate Nucleus
LFP	Local Field Potential
STN	Subthalamic Nucleus
GPi	Globus Pallidus
FDA	Food and Drug Administration
sEMG	surface-Electromyography
Acc	Accelerometer Signal
HFS	High Frequency Stimulation
ISI	Inter Spike time Interval
NN	Neural Network
DT	Decision Tree
DTC	Decision Tree Classifier
DTP	Decision Tree Predictor
TBAG	Tree Bagger

LIST OF ABBREVIATIONS (Continued)

TBAGP	Tree Bagger Predictor
SVM	Support Vector Machine
SNR	Signal to Noise Ratio
OUP	Ornstein Uhlenbeck Process
PP	Poisson Process
BM	Brownian Motion
IG	Inverse Gaussian
MSE	Mean Square Error
MER	Micro Electrode Recording
FPT	First Passage Time
RMM	Riccaiardi's Movement Method
FIE	Fortet Integral Equation
ISE	Integral Square Error
MAD	Median Absolute Error
IQR	Inter Quartile Range
PCA	Principal Component Analysis
FA	Factor Analysis
ICA	Independent Component Analysis

SUMMARY

The main motive behind the research work presented in this thesis, is to provide the proof of concept for the design of an automated, next generation, adaptive closed-loop deep brain stimulation (DBS) system. In this work we developed various automated tremor prediction algorithms based on surface-Electromyography (sEMG) and Accelerometer (Acc) signals measured at symptomatic extremities. We also performed the mathematical modeling of neuronal activities measured from the affected part of the brain in case of movement disorder patients. This provides theoretical background to further improve the existing state of the art DBS system so that it can provide maximum benefits to the patients. This thesis work can be subdivided into two parts:

- To develop automated tremor prediction algorithms for Parkinson's Disease (PD) and Essential Tremor (ET) patients using various machine learning techniques such as Neural Network (NN), Decision Tree (DT), Tree Bagger (TBAG) and Support Vector Machine (SVM).
- To provide a stochastic model for the neuronal spiking activities measured from the subthalamic nucleus (STN) of PD patients and Venteral Intermediate Nucleus (VIM) of ET patients during DBS implantation which can further be used in adaptively controlling the stimulation parameters.

DBS is a surgically-implanted battery-operated electrodes which sends High Frequency electrical Stimulation (HFS) to targeted areas of the brain [7]. DBS has provided remarkable therapeutic benefits to PD and ET patients when their disease symptoms are disabling. Despite the long history of the treatment based on DBS [8], its underlying principles and working mechanisms are still not clear. The existing FDA approved DBS systems operate open-loop, that is, the physician sets the DBS stimulation

parameters, such as frequency, pulse amplitude, and pulse duration, with visual feedback from the patient. DBS stimulation is provided continuously and its parameters remain constant until the physician changes them. This implies that existing DBS technology is neither adaptive to the patients needs nor able to follow the patients disease progression over time.

To design an adaptive closed-loop DBS system we need to adaptively change the DBS stimulation parameters as per the patients need and also make it an automated ON-OFF controlled system. The next generation adaptive closed-loop DBS system design requires the identification and processing of suitable physiological signals that contain information related to the real-time response of the brain to DBS stimulation. The mathematical modeling of neuronal brain activities measured at the site of the DBS implant would shed light into the mechanisms of DBS system and therefore can provide effective DBS treatment to PD and ET patients in alleviating their severe disease symptoms [9]. The effect of DBS parameters on mathematical model parameters can predict the reappearance of diseease symptoms when DBS is turned OFf and also can be used in optimizing DBS parameters [10–13]. However the mathematical model based on the neuronal brain activities measured at the site of the DBS implant would require changes in the currently approved DBS system whose testing and approval could take years and considerably delay closed loop DBS commercialization. Therefore to overcome this limitation the authors of [6] have proposed a closed loop DBS design based non-invasive surface electromyogram (sEMG) and accelerometer (Acc) signals measured from patient's symptomatic extremities. As this design was based on manual algorithm which involves manual training and manual setting of several threshold parameters therefore it's commercial implimentation is unfeasible.

SUMMARY (Continued)

This thesis work shows the implementation of various automted tremor prediction algorithms in case of PD and ET patients based on which we can design a commercially viable closed loop DBS system. To implement automated tremor prediction algorithms in PD and ET patients we explored various machine learning techniques. We compared the performance of tremor prediction algorithms which are implemented using NN, DT, TBAG and SVM in ET and PD patients to choose best among them. In this thesis work we also performed the mathematical modelling of neuronal spiking activities recorded from Ventral Intermediate Nucleus (VIM) of thalamus of ET patients and the subthalamic nucleus (STN) of PD patients using Ornstein Uhlenbeck Process (OUP). The parameter extraction of OUP ia performed using the Fortet Integral Equation (FIE) [14, 15], which is based on the minimization of maximum Kolmogorov-Smirnov statistical error criteria. This mathematical modelling is performed on 19 VIM recordings from ET patients and 10 STN recordings from PD patients. We statistically compared the results obtained from the OUP whose parameters were obtained using FIE method with the OUP in which the model parameters were extracted using the moments method based on the Ricciardi's approach [16] as in [17,18] using a directional Wilcoxon signed rank test [19] and we concluded that the model parameter estimated based on the FIE method gives overall better results compared to the moment method in case of ET and PD patients. Therefore mathematical modelling of neuronal spiking activities in case of ET and PD patients can be performed by OUP in which model parameters are extracted using FIE method. These results may have various implications in designing the next generation automated adaptive close loop DBS system.

The introduction chapter of this thesis summarizes the background about ET and PD patients. The second chapter presents all the automated tremor prediction algorithms in case of PD patients with their

performance comparision. The third chapter of thesis shows the implementation of various automated tremor prediction algorithms is case of ET patients. In chapter four of this thesis we perform the mathematical modelling of neuronal spiking activities using OUP in which model parameters were extracted using FIE method. In conclusion chapter we compare the various machine learning technique based tremor prediction algorithms is case of ET and PD patients. Finally, we propose the future directions to this study.

CHAPTER 1

INTRODUCTION

Essential Tremor (ET) and Parkinson's Disease (PD) are the most prevalent progressive neurological movement disorders. The underlying pathophysiology for these diseases are still unknown and there is no cure at present. However, there are medication therapies which can control the symptoms of these diseases, but if the symptom severity increases to a disabling level, then surgical procedures such as deep brain stimulation (DBS) can used for further treatment. DBS provides stimulation either to the Ventral Intermediate Nucleus (VIM) of thalamus in case of ET/PD or to the subthalamic nucleus (STN)/globus pallidus (GPi) in case of PD, DBS is thought to block the abnormal nerve signals responsible for symptoms, such as bradykinesia, rigidity, tremor, and gait difficulties. DBS provides therapeutic benefits in case of PD and ET by changing the brain activities in a controlled and reversible manner but its underlying mechanism is still unknown [20].

1.1 Essential Tremor

ET is a progressive neurological disorder [21]. The progression of the disease varies from patient to patient as in some cases it may be slow and for others it may be very rapid [22], [23]. ET is also referred to as kinetic and / or action tremor as it occurs only when the affected muscle exerts effort, i.e., in posture (kinetic) or in action, and is characterized by a tremor frequency range of 4-12 Hz [24]. ET can affect the head (neck), jaw, voice and other parts of the body but in most cases tremor originates from the arm [24]. Statistics of this disease shows that the prevalence of this disease is up to 10% of

the population in the United States. It also indicates that the risk factor for this disease increases as the age increases (approximately 4% for persons in the age group of 35-40 years and about 5% for those who are above 60 years [25]). The occurrence of ET patient is approximately ten times that of PD patients. Many cases of ET are found to be familial but underlying pathophysiology is still unknown [26]. Several physiological, clinical and imaging studies show the involvement of the cerebellum and/or cerebellothalamocortical circuits [27]. There is no cure for this disease but there are treatments which can control the symptoms and improve the quality of life to an extent. The treatment depends on the severity of the tremor; if it is less severe, then medications the beta-blockers propranolol and the antiepileptic primidone are effective [28]. If medication does not work and the severity of the disease is disabling, then surgical procedures such as thalamotomy [29] and DBS [30] may be used. In the thalamotomy surgical procedure, a small volume of the tissue in thalamus area is removed by using either stereotactic radio surgery or radio frequency (RF) ablation this procedure is irreversible. DBS, which involves the placement of electric probe inside VIM of thalamus and is connected to a pacemaker device placed near collarbone to power the electrode. DBS provides continuous, high frequency electrical stimulation to target area of the brain and its effects are reversible. Currently, the FDA approved DBS system operates open-loop, i.e., the stimulation parameters do not change over time. The next-generation of DBS system is envisioned to adaptively change the stimulation parameters according to the needs and condition of patient [31].

1.2 Parkinson's Disease

PD is a gradual progressive neurodegenerative disorder of the central nervous system, which is characterized by symptoms such as tremor, rigidity, slowness of movement and postural instability. In

United states approximately 0.37% (1̃ million) people are suffering from PD. The risk factor for PD increases with age and prevalence of this disease rises from 1% for age over 60 years to 4% for age over 80 years [32]. This disease is caused due to the loss of subgroups of dopaminergic neurons in the substangia niga, a region of the mid-brain that controls movements and is characterized by a rhythmic tremor in the 4 - 12 Hz frequency band. The insufficient dopaminergic neurons in the substangia niga disturbs the direct and indirect pathways of transmission of signals from the motor cortex area to the basal ganglia (BG) which is the cause for most of the Parkinsonian symptoms [20, 33, 34]. This disease cannot be cured but there are medical procedures which can control the symptoms of this disease [33]. The medication therapies which can control the symptoms are levodopa in combination with dopa decarboxylase inhibitor or COMT inhibitor, dopamine agonists and MAO-B inhibitors [35]. In advanced stage PD medication therapies become ineffective and/or start producing side-effects such as nausea, dyskinesias and joint stiffness [35] then the surgical procedures such as DBS relieve patients from most of their debilitating motor symptoms and improve their quality of life to a larger extent [36–39]. Currently approved DBS (from Medtronic) uses battery-operated surgically-implanted electrodes to deliver HFS to the neurons in the brain that control movement. DBS is particularly effective at suppressing involuntary rhythmic tremor in the $4 - 12$ Hz frequency band [40]. The target area of the stimulation for PD patients is either the internal segment of GPi or STN as it benefits not only tremor but also other symptoms such as rigidity, bradykinesia, gait problems, and dyskinesias.

1.3 Current state-of-the-art of DBS system

In case of healthy subjects, the neurons within the GPi and the STN in the basal ganglia resonates at around 70 Hz; in case of PD and ET patients, due to decrease in dopamine level, the resonant frequency

reduces to 30 Hz [41]. DBS uses a surgically-implanted battery-operated medical device which consists of three components: the lead, the extension, and neurostimulato as shown in Figure 1 [1].

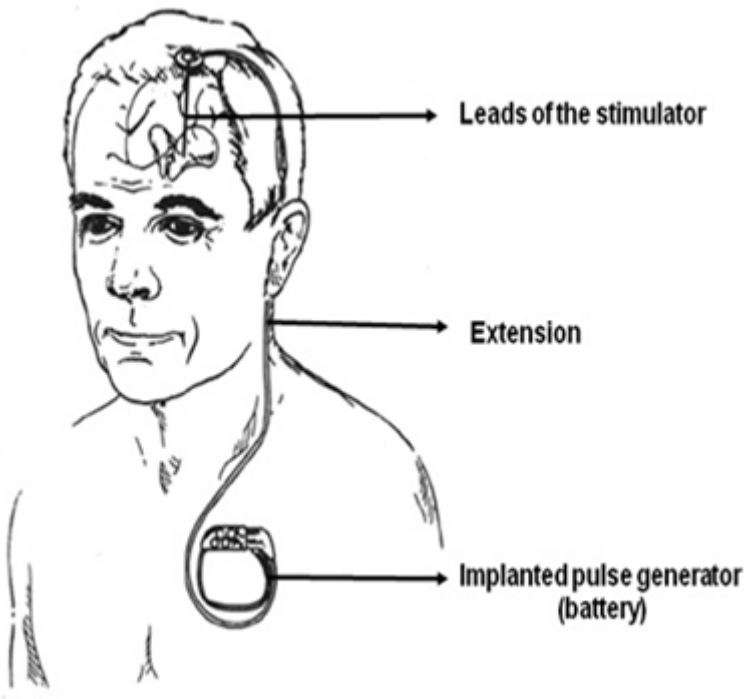

Figure 1. DBS system components (Lead, Extension and pulse generator).

[1]This figure is taken from http://www.med.unc.edu/neurology/divisions/movement-disorders/copy_of_deep-brain-stimulation.

The lead is a thin insulated wire consisting of four thin insulated electrodes (electrodes 0, 1, 2, 3) whose tips are implanted within the targeted brain area with electrode spacing of 0.5 mm. The neurostimulator is similar to a cardiac pacemaker device and consists of a small battery and programmable computer chip to send electrical pulses to control disease symptoms. It is implanted under the skin below the collarbone. The extension is an insulated wire that is passed under the skin and connects the lead to the neurostimulator to send the signal from neurostimulator to the electrodes. DBS system delivers High Frequency electrical Stimulation (HFS) through the lead to targeted areas such as VIM of thalamus in case of ET/PD or to the STN/GPi in case of PD in the brain that control movement.

Activa is the only Food and Drug Administration (FDA) approved DBS system from Medtronic. DBS can operate in monopolar stimulation mode or in in bipolar stimulation mode. In case of monopolar stimulation mode, the pulse generator is the anode and one or more of the four electrodes can be the cathode(s) in bipolar stimulation mode, the cathode(s) as well as the anode(s) are provided by the electrodes. DBS surgery can be unilateral (for ET patients) or bilateral (for PD patients) in which the leads are surgically implanted in the brain and connected to one or more neurosimulators, respectively. In the existing open-loop system, the physician sets the stimulation parameters such as frequency, pulse amplitude, and pulse duration with visual feedback from the patient. The stimulation is provided continuously and parameters remain constant until physician make any changes into it. The existing DBS technology is non-adaptive to patient's needs and is not able to follow the patient's disease progression over time. We therefore say that current DBS systems operate open-loop.

1.4 Adaptive ON-OFF controlled Closed-Loop DBS system

To redesign the current DBS system such that it can adapt to the variation in patient's tremor condition, it is necessary to design an adaptively controlled closed-loop DBS system. The closed-loop DBS system design requires suitable physiological signal that contains information related to the real time response of brain to electrical stimulations for adaptive control of the stimulation parameter and information related to reappearance of the tremor for adaptive on-off control. The best choice of the physiological signal would be the actual neuronal brain activity which can be measured either from individual neurons called micro-recording represented by cell firing, or from group of neurons called macrorecording represented by local field potential. To measure these signals during stimulation off times require changes to the current FDA approved DBS system which requires long testing and approval times and will delay its commercialization. To overcome this limitation, the alternative choice is non-invasively recorded surface-electromyogram (sEMG) signal in correlation with accelerometer (Acc) signal [42] which can be used to implement the adaptive on-off control in existing state of the art DBS system.

Many researches are developing an adaptive closed-loop DBS controller. The study performed in [43] shows that closed-loop control of DBS amplitude can regulate the spectrum of the local field potential and therefore can normalize the aberrant pattern of neuronal activity present in tremor. One study shows that the combination electrochemical monitoring and mathematical modeling can potentially provide an automatic algorithm to adjust the postoperative DBS parameters [44]. Some researches to design a close-loop DBS system [45] used the optimization of stimulation pattern, such as phase resetting and delayed feedback [46–48] using a pulse train with random frequency [11]. As these ap-

proaches are based on mathematical modeling of recorded electrical signals from the key areas of the brain therefore these closed-loop DBS system designs will need further approval from Food and Drug Administration for its commercial application. To overcome this limitation the authors of [42, 49] proposed a DBS closed-loop design based on non-invasively recorded sEMG/Acc signals. In [6] authors showed that a closed-loop DBS system can be designed in case ET and PD using manual algorithm based on non-invasively measured sEMG/Acc signals which contain tremor information. In [42] it was shown that DBS could be switched OFF for up to 50% of the time without patients experiencing any discomfort. In this thesis work we are taking one step forward to designing a fully automated tremor prediction algorithms in ET and PD patients based on various machine learning algorithms which does not require manual thresholding of the parameters.

1.5 Motivation and Impacts

The motivation behind this work is to design an automated, controlled closed-loop DBS system for movement disorders because of the two major shortcomings in the existing DBS system. First, the current DBS system operates open loop, i.e., it continuously stimulates the brain area which controls the movement with HFS. This can be avoided by using the HFS pulses just before the reappearance of the tremor in case of PD and ET patients. The reappearance of the tremor can be predicted by using some signals measured from the PD and ET patients which contains the tremor prediction information. By implementing the closed-loop algorithm we can avoid the high injection of the current inside the brain.

Second, the existing DBS system is non-adaptive in nature meaning the stimulation parameters remains constant until the physician changes them. Even though the disease symptoms may change over the time, but the stimulation parameters doesn't change according to patient's disease progression

over the time. To make the current DBS system adaptive in nature, we have to record and process the brain activities measured through the implanted DBS electrodes. The mathematical modeling of the inter spike time interval (ISI) measured through micro electrode during DBS surgery may provide us some knowledge about the brain activities in case of ET and PD patients.

The next generation adaptive close-loop control DBS systems will have following major impacts:

1. As the next generation DBS system will provide the HFS only on the reappearance of the tremor therefore it will require less power, which in turn will prolong the battery life. The prolonged battery life will reduce the recurring battery implantation surgery cost and risks.
2. It will reduce the injection of the current inside the brain which will avoid the possibility of destroying healthy cells.
3. It may also provide the run time activities of the brain which could be helpful in understanding the pathophysiology of the disease and also the working mechanism of DBS system.

1.6 Outline of the work

The introduction chapter of this thesis provides some background about the ET and PD diseases which includes the symptoms of the diseases, statistics about the population affected by these diseases, medication based initial treatments of these diseases and surgical based treatments in case of severe disease symptoms. As DBS is one of the surgical procedures which is widely used to relieve ET and PD patients from most of their debilitating symptoms. In this chapter we discuss some of the possible underlying mechanisms involved in DBS which can be responsible to provide the therapeutic benefits to

the patients. We discuss about the existing state of the art DBS system and its shortcomings followed by the discussion about the design of an automated adaptive ON-OFF controlled closed-loop DBS system.

The second chapter introduces the automated tremor prediction algorithms for PD patients using various machine learning techniques. The input parameters for all the tremor prediction algorithms are estimated from non-invasively measured sEMG and Acc signals; in this chapter we discuss the data collection procedure used. This chapter describes all the parameters used for tremor prediction and proposed all the machine learning techniques such as NN, DT, TBAG and SVM based on which all automated tremor prediction algorithms are designed. The training of machine learning technique based tremor prediction algorithms in case of PD patients is also presented in this chapter. This chapter also discusses the performance matrix involved in analyzing the algorithms. This chapter concludes with the results and discussion of the various automated tremor prediction algorithms in case of four PD patients.

The third chapter deals with the implementation of automated tremor prediction algorithms for ET. In case of ET patients five different automated tremor prediction algorithms are proposed two of them also involve a condition classifier before tremor predictor. The conditions classifier section involves the discussion about the input parameter extraction for the classifier and its implementation. Finally, in this chapter we provide the individual tremor prediction summary for all tremor prediction algorithms followed by a comparative analysis amongst all the algorithms.

The fourth chapter derives mathematical models for the neuronal spiking activities recorded from the STN of PD patients and VIM of ET patients during the micro-electrode recording of the affected areas of the brain during DBS surgery. To derive a mathematical model for neuronal activities in diseased part of the brain, we propose to use, following well established literature, the Ornstein-Uhlenbeck Process

(OUP). In this work, we propose to extract the OUP parameters by using Fortet Integral Equation (FIE) method. Furthermore, we statistically compare the performance of OUP with some other stochastic processes such as Poisson Process (PP), the Brownian Motion (BM) and the OUP whose parameters are extracted using a moment method. We show that the performance of OUP in which the parameters are extracted using FIE method is superior than the other stochastic processes. This mathematical modeling can be further used to provide understanding of neuronal activities in the affected part of the brain and also can be useful in designing an adaptive close-loop DBS in case of PD and ET patients.

In the conclusion chapter of this thesis we compare the machine learning technique based tremor prediction algorithms in case of PD and ET patients for next generation closed-loop DBS system. As the future direction of the work we propose to improve the processing of the sEMG and Acc signal. We also propose to explore some other methods such as Principal Component Analysis (PCA), Factor Analysis (FA) or Independent Component Analysis (ICA) to extract the optimum number of parameters from filtered sEMG and Acc signals. Furthermore a rigorous exercise can also be undertaken to find out the best combination of parameters or options for various machine learning techniques used in this work. For the modeling of neuronal spiking activities we can further investigate more complex stochastic process such as Feller process.

This thesis work provides the theoretical concept for the design of an automated next generation adaptive closed loop DBS system which in turn can improve the existing DBS system design for the treatment of PD and ET patients.

CHAPTER 2

TREMOR PREDICTION ALGORITHM IMPLEMENTATION IN PARKINSON'S DISEASE PATIENTS USING MACHINE LEARNING TECHNIQUES

Part of the content of this chapter appeared [1]: Shukla, P., Basu, I., Graupe, D., Tuninetti, D., and Slavin, K. V.: A neural networkbased design of an on-off adaptive control for deep brain stimulation in movement disorders. In Engineering in Medicine and Biology Society (EMBC), 2012 Annual International Conference of the IEEE, 2012.

2.1 Background

To redesign the current DBS system such that it can adapt to the variation in patient's tremor condition, it is necessary to design an adaptively controlled closed-loop DBS system. To design a closed-loop DBS system, we need to adaptively control the DBS stimulation parameters as well as the time intervals when DBS stimulation is administered. This requires the identification of suitable physiological signals that contain information related to the real-time response of the brain to DBS stimulation. In particular, we are interested in a simple but robust ON-OFF control of DBS such as when stimulation is switched OFF and the patient does not experience tremor, the system tracks few physiological signals and predicts when tremor is about to reappear. When tremor recurrence is predicted, stimulation is switched ON for a fixed amount of time. The authors showed in [42] that in most of the cases, it is possible to switch

OFF stimulation for more than 50% of the time, which gives a considerable saving in battery life and reduces the amount of current injected in the brain.

The neuronal brain activity measured at the site of the DBS implant would offer the necessary predictive information about tremor reappearance. However, measuring from the stimulating electrodes would require changes in the currently approved DBS system whose testing and approval could take years and considerably delay closed-loop DBS commercialization. To overcome this limitation the authors of [42, 49] proposed a DBS closed-loop design where the controller inputs are parameters estimated from non-invasively recorded sEMG/Acc signals that correlate with the tremor symptoms. Such an automated tremor predictor must achieve the following objectives:

- Goal 1: The onset of the tremor should be predicted just a few seconds before the occurrence of the tremor so that the patient does not experience any discomfort due to tremor.
- Goal 2: Any kind of voluntary movements and posture initiations should not be predicted as tremor so as to increase the DBS-OFF time.

In [49], a reliable predictor of tremor onset for Essential Tremor was obtained by using entropy measures, in particular approximate and wavelet entropy. Furthermore, we extended our work in [6] and designed a manual closed-loop ON-OFF DBS system based on surface electromyogram (sEMG) and accelerometer (Acc) signals measured non-invasively from the patient's symptomatic extremities. We extracted several features from the sEMG and Acc signals and manually designed thresholds for a tremor prediction algorithm that was shown to achieve an overall sensitivity of 100% along with an accuracy of 80.2% in case of 4 PD patients. Based on statistical tests, we concluded that the predicted

tremor reappearance times differ from random prediction outcomes. Towards the design of a fully automated closed-loop DBS system suitable for commercial implementation, in [1] we developed a tremor predictor based on a feed-forward back-propagation Neural Network (NN), which achieved an overall sensitivity of 92.3% and accuracy of 75.8%, when tested on 2 Parkinson's Disease (PD) patients. As the results were limited to 33 trials for two PD patients we extended this work and implemented on 92 trials for 4 PD patients; moreover, we have implemented the tremor predictor algorithms in 4 PD patients based on various other self adaptive machine learning techniques such as decision tree (DT), treebagger (TBAG) and support vector machine (SVM).

NN-based predictors, with physiological signals as inputs, have been widely used in clinical applications such as for predicting, for example, epileptic seizures [50] and sleep apnea [51]. In this work, we implemented various other machine learning algorithms such as DT, TBAG and SVM along with feed-forward back-propagation NN to predict tremor reappearance in PD patients.

Finally, we show that in case of 4 PD patients, the NN based tremor prediction algorithm successfully predicts tremor in 86 out of 92 trials with an overall accuracy of 76.09% and sensitivity of 91.05%, the DT based tremor prediction algorithm successfully predicts tremor in 92 out of 92 trials with an overall accuracy of 85.87% and sensitivity of 100.00%, the TBAG based tremor prediction algorithm successfully predicts tremor in 91 out of 92 trials with an overall accuracy of 78.26% and sensitivity of 98.41% and the SVM based tremor prediction algorithm successfully predicts tremor in 88 out of 92 trials with an overall accuracy of 83.70% and sensitivity of 94.29%. The overall summary of all tremor prediction algorithms in case of PD patients is summarized in Table VII. The DT based tremor prediction algorithm has achieved the highest performance among all other tremor prediction algorithms with

TABLE I

OVERALL TREMOR PREDICTION SUMMARY FOR ALL MACHINE LEARNING TECHNIQUES BASED TREMOR PREDICTION ALGORITHMS. LEGEND: N = TOTAL # OF TRIALS, NTD = TOTAL # OF NO TREMOR DETECTED TRIALS, A = ACCURACY IN %, S = SENSITIVITY IN %, FA = FALSE ALARM RATE IN % AND MCC = MATTHEWS CORRELATION COEFFICIENT.

TREMOR PREDICTION ALGORITHM	**N**	**NTD**	**TP**	**TN**	**FP**	**FN**	**A (%)**	**S (%)**	**FA (%)**	**Mcc**
NN	92	11	61	9	16	6	76.09	91.05	18.18	0.37
DT	92	11	71	8	13	0	85.87	100.0	27.27	0.57
TBAG	92	11	62	10	19	1	78.26	98.41	9.09	0.45
SVM	92	11	66	11	11	4	83.70	94.29	0.00	0.51

an overall accuracy of 85.87% and sensitivity of 100.00%. This work shows the possibility of DT-based closed-loop DBS system design without making any modifications to the existing electrodes implanted in the brain.

2.2 Data Set

Four PD patients were recruited for the study from the Movement Disorder Clinic at Rush University Medical Center. Patient details are listed in Table VIII. Informed consent approved by the IRB was obtained from all patients. The four PD patients had DBS electrodes (Medtronic DBS lead model 3389) stereotactically implanted in the STN. All patients had dominant tremor in one or both arms and their symptoms were well controlled by the combination of DBS stimulation and medications. All four patients had one recording session each in the Neural Control of Movement Laboratory (NCML) at UIC. On the testing day, the patients were on their usual medication and a series of sEMG recordings

were done from the the extensor digitorum communis (upper forearm). The recording setup was as in [52]. The sEMG signal was amplified (gain set to 1,000) and bandpass filtered between 20Hz and 450Hz (Delsys Inc., Boston, MA). Along with sEMG, acceleration data was recorded from the finger tip (with a calibrated Coulbourn type V 94-41 miniature solid-state piezoresistive accelerometer having a resolution of 0.01g). Both sEMG and accelerometer data were sampled at $f_s = 1000$Hz. The experiment setup is shown in Figure 2.

In the beginning of the experiment, the patient was comfortably seated in an upright position. The arm of the chair served as the supportive surface for the patient's forearm. DBS stimulation was switched OFF for some time before recording started. Then a trial started with the stimulation ON for 20s to 50s followed immediately by an interval with stimulation OFF. The total duration of each trial, T, was between 50s to 100s. In each trial, the patient was in one of the following three states:

R: Rest with his/her hand completely relaxed and hanging from the chair's arm rest.

P: Holding a Posture, with his/her wrist and hand in a neutral extended position.

A: Performing a voluntary Action such as reaching for his/her opposite shoulder or flexion of the wrist.

In states P and A, the movement/posture was initiated either before or after switching the stimulation OFF. There were 15 to 20 such trials recorded for each patient. After stimulation was switched OFF at time t_{OFF}, the first instant t_{tr} when tremor visibly reappeared was noted. Reappearance of tremor was also verified by thresholding the acceleration data at $0.2 m/s^2$ for states R and P.

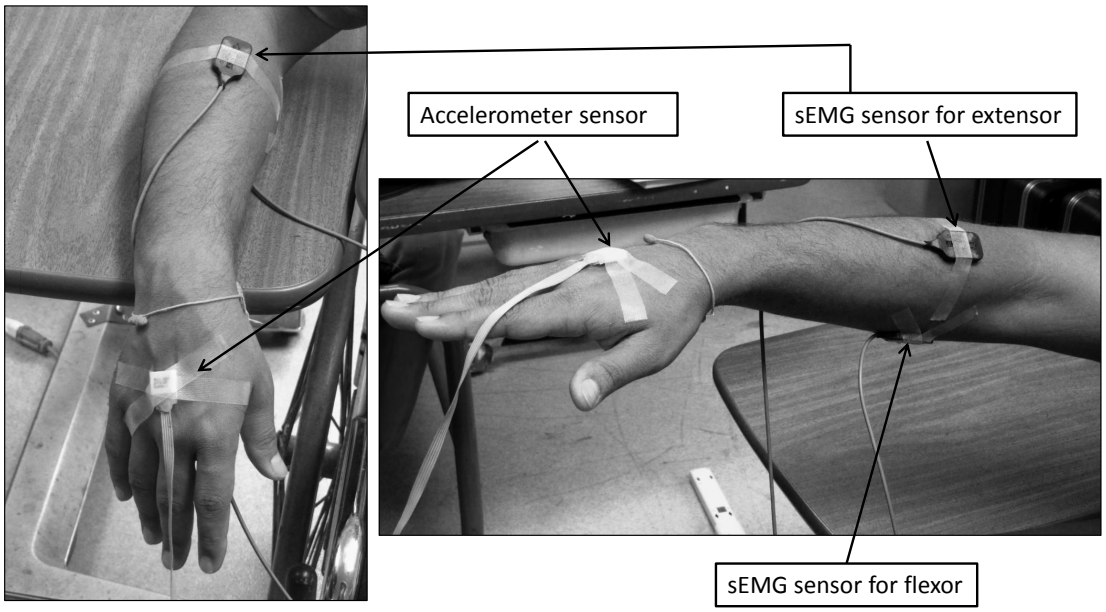

Figure 2. Hand position with sEMG (flexor and extensor) and Acc sensors during posture condition. Figure from [6].

2.3 Input parameters for tremor predictor algorithms

The tremor predictor inputs are a combination of spectral, entropy and recurrence measures from the *smoothed sEMG* and Acc signals. The smoothening of the raw extensor signal $x(t)$ was performed by calculating the power over windows of 50 ms (equivalent to 50 samples) duration that slide over every sample. The smoothed sEMG signal will be denoted as $x_s(t)$. The sEMG was smoothed to extract the lower frequency tremor bursts by averaging out the higher frequency oscillations inside the sEMG bursts. The smoothening of the signal is mathematically equivalent to the low pass filtering. Finally, a set of parameters were calculated based on smoothed sEMG and Acc signals using windows of 1 sec

TABLE II

DETAILS OF PD PATIENTS

Patient#	age	gender	DBS parameter			active contacts	DBS implant	hand tested
			amplitude	frequency	pulse width			
PD1	46	M	2.8 V	180 Hz	80 μs	1-0+	2008	R
PD2	45	M	2.5 V	185 Hz	60 μs	1-2-C+	2002	L
PD3	52	F	2.8 V	185 Hz	120 μs	0-C+	2004	R
PD4	60	F	2 V	145 Hz	60 μs	1-3-C+	2009	R

(equivalent to 1000 samples) with an overlap of 0.75 sec thus producing a sample every 0.25 sec. The first parameter sample was obtained after an initial delay of 1.05 sec. A description of all the parameters that were used for tremor prediction in case of PD patients is as follows:

1) The *mean frequency* is the expected value of the frequency distribution over the spectrum range considered

$$F_{\text{mean}} = \frac{\sum_{n=1}^{N} f_n P_n}{\sum_{n=1}^{N} P_n},\ N = 37, \tag{2.1}$$

where P_n is the power of a 1s window of the smoothed sEMG at frequency band centered around f_n, $n \in [1:N]$, calculated by using a 512-point Fourier transform. As F_{mean} involves the power of sEMG and Acc signals centered around different frequencies, therefore it is expected that F_{mean} will have greater value in the absence of a tremor compared to the presence of tremor or just before the appearance of tremor.

2) The *Peak Frequency* and the *Power at Peak Frequency*: The frequency band of interest is from $f_4 = 3$Hz to $f_{19} = 18$Hz, which carries tremor information. For each band we calculate the power P_n; the frequency band with maximum power has index $i^\star$ which is given by:

$$i^\star = \arg \max_{n \in [4:19]} \{P_n\}. \tag{2.2}$$

The *peak frequency* and the *power at peak frequency*, whose utility is explained in [6], are respectively

$$F_{\max} = f_{i^\star}, \quad P_{\max} = \frac{P_{i^\star}}{\sum_{i \in [20:37]} P_i}. \tag{2.3}$$

In (Equation 2.3) $P_{\max}$ is normalized by the power of signal outside the tremor frequency range because the power at $F_{\max}$ must be compared over different trials, which might have significantly different power outside the range of interest.

3) The *mean power in n-th frequency band* is obtained by decomposing the smoothed sEMG signal into $M = 10$ frequency bands with Daubechies4 wavelets. Let $X_j(t)$ denote the signal in the j-th frequency band, $j \in [1 : M]$. The mean power in j-th frequency band is defined as

$$\overline{P_j} = \frac{1}{\Delta_T} \sum_{t \in \Delta_T} |X_j(t)|^2, \ \Delta_T = 1\text{s}. \tag{2.4}$$

The mean power in the frequency band of $(8-16)$ Hz was used for the tremor prediction algorithms. The frequency band of $(8-16)$ Hz was used because it was seen that this frequency band contains most

of the predictive information [42] which can specially distinguish between the voluntary movement and actual tremor condition. Moreover, this band also overlaps with the typical action/postural tremor frequency band.

4) The *sample entropy* $\mathrm{SpEn}(U,m,r)$ for a time series U (here the smoothed sEMG signal) of length L involves two input parameters m and r, which are the pattern length and the similarity criterion, respectively. It is defined as

$$\mathrm{SpEn}(U,m,r) = \lim_{L\to\infty} -\log \frac{B_{m+1}(r)}{B_m(r)}, \tag{2.5}$$

where $B_{m+1}(r)/B_m(r)$ represents the conditional probability that the two sub-sequences of U matches point-wise for m points will also match within a tolerance r at the next point; therefore a lower $\mathrm{SpEn}(U,m,r)$ value reflects a high degree of regularity [53]. Here $m = 2, r = 0.14\sigma$, where σ is the standard deviation of the smoothed sEMG signal.

5) The *recurrence rate* involves the calculation of a recurrence matrix with elements, $R_{i,j}$, $(i,j) \in [1:P], P = L-(E-1)\tau$, for $U = \{x(i),\ i \in [1:L]\}$ of length L considering $E = 5,\ \tau = 3,\ L = 1000$ as described in [54]. From $R_{i,j}$ the recurrence rate R is calculated as

$$\mathsf{R} = \frac{1}{P^2}\sum_{i,j} R_{i,j} \tag{2.6}$$

and quantifies possible non-linear synchronization in the sEMG signal (it corresponds roughly to the probability that a specific state of the dynamical system, reconstructed using a method of delayed vector construction, will recur [54]).

6) The (Shannon) entropy is a measure of unpredictability and is often used to quantify the amount of order/disorder in a signal. In information theory, the entropy of a discrete random variable (RV) X is defined as [55]:

$$H(X) = -\sum_{i=1}^{K} p_i \log p_i \tag{2.7}$$

where $p_i = \mathbb{P}[X = x_i]$, $i \in \{1,...,K\}$, is the probability mass function and K is the number of possible outcomes for X. Based on Equation 2.7, the *Wavelet Entropy*, $H_{\text{wt}}(t)$ of $x_s(t)$, is calculated as [56]:

$$H_{\text{wt}}(t) = \sum_{j=1}^{M} \bar{x}_j(t) \log \frac{1}{\bar{x}_j(t)}. \tag{2.8}$$

where,

$$\bar{x}_j(t) = \frac{|x_j(t)|^2}{\sum_{k=1}^{M} |x_k(t)|^2},\ j \in \{1,...,M\}. \tag{2.9}$$

$\bar{x}_j(t)$ represents the normalized power of $x_j(t)$ and hence can be treated as a probability mass function whose (Shannon) entropy is estimated by $H_{\text{wt}}(t)$. This parameter was calculated only for PD sEMG. For each window of $x_s(t)$, the wavelet entropy was calculated as the average of $H_{\text{wt}}(t)$ over the time window.

2.4 Machine Learning Techniques for Tremor Prediction Algorithm

In this work we developed various automated tremor prediction algorithms for four PD patients which are based on different machine learning techniques: Neural Networks (NN), Decision Tree (DT), Tree Bagger (TBAG) and Support Vector Machine (SVM). We compared their performances using

various criteria to choose the best among all machine learning techniques. First, we discuss the main features of all tremor prediction algorithms.

2.4.1 Neural Network (NN)

A NN consists of many neurons/nodes arranged in different layers, referred to as input, hidden and output layers. A NN is a connectionist architecture based on functional and/or structural aspects of the human brain. It consists of a massive set of interconnected neurons working in unison to solve a specific problem. A NN is an adaptive network that changes its organization based on the information it receives that is defined by: (i) the interconnection between different neurons (weights), (ii) the learning process for updating the weights of the interconnection between the neurons and the bias at each neuron and (iii) the activation function that converts a neuron weighted input to its output activation, which we introduce next. To predict the onset of the tremor for the problem at hand, we propose to use a *feed-forward back-propagation NN* [57]. The term "feedforward" describes that the neural network processes and recalls patterns in forward manner. In this type of NN architecture the neurons are connected only in forward direction, i.e., each layer of the NN contains connections to the next layer, but there are no connections in backward direction. The second term "backpropagation" describes the direction of error propagation during the NN training, i.e., the error propagates from output layer to the input layer. As the feed-forward back-propagation NN architecture is very popular and efficient networks in modeling complex input-output relationships [57], we implemented this network for tremor prediction in PD patients. There are various other NN such as radial basis function network, recurrent neural network and LAMSTAR which can also be applied for tremor prediction algorithms.

Our NN architecture consists of an input layer with six neurons, two to three hidden layers each with 20 neurons and an output layer with two neurons. Each layer has its own weight matrix, bias vector, input vector and output vector, whose dimensions are given by the number of neurons/nodes in the layer. For the j-th node in a layer, let $\mathbf{w}_j = [w_{j,1}, ..., w_{j,n}]$ be its weight vector, $\mathbf{x}_j = [x_1, ..., x_n]$ be its input vector, b_j be its bias and o_j be its output (here n indicates the number of neurons in the preceding layer). The initialization of weight/bias in NN is one of the most effective ways in speeding up the training of neural network. There are various weight/bias initialization methods such as least-squares method [58, 59], statistically controlled activation weight initialization method [60] and Nguyen and Widrow Randomization method [61]. In this work to speed up the training process the initialization of the weight/bias is performed by Nguyen-Widrow Randomization technique [61]. This algorithm chooses the initial values of weights and biases in order to distribute the active region of each neuron approximately evenly across the layer's input space.

The *net input* at j-th node is defined by

$$o_j := \sum_{\ell=1}^{n} w_{j,\ell} x_\ell + b_j \tag{2.10}$$

The net output at j-th neuron is a function $f(o_j)$ of the net signal o_j, where f is the *activation function*. For nodes in the input layer, we choose the activation function $f(o_j) = \tanh(o_j)$, while for nodes in the hidden or output layer, $f(o_j) = o_j$. The net output values of the nodes in one layer becomes the input values of the nodes in the next layer (here for notation convenience we omitted the layer index).

Weights and bias are chosen so as to minimize the mean square error (MSE). The *net error* over all P input-output pairs at the N-node output layer is

$$E_{net}(\mathbf{w},\mathbf{b}) := \sum_{p=1}^{P} \frac{1}{N} \sum_{k=1}^{N} e_{p,k}^2, \tag{2.11}$$

where $e_{p,k} := d_{p,k} - y_{p,k}$ is the training error at k-th output layer for the p-th input-output pair (defined as the difference between the desired/ground truth output $d_{p,k}$ and the NN predicted output $y_{p,k} = f(o_{p,k})$, and where $\mathbf{w}$ is the weight vector and $\mathbf{b}$ the bias vector. Here $N = 20$, and $P = 9$, 15, 10 and 17 for PD1, PD2, PD3 and PD4 respectively.

In our NN design we use the derivative-based Levenberg-Marquardt (LM) algorithm for the learning phase to optimize $(\mathbf{w},\mathbf{b})$. In the LM learning algorithm the weight and bias update is based on the second-order derivative of the total error function in (Equation 2.11) [62, 63]. It is formulated in terms of the Hessian matrix $\mathbf{H}$ of (Equation 2.11) with respect to $(\mathbf{w},\mathbf{b})$ which is approximated in term of Jacobian matrix $\mathbf{J}$ as $\mathbf{H} \approx \mathbf{J}^T\mathbf{J} + \mu\mathbf{I}$, with $\mathbf{I}$ is the identity matrix. Finally, the weights or bias at iteration k, indicated here as z_k, is updated as

$$z_{k+1} = z_k - \left(\mathbf{J}_k{}^T\mathbf{J}_k + \mu\mathbf{I}\right)^{-1}\mathbf{J}_k\mathbf{e}_k \tag{2.12}$$

where μ is the non-negative combination coefficient ($\mu \to 0$: Gauss-Newton algorithm; $\mu \to \infty$: steepest decent algorithm) and $\mathbf{e}$ is the error vector that contains all the $e_{p,k}$ in the definition error in (Equation 2.11) [62, 63].

2.4.2 Decision Tree (DT)

A DT consists of a root node n_R, intermediate nodes $\mathbf{n}$, and terminal nodes $\mathbf{n}_T$. The input data set is subdivided into smaller and smaller subsets such that the data in each of the descendants subsets are 'purer' than the data in the parent subset, i.e., the descendants subsets contains majority of one class data compared to the data in the parent subset. To implement a DTC, we calculate the *node proportions* $p(k|n)$, where $k = 1,2,3,\ldots,K$ for K equal to the total number of classes for classification, which is defined as the proportion of k class data at node n. In our analysis $K = 2$ as we have two classes for classification one is tremor and other is no-tremor. Based on the proportions calculated for each state at a given node n, the *impurity* of node n is a non-negative function

$$i(n) = \phi\big(p(1|n),\ldots,p(K|n)\big), \tag{2.13}$$

implemented in this work by using the *Gini index* defined as [64]

$$i(n) = 1 - \sum_{k=1}^{K} p(k|n)^2. \tag{2.14}$$

The *goodness of the split* at a node n is calculated in term of *decrease in impurity* $\Delta i(t)$, which divides the node n into nodes n_r and n_l, the right and the left nodes respectively, such that the proportion p_l of classes goes into left node n_l and the proportion p_r of classes goes into right node n_r; $\Delta i(t)$ is defined as

$$\Delta i(s,n) = i(n) - p_l i(n_l) - p_r i(n_r) \tag{2.15}$$

where $s \in S$ and S is a set of binary splits at each node generated by a set of binary questions [64]. Finally, the split criteria s^* is chosen for root node n_R which gave the largest decrease in impurity, i.e.,

$$\Delta i(s^*, n_R) = \max_{s \in S} \Delta i(s, n_R). \tag{2.16}$$

Based on $\Delta i(s^*, n_R)$, the root node n_R is split into two nodes n_1 and n_2 and the same procedure is recursively repeated for node n_1 and n_2. The decision tree is terminated at nodes $\mathbf{n}_T$ if no significant decrease in impurity measure was further possible. After creating maximum tree which consists of several levels, it is optimized by pruning some of its nodes and sub trees. In our algorithm maximum trees are pruned by implementing an optimal pruning scheme in which a pruned tree with least error rate is selected from a set of pruned trees [64, Section 10.2].

2.4.3 Tree Bagger (TBAG)

Brieman proposed a new method for classification and named it Tree Bagging [65, 66]. The word 'Bagging' is coined by joining two terms **B**ootsrap and **agg**regating. Thus the name of the algorithm itself gives clue about its methodology. Bagging is a statistical learning algorithm based on ensemble of several statistical predictors that are derived from the re sampling of training data set using bootstrap [67,68] algorithm. Bagging not only improves the stability and accuracy of statistical learning algorithm used, but also avoids over fitting of statistical learning algorithm. It is possible to use any machine learning algorithm method in bagging, but it is used with decision trees in most cases. Here we use tree bagger, i.e. bagging with decision tree for classification. In a nutshell, tree bagger is a method for prediction that generates ensemble of decision tree based predictors by making an ensemble of training

data set using bootstrap algorithm and then uses a majority vote for the aggregation of ensemble of predictors to generate a final predictor. Bootstrapping algorithm helps in generating several training data sets from a single training data set with same number of samples as in the original data set.

Consider a classification problem with training data set $\mathcal{D}$ with N samples, consisting of data elements $\{(\mathbf{x_1}, y_1), \ldots, (\mathbf{x_N}, y_N)\}$, where $\mathbf{x_1}, \ldots, \mathbf{x_N}$ are input vectors corresponding to class labels $y_1, \ldots, y_N$. Now we assume that we have a predictor $\varphi(\mathbf{x_l}, \mathcal{D})$ (generated from a classifier algorithm) that predicts the class label y_l for a given value of $\mathbf{x_l}$, ($l \in [1, ..., N]$) based on classifier generated using the training data set $\mathcal{D}$. To improve the performance of the classifier, we intend to use multiple predictors in place of single predictor. Therefore, we generate $\mathcal{D}_k^B$ training data sets each of sample size N, using bootstrapping method where B denotes that the training data belongs to TBAG method and $k \in [1, ..., M]$, where M is the total number of trees used in TBAG algorithm. We used 150 trees to implement TBAG algorithm therefore in our analysis $M = 150$. To prepare $\mathcal{D}_k^B$ of sample size N, random samples are drawn but with replacement from original set $\mathcal{D}$. Because of such replication, it is possible to have repeated samples of $(\mathbf{x_l}, y_l)$ in particular bootstrap training data set $\mathcal{D}_k^B$. On the other hand, it may also happen that a particular sample $(\mathbf{x_l}, y_l)$ is completly absent in $\mathcal{D}_k^B$. Finally, with the help of ensemble of training data set $\mathcal{D}_k^B$, an ensemble of predictors $\{\varphi(\mathbf{x_k}, \mathcal{D}_k^B)\}$ is generated. Out of this ensemble, bagging predictor is chosen based on the majority of votes. i.e.

$$\varphi_B = \text{majority of vote} \quad \varphi(\mathbf{x}, \mathcal{D}) \tag{2.17}$$

The most crucial component that decides the chance of improvement in accuracy through bagging is the stability of procedure to construct φ. If changes in $\mathcal{D}^B$ makes a very small change in φ, then bagging predictor φ^B will be very close to φ and no improvement will be observed. But with instabilities in the procedure, very small changes in $\mathcal{D}^B$ will ensue a large change in φ and thus results in a bagging predictor φ^B that improves accuracy of classifier significantly. In [65], an analysis of instabilities of various procedures for its suitability in bagging was presented. It is found that except k-means method, all other methods such as neural nets, classification, regression trees were unstable and can be used in bagging methodology.

The reason for improvement in accuracy in bagging classifier can be explained as follows: Let assume that in a classification problem, $\varphi(\mathbf{x},\mathcal{D})$ predicts a class label $j \in \{1,\ldots,J\}$. This predictor can be charecterized by $Q(j|\mathbf{x}) = P(\phi(\mathbf{x},\mathcal{D}) = j)$. Let $P(j|\mathbf{x})$ denotes the probability of getting class j for input $\mathbf{x}$. $Q(j|\mathbf{x})$ refers to the relative frequency of getting class label j, with input $\mathbf{x}$ from multiple predictors generated from many independent replicas of the learning set $\mathcal{D}$. The probability of getting correct classification for input $\mathbf{x}$ is

$$\sum_j Q(j|\mathbf{x})P(j|\mathbf{x}) \tag{2.18}$$

The net probability of getting accurate classification is

$$r = \int \left[\sum_j Q(j|\mathbf{x})P(j|\mathbf{x})\right] P_{\mathrm{X}}(\mathrm{d}\mathbf{x}) \tag{2.19}$$

where, $P_X(\mathrm{d}\mathbf{x})$ denotes the probability distribution of $\mathbf{x}$. Since the probability of getting accurate classification is always less than or equal to the total probability distribution of a classifier, we have

$$\sum_j Q(j|\mathbf{x})P(j|\mathbf{x}) \leq \max_j P(j|\mathbf{x}) \tag{2.20}$$

where equality holds if

$$Q(j|\mathbf{x}) = \begin{cases} 1 & \text{if } P(j|\mathbf{x}) = \max_i P(i|\mathbf{x}) \\ 0 & \text{else} \end{cases}$$

Now using Bayes predictor $\phi^*(\mathbf{x}) = \arg\max_j P(j|\mathbf{x})P_X(\mathbf{x})$, the maximum value of classification rate is

$$r^* = \int \max_j P(j|\mathbf{x})P_X(\mathrm{d}\mathbf{x}) \tag{2.21}$$

Order-correct ϕ is a predictor that predicts a particular class with higher rate than any other predictor, provided that input $\mathbf{x}$ results in same class, that is, $\arg\max_j Q(j|\mathbf{x}) = \arg\max_j P(j|\mathbf{x})$. The aggregated predictor is: $\phi_A(\mathbf{x}) = \arg\max_j Q(j|\mathbf{x})$. The correct classification at $\mathbf{x}$ for aggregate predictor is

$$\sum_j I(\arg\max_j Q(j|\mathbf{x}) = j)P(j|\mathbf{x}) \tag{2.22}$$

where, $I(.)$ is the indicator function. The expression for correct probability for ϕ_A is

$$r_A = \int_{\mathbf{x}\in C} P(j|\mathbf{x})P_X(\mathrm{d}\mathbf{x}) + \int_{\mathbf{x}\in C'} \left[\sum_j I(\phi_A(\mathbf{x}) = j)P(j|\mathbf{x})\right] P_X(\mathrm{d}\mathbf{x}) \tag{2.23}$$

where, C is the set of all inputs $\mathbf{x}$ at which ϕ is order-correct. Hence the optimal aggregated predictor ϕ_A is generated from far from optimal order-correct ϕ's.

Out of bag error estimate in Tree bagger algorithm is another important parameter, as it provides an opportunity to use training data as testing data. As mentioned before, bagging generates an ensemble of sample using bootstrapping with replacement option. Therefore, there will be a classifier with a training data set that misses a particular record of pair $(\mathbf{x}_i, y_i)$ from the original data set. Such sets are termed as out of bag examples. Obviously there will be N such subsets (each corresponding to a record in the original data set) for the original training data set of sample size N. Out of bag estimate for the generalization error is the error rate of the out of bag classifier on the training set (as compared to known y_i's). The study of error estimates for bagged classifiers in [69], gives empirical evidence to show that out of bag estimate is as accurate as using a test set of the same size as the training set. Therefore, using the out of bag error estimate removes the need for a set aside test set.

2.4.4 Support Vector Machine (SVM)

Statistical classification methods automatically segregate a given input data into different sets. The schemes for separation of data is learned through a training data set. The sole aim is to generate a generalized classifier that segregate any known or unknown data set into its components without any error. There will be no loss of generality if classification problems are reduced to binary classification. SVM is one of the best method suitable for such classification [70]. First we consider the simplest case wherein it is possible to classify a data set into two classes by linear classifiers. For the case of linear classifiers it desirable to find a suitable plane (or line) that separate data with maximum margin. The

classification boundary, which best generalizes the data classification, is known as the optimal separating hyperplane.

We consider a binary classification problem given by (Equation 2.24), where classification can be performed using a hyperplane defined by (Equation 2.25)

$$\mathcal{D} = \{(\mathbf{x_1}, y_1), \ldots, (\mathbf{x_N}, y_N)\},\ x \in \mathbb{R}^n, y \in \{-1, 1\} \tag{2.24}$$

$$f(\mathbf{x}) = sgn(\mathbf{w}.\mathbf{x} - b) \tag{2.25}$$

In (Equation 2.25) (.) represents the **dot products** and $\mathbf{w}$ denotes the normal vector to the hyperplane. For optimal separating hyperplane, [71] proposed a canonical hyperplane $H : y = \mathbf{w}.\mathbf{x} - b = 0$ such that it is equidistant from the parallel hyperplanes $H_1 : y = \mathbf{w}.\mathbf{x} - b = +1$ and $H_2 : y = \mathbf{w}.\mathbf{x} - b = -1$ with no data points lying between H_1 and H_2. Thus the distance between H_1 and H_2 would be

$$2 \times \frac{|\mathbf{w}.\mathbf{x} - b|}{\|\mathbf{w}\|} = \frac{2}{\|\mathbf{w}\|} \tag{2.26}$$

An optimal hyperplane requires this distance to be maximized. Hence require minimization of $\|\mathbf{w}\| = \mathbf{w}^T\mathbf{w}$ under the constraint

$$y_i(\mathbf{w}.\mathbf{x_i} - b) \geq 1 \tag{2.27}$$

The constraint given in (Equation 2.27) ensure that no points lie between H_1 and H_2. Here y_i is $+1$ for data in positive class and -1 for data in negative class. Thus the optimization problems becomes

$$\min_{\mathbf{w},b} \frac{1}{2}\mathbf{w}^T\mathbf{w} \quad \text{subject to} \quad y_i(\mathbf{w}.\mathbf{x_i} - b) \geq 1 \tag{2.28}$$

The solution to (Equation 2.28) is defined by the saddle point of Lagrange

$$\mathscr{L}(\mathbf{w}, b, \alpha) \equiv \frac{1}{2}\mathbf{w}^T\mathbf{w} - \sum_{i=1}^{N} \alpha_i y_i(\mathbf{w}.\mathbf{x_i} - b) + \sum_{i=1}^{N} \alpha_i \tag{2.29}$$

where, $\alpha_1, \alpha_2, \ldots, \alpha_N$ are Lagrange multipliers. This needs to be minimized with respect to $\mathbf{w}, b$ and maximized with respect to $\alpha_i \geq 0$. This reduces the optimization problem to its dual form ($\mathscr{L}_\mathscr{D}$) which is a quadratic problem (QP) where object function is dependent on α_i.

$$\mathscr{L}_\mathscr{D} \equiv \sum_{i=i}^{N} \alpha_i - \frac{1}{2}\sum_{i,j}^{l} \alpha_i \alpha_j y_i y_j \mathbf{x}_i.\mathbf{x}_j \tag{2.30}$$

Solution of Lagrangian multiplier α_i gives the value of $\mathbf{w}$

$$\mathbf{w} = \sum_{i=1}^{N} \alpha_i y_i \mathbf{x}_i \tag{2.31}$$

Optimal classifier hyperplane is then

$$f(x) = sgn\left(\left(\sum_{i=1}^{N} \alpha_i y_i \mathbf{x}_i\right).(\mathbf{x}) - b\right) \tag{2.32}$$

which is in the form of dot product of training vector $\mathbf{x}_i$. This hyperplane considers data to be ideal that is completely noise free, but acual data would be noisy and thus there would be data points lying between H_1 and H_2. Therefore, constrained given by (Equation 2.27) would not hold in a strict sense. This can be taken into account by using a finite valued penalty function C in our analysis which penalizes the failure of a data point to reach the correct margin. Thus the optimization problem of (Equation 2.28) is modified as:

$$\min_{\mathbf{w},b,\xi} \frac{1}{2}\mathbf{w}^T\mathbf{w} + C\sum_{i}^{N}\xi_i \quad \text{subject to} \quad y_i(\mathbf{w}^T\mathbf{x}_i - b) \geq 1 - \xi_i, \qquad 1 \leq i \leq N \tag{2.33}$$

where the new variables ξ_i are slack variables. These variables converts a hard margin problem (where no margin failure, i.e. no presence of any data points between two parallel hyperplanes) into a soft margin problem (where a little bit of data point intrusion is allowed between two hyperplane). C is a parameter that optimizes the distance between two hyperplanes and the number of occurrences of margin failures.

The constrained optimization problem in (Equation 2.33) is solved using Lagrange as before and thus reduces to:

$$\max_{\alpha} \mathscr{L}_{\mathrm{D}} \equiv \sum_i \alpha_i - \frac{1}{2}\sum_{i,j}\alpha_i\alpha_j y_i y_j \mathbf{x}_i.\mathbf{x}_j \tag{2.34}$$

$$\text{subject to} \quad 0 \leq \alpha_i \leq C, \quad \sum_i \alpha_i y_i = 0 \tag{2.35}$$

For non-linearly separable data SVM can be used to generate an optimal separating hyperplane in a high dimensional feature space after mapping the input vectors $\mathbf{x}$ to the feature space. Let the mapping

function from the input space to the high dimensional feature space be $\Phi(.)$. Define the kernel function as $K(\mathbf{x}_i,\mathbf{x}_j) = \Phi(\mathbf{x}_i).\Phi(\mathbf{x}_j)$, i.e. the kernel function in the input space is equivalent to a dot product in high dimensional space. Thus the introduction of kernel function can generalize SVMs for non-linear classifiers. This forms a case of generalized optimal hyperplane, the solution to which can be found by using the method of Lagrange multipliers as before. Let $u = \sum_{i=1}^{N} y_i\alpha_i K(\mathbf{x}_i,\mathbf{x}) - b$ defines a generalized hyperplane. Non-linearties may change the quadratic form pertaining to the solution of Lagrange's multiplier, however duality turns the objective function into a quadratic form as follows:

$$\mathscr{L}_{\mathfrak{D}} \equiv \sum_{i=i}^{N} \alpha_i - \frac{1}{2}\sum_{i,j}^{l} \alpha_i\alpha_j y_i y_j \Phi(\mathbf{x}_i).\Phi(\mathbf{x}_j) \tag{2.36}$$

$$\text{subject to} \quad 0 \leq \alpha_i \leq C, \quad \forall i \quad \text{and} \quad \sum_{i=1}^{N} \alpha_i y_i \tag{2.37}$$

where the Quadratic Problem (QP) given by (Equation 2.36) can be solved by Sequential Minimal Optimization (SMO) method. A function qualifies to be used as a Kernel function if and only if it satisfies the Mercer's condition that makes QP problem positive definite [72]. According to Mercer's condition, a transformational function Φ and an expansion

$$K(\mathbf{x},\mathbf{y}) = \sum_{i} \Phi(\mathbf{x})_i.\Phi(\mathbf{y})_i \tag{2.38}$$

if and only if, for any $g(\mathbf{x})$ such that $\int g(\mathbf{x})^2 \mathrm{d}\mathbf{x}$ is finite then

$$\int K(\mathbf{x},\mathbf{y})g(\mathbf{x})g(\mathbf{y})\mathrm{d}\mathbf{x}\mathrm{d}\mathbf{y} \geq 0 \tag{2.39}$$

This method of generating kernel functions is based on the work, [73–75]. Some mapping methods that qualify as kernel functions are polynomial, radial basis function, multilayer perceptron, Fourier series, splines, additive kernel and tensor products. In this study Gaussian radial basis kernel function $K(\mathbf{x}_i, \mathbf{x}_j) = \exp^{-\|\mathbf{x}_i - \mathbf{x}_j\|^2} / 2\sigma^2$ is used because of its capability to handle non linear relation between the class labels and attributes. Also, it is numerically less complex than other polynomial kernel functions which have more hyperparameters than radial basis kernel function.

The training of SVM is done by maximizing the objective function in the region where a solution to the dual problem exists. Only those optimal solutions are considered which satisfies Karush-Kuhn-Tucker KKT conditions:

$$\alpha_i = 0 \Leftrightarrow y_i u_i \geq 1, \tag{2.40}$$

$$0 < \alpha_i < C \Leftrightarrow y_i u_i = 1 \tag{2.41}$$

$$\alpha_i = C \Leftrightarrow y_i u_i \leq 1 \tag{2.42}$$

SMO is an algorithm used for solving quadratic programming optimization problem that is an essential part of training the SVM. It works by iteratively breaking the bigger QP problem into smallest possible ones. These sub-problems are then solved analytically by jointly optimizing two Lagrange multipliers at a time and updating the SVM with their new optimal values. Thus computationally intensive matrix operations as well as in-loop numerical QP optimizations are avoided, making it less susceptible to precision errors. This reduces the training set size as compared to the PC (standard projected con-

jugate gradient) algorithm thus improving upon the training time as well as its ease of implementation. SMO can be implemented in two major steps [72]:

1. An analytic method to solve for the two Lagrange multipliers
2. A heuristic approach for selecting two multipliers used for optimization

2.5 Training of Machine Learning Algorithms

The NN (Section 2.4.1) is trained with the following six parameters extracted from a subset of the recorded sEMG and accelerometer signals: Mean power in the frequency band 8-16Hz of the sEMG signal defined in (Equation 2.4); Power at peak frequency of the sEMG and of the accelerometer signal defined in (Equation 2.3); Peak frequency of the sEMG and of the accelerometer signal defined in (Equation 2.3); and Sample entropy of the sEMG signal defined in (Equation 2.5). The feedforward backpropagation NN architecture with its atributes, inputs and outputs for Tremor and Non-Termor events is shown in Figure 4. The NN structure is built off-line during the training phase and the parameters to which the trained NN will converge remain fixed in the testing phase. The parameters of the NN will not adapt to the patients conditions.

The training of DT (Section 2.4.2), TBAG (Section 2.4.3) and SVM (Section 2.4.4) is performed by using eight extracted parameters from smoothed sEMG and accelerometer signals: Peak frequency and Power at peak frequency of sEMG and of the accelerometer signal as in (Equation 2.4); Mean power in 8-16Hz frequency band of sEMG signal as defined in (Equation 2.4); Recurrence rate of sEMG signal as in (Equation 2.6); Sample entropy and Wavelet entropy of the sEMG signal as defined in (Equation 2.5) and (Equation 2.9) respectively.

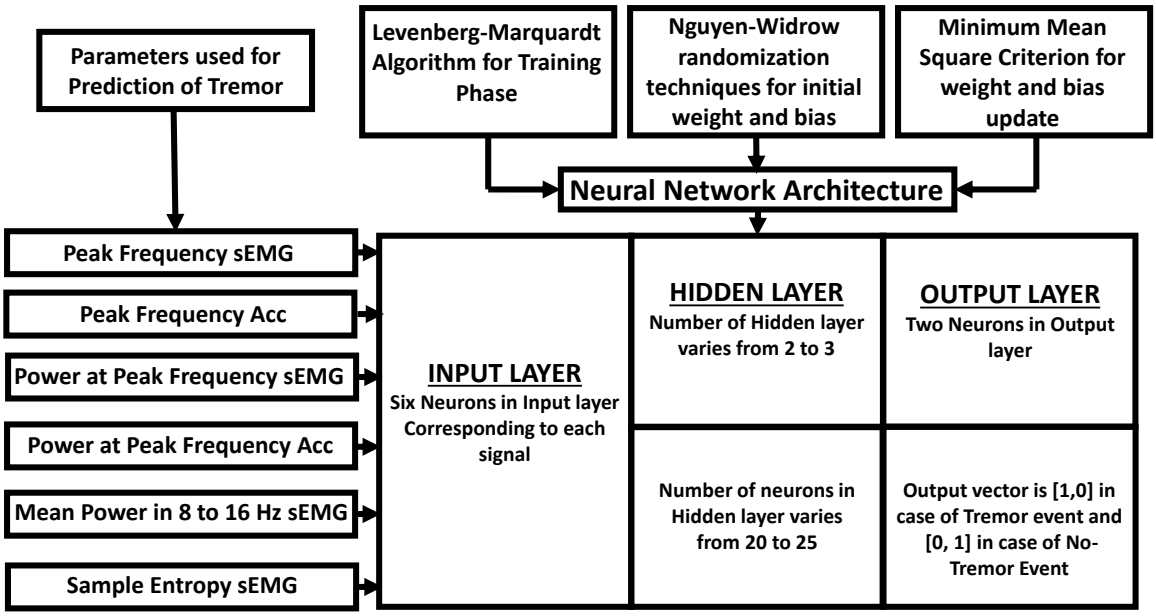

Figure 3. Feedforrward backpropagation NN arctitecture with its attributes, input and output sequence for Tremor and Non-Tremor events.

The time series of all extracted parameters from the sEMG and accelerometer signals are divided into two regions: tremor region and no-tremor region, visually separated by two sided bold arrow with name of Tremor Start Time (t_{tr}) as shown in Figure 4. In order to define an input-output vector pair, a particular time step (shown in Figure 4 by dotted bold vertical line) is chosen from the given time series. The time series points (indicated by the arrows in Figure 4) on the dotted bold vertical line forms the input vector which consists of six elements in case of NN based prediction algorithm (as shown in Figure 4) and eight elements in case of all other prediction algorithms corresponding to each extracted parameter at the particular time step. In case of NN, if the time step lies before two sided bold

arrow with name of Tremor Start Time, t_{tr} the output vector/ground truth is [0,1] otherwise it is [1,0]. For example, in Figure 4 the chosen time step lies after Tremor Start Time, t_{tr} (shown by two sided bold arrow)therefore, the output vector is [1,0]. In case of DT, TBAG and SVM, by training the algorithms to transition from Non-Tremor to Tremor at the time instant where tremor was visually detected, the prediction of tremor for some of the trials turned out to be 'delayed' by 0.5s to 2.5s; for this reason, we train the algorithms to transition from Non-Tremor to Tremor 2.5s before tremor was visually observed to capture the building up of the tremor as shown by bold dotted vertical line in Figure 4. For DT, TABG and SVM, the output vector/ground truth is '0' if time instance lies 2.5 seconds before tremor starts (tremor starting point is shown by bold dotted vertical line) and '1' otherwise as shown in Figure 4. The DT, TBAG and SVM structures are built during off-line training phase and remains fixed during testing phase. The structures of DT, TBAG and SVM will not adapt to the patients conditions during run time.

The training of NN, DT, TBAG and SVM is performed by using 9/16, 15/26, 9/18 and 16/32 sEMG/acc data sets for PD1, PD2, PD3 and PD4 respectively. All the machine learning algorithms are first trained with the original data set in order to adjust their parameters. The second phase of training is performed by using the same training set, but this time the different trials are uniformly permuted at random. This second phase serves to further tune their parameters. Finally, the so trained NN, DT, TBAG and SVM are fed with the parameters extracted from the sEMG and accelerometer signals as inputs and is used to predict the onset of tremor after the stimulation turned OFF for all trials.

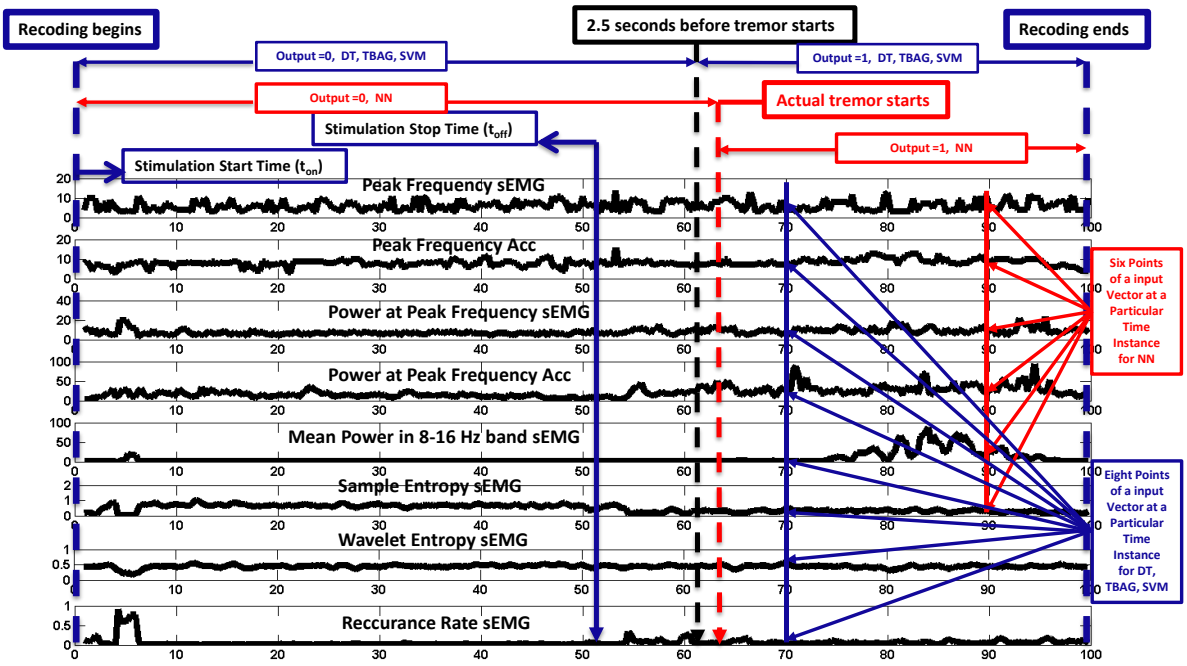

Figure 4. Inputs and output for theNN, DT, TBAG, SVM based predictor in a particular trial used for training. The bold vertical black line, set at 2.5 sec before tremor was visually observed, divides the time series of the extracted parameters into Tremor (output equals 1) and No-Tremor regions (output equals 0) in case of DT, TBAG and SVM. For NN the red bold vertical line divides the time series of the extracted parameters into Tremor (output equals 1) and No-Tremor regions (output equals 0). A time instance in the 'tremor region' is shown via a thin vertical line: the six elements of the corresponding input vector in case of NN and eight element in case of DT, TBAG and SVM are indicated by six arrows, which results in an output equal to 1.

2.6 Performance Matrices for Tremor Prediction Algorithms

To analyze the prediction performance, each considered trial is classified based on the prediction outcome as follows: let T be the total duration of a trial, t_{ON} and t_{OFF} be the times when stimulation was switched ON and OFF respectively, and t_{tr} and t_{pr} be the times when tremor was detected and predicted using different tremor prediction algorithms, during the stimulation OFF period, respectively. Trials where tremor was detected over the recorded interval after stimulation was OFF, i.e $t_{tr} < T$, are denoted as TD (Tremor Detected), while those where tremor was not detected, i.e $t_{tr} > T$, are denoted as NTD (No-Tremor Detected). In particular we classify as follows [6] (as shown in Figure 5).

For TD:

• If $[(t_{tr} > t_{pr})$ and $(t_{tr} - t_{pr}) < \max(5s, 0.5(t_{pr} - t_{OFF}))]$ or $[(t_{tr} < t_{pr})$ and $(t_{pr} - t_{tr}) < 1s]$, then the algorithm successfully predicts tremor and this outcome is classified as a *true positive (TP)*. This is a bit different from the classical TP definition, in that we require that the prediction be at most 50% of the tremor free OFF period or 5s (whichever is greater) before actual tremor reappears. This allows penalizing too early prediction outcomes.

• If $(t_{tr} > t_{pr})$ and $(t_{tr} - t_{pr}) > \max(5s, 0.5(t_{pr} - t_{OFF}))$, then the prediction is too early and the outcome is classified as *false positive (FP)*.

• If $(t_{tr} < t_{pr})$ and $(t_{pr} - t_{tr}) > 1s$, then the prediction is too late and the outcome is classified as *false negative (FN)*.

For NTD:

• If the algorithm does not predict any tremor over the entire interval $T - t_{OFF}$, then it is classified as *true negative (TN)*.

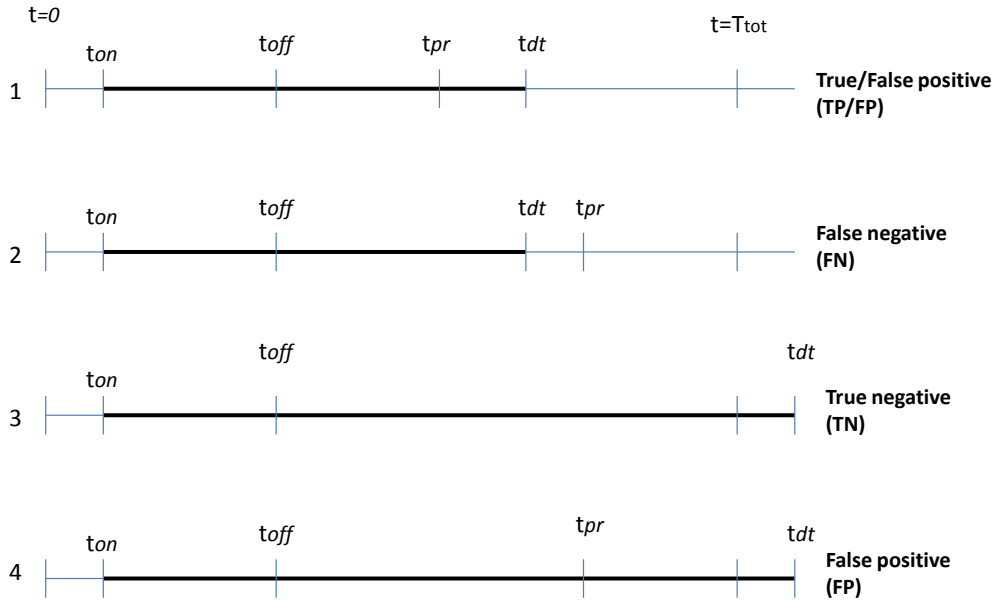

Figure 5. Timing points for events from DBS-ON time (t_{on}) to tremor detection time (t_{tr}) marked in bold line. There are 4 possible scenarios: 1,2 are TD trials, in 1 the tremor is predicted before its detection (TP/FP) and in 2 tremor is predicted after its detection (FN); 3,4 are NTD trials, in 3 tremor is not predicted over the entire interval *TN* and in 4 tremor is predicted *FP*. *Notation*: T_{tot} is the total duration of a trial, t_{on} and t_{off} are the times when DBS was switched ON and OFF respectively, t_{tr} and t_{pr} are the times when tremor was detected and predicted using the algorithm, respectively. Figure from [6].

• If the algorithm predicts tremor over the entire interval $T - t_{OFF}$, then it is classified as *false positive (FP)*.

2.6.1 Performance Evaluation.

For the algorithm to perform well, the total number of TP and TN must be maximized while minimizing FP and eliminating FN. This would achieve the maximum "tremor-free" interval when the stimulation is OFF. In order to quantify this, the following performance metrics are defined as:

$$\mathsf{Accuracy(A)} = \frac{\#TP + \#TN}{\#TP + \#TN + \#FP + \#FN}, \tag{2.43}$$

$$\mathsf{Sensitivity(S)} = \frac{\#TP}{\#TP + \#FN}, \tag{2.44}$$

$$\mathsf{FalseAlarm(FA)} = \frac{\#NTD - \#TN}{\#NTD}. \tag{2.45}$$

$$\mathsf{Mcc} = \frac{(\#TP)(\#TN) - (\#FP)(\#FN)}{\sqrt{(\#TP + \#FP)(\#TP + \#FN)(\#TN + \#FP)(\#TN + \#FN)}} \tag{2.46}$$

Mcc in (Equation 2.46) defines the Matthews correlation coefficient [76] which measures the quality of a binary classifier. The value of Mcc lies in the range of -1 to 1, where 1 represents a perfect prediction, 0 represents no better than random prediction and -1 indicates that there is no agreement between prediction and observation. The sensitivity in (Equation 2.44) should be very high (above 90%) as we do not want to miss any of the tremor events. Accuracy in (Equation 2.43), which is the ratio between the correctly predicted trials and the total number of trials, should be high (over 80%). The false alarm rate in (Equation 2.45) is proportional to the number of early tremor predictions in case of NTD trials and hence should be low (less than 20%).

Furthermore, three timing ratios are defined as:

$$R_{\mathrm{pd}} = \sum(t_{\mathrm{pr}} - t_{\mathrm{off}}) / \sum(t_{\mathrm{dt}} - t_{\mathrm{off}}), \tag{2.47}$$

$$R_{\mathrm{dt}} = \sum(t_{\mathrm{dt}} - t_{\mathrm{off}}) / \sum(t_{\mathrm{dt}} - t_{\mathrm{on}}), \tag{2.48}$$

$$R_{\mathrm{pt}} = \sum(t_{\mathrm{pr}} - t_{\mathrm{off}}) / \sum(t_{\mathrm{pr}} - t_{\mathrm{on}}), \tag{2.49}$$

Where the summation is over all the experimental trials for each patient. For those trials where tremor was not detected i.e. the exact time of tremor reappearance was not known, we considered total recording time T_{tot} as tremor detected time, t_{tr} whereas the minimum of T_{tot} and T_{fd} is taken as tremor predicted time i.e. t_{pr} = min(T_{tot}, t_{fd}). T_{fd} is a maximum duration for which stimulation remains OFF. In practical cases, T_{tot} would be the time when the stimulation switches ON automatically after some fixed duration of time in the absence of a tremor prediction. Therefore, in case of NTD trials we can consider T_{tot} - t_{off} to be the time interval when stimulation is OFF.

R_{pd} is the ratio between the predicted delay to the actual delay in tremor, hence R_{pd} provides a measure of how good the prediction is, i.e., a higher value indicates that the predicted delay t_{pr} is closer to the actual delay t_{tr} which is desirable. The other two timing ratios, R_{dt} and R_{pt}, provide a measure of the fraction of time the stimulation is OFF with an ideal predictor (which would predict the exact time when tremor re-appeared) and the one designed. To assess whether a particular patient is suited for this type of application, the R_{dt} timing ratios can be used as a measure. If the value of R_{dt} is very low, i.e., if the stimulation is OFF for just 10% of the total time, then it is better just to have DBS-ON continuously.

2.7 Results and Discussion

Based on the prediction time t_{pr} each trial was classified as TP, TN, FP and FN as described in Section 2.6. For the performance evaluation of the prediction algorithms we have calculated accuracy (A) using (Equation 2.43), sensitivity (S) using (Equation 2.44), false alarm (FA) using (Equation 2.45) and Mcc using (Equation 2.46). We have also calculated some timing ratios using t_{pr}, t_{dt}, t_{off} and t_{on} which are R_{pd} as in (Equation 2.47), R_{dt} as in (Equation 2.48), and R_{pt} as in (Equation 2.49). All the performance parameters such as A, S, FA, Mcc, R_{pd}, R_{dt} and R_{pt} are calculated for each individual patient and overall for each algorithm. The Mcc value is not calculated for the cases where TN = 0 and FN = 0 to avoid the indeterminate form. The FA is not calculated for PD3 as there is no NTD trial. The performance metrics for all algorithms in case of PD patients are summarized in following subsections.

2.7.1 Tremor prediction results for NN based algorithm

The NN based tremor predictor achieved an overall sensitivity of 91.05% by correctly predicting tremor in 86/92 trials in case of all four PD patients. It achieved S >90% in all PD patients except for PD4, where it achieved sensitivity of 88.89%. The A was found to be more than 75% individually and overall. The A is quite high which is desirable but there are 6 trials where the algorithm missed to predict the tremor event. Out of 11 NTD trials, this algorithm predicts no tremor in case of 9 trials and achieved an overall FA of 18.18%. The overall Mcc value for this algorithm is 0.37 which shows strong correlation between the predicted and actual classification for all PD patients. The R_{pd} >70% in all PD patients except PD3 (69.70%) which means that the predictor loses less than 30% of the actual delay period due to early prediction.

TABLE III

PREDICTION RESULTS FOR EACH PD PATIENT AND OVERALL USING NN BASED TREMOR PREDICTION ALGORITHM. LEGEND: N = TOTAL # OF TRIALS, A = ACCURACY IN %, S = SENSITIVITY IN %, FA = FALSE ALARM RATE IN %.

PAT #	**N**	**NTD**	**TP**	**TN**	**FP**	**FN**	**A (%)**	**S (%)**	**FA (%)**	**Mcc**	R_{pd}	R_{dt}	R_{pt}
PD1	16	2	12	0	3	1	75.00	92.31	NC	NC	71.00	34.05	25.90
PD2	26	1	19	1	4	2	76.92	90.48	00.00	0.27	80.60	35.68	28.96
PD3	18	0	14	0	3	1	77.78	93.33	NA	NC	69.70	15.45	11.75
PD4	32	8	16	8	6	2	75.00	88.89	0.00	0.51	90.20	43.38	35.77
ALL	92	11	61	9	16	6	76.09	91.05	18.18	0.37	NC	NC	NC

2.7.2 Tremor prediction results for DT based algorithm

The tremor prediction algorithm based on DT achieved an overall sensitivity of 100% by successfully predicting tremor in all trials in all PD patients. This algorithm showed an overall accuracy of 85.87%. The minimum and maximum accuracy are 81.25% and 88.89% in case of PD1 and PD3 patients respectively. In case of PD4, DT based tremor prediction algorithm achieved FA of 37.50% by predicting tremor in 3 NTD trials. This algorithm predicted tremor in 3 NTD trials and achieved an overall FA of 27.27%. The $R_{pd} >$75% in all PD patients except PD3 (71.79%), which means that the DT based predictor loses less than 25% of the actual delay period due to early prediction. This algorithm achieved an overall Mcc value of 0.57 which means the predicted classification results are strongly correlated to the actual classification results.

TABLE IV

PREDICTION RESULTS FOR EACH PD PATIENT AND OVERALL USING DT BASED TREMOR PREDICTION ALGORITHM. LEGEND: N = TOTAL # OF TRIALS, A = ACCURACY IN %, S = SENSITIVITY IN %, FA = FALSE ALARM RATE IN %.

PAT #	**N**	**NTD**	**TP**	**TN**	**FP**	**FN**	**A (%)**	**S (%)**	**FA (%)**	**Mcc**	R_{pd}	R_{dt}	R_{pt}
PD1	16	2	11	2	3	0	81.25	100.0	0.00	0.56	78.04	34.05	28.72
PD2	26	1	21	1	4	0	84.61	100.0	0.00	0.41	78.89	35.68	30.43
PD3	18	0	16	0	2	0	88.89	100.0	NA	NC	71.79	15.45	11.60
PD4	32	8	23	5	4	0	87.50	100.0	37.50	0.69	81.29	43.38	38.37
ALL	92	11	71	8	13	0	85.87	100.0	27.27	0.57	NC	NC	NC

2.7.3 Tremor prediction results for TBAG based algorithm

The TBAG algorithm predicted successfully in 91 out of 92 trials in case of 4 PD patients and achieved an overall sensitivity of 98.41%. The overall FA for this algorithm is 9.09% as this algorithm miss predicted tremor only in 1 out of 11 NTD trials. This algorithm has 19 FP trials and therefore achieved overall accuracy of 78.26%. The minimum and maximum accuracy turned out to be 88.33% and 75% in case of PD3 and PD4 patients respectively. This algorithm showed R_{pd} value $>$75% in all PD patient except PD3 where it achieved only R_{pd} value of 73.43%. Therefore this tremor prediction algorithm loses less than 25% of the actual tremor delay period due to early prediction. The overall Mcc value for this algorithm is 0.45 which clearly shows that there is strong correlation between the predicted tremor classification results and the actual tremor classification results.

TABLE V

PREDICTION RESULTS FOR EACH PD PATIENT AND OVERALL USING TBAG BASED TREMOR PREDICTION ALGORITHM. LEGEND: N = TOTAL # OF TRIALS, A = ACCURACY IN %, S = SENSITIVITY IN %, FA = FALSE ALARM RATE IN %.

PAT #	**N**	**NTD**	**TP**	**TN**	**FP**	**FN**	**A (%)**	**S (%)**	**FA (%)**	**Mcc**	R_{pd}	R_{dt}	R_{pt}
PD1	16	2	11	2	3	0	81.25	100.0	0.00	0.56	80.30	34.05	29.31
PD2	26	1	19	1	4	0	76.92	100.0	0.00	0.33	78.71	35.67	30.39
PD3	18	0	15	0	2	1	88.33	93.75	NA	NC	73.43	15.46	12.36
PD4	32	8	17	7	8	0	75.00	100.0	12.50	0.56	82.09	43.37	38.60
ALL	92	11	62	10	19	1	78.26	98.41	9.09	0.45	NC	NC	NC

2.7.4 Tremor prediction results for SVM based algorithm

For the comparison of performances of different machine learning techniques, we have also implemented SVM based tremor prediction algorithm. This algorithm could not accurately predict the 4 out of 92 trials in all PD patients and therefore achieved an overall sensitivity of 83.70%. Patient-wise, it showed sensitivity of 100.0% in PD1 with 0 miss prediction, sensitivity of 95.45.0% in PD2 with 1 miss prediction, sensitivity of 88.24% in PD3 with 2 miss prediction and sensitivity of 94.74% in PD4 with 1 miss prediction. The overall accuracy of 83.70% shows that this algorithm correctly predicts tremor in 83.87% of total PD trials. Correct tremor prediction means that the tremor was not predicted too early in case of the TD trials and no tremor was predicted in NTD trials. The FA of this tremor algorithm is 0% as this algorithm predicted no tremor for all 11 NTD trials. The R_{pd} value for PD2 and PD3 is $\sim$ 75% and for PD1 and PD4 $\sim$ 85%, therefore the loss of tremor prediction delay in case of PD2 and

PD3 is $\sim$ 25% and in case of PD1 and PD4, it is $\sim$ 15%. The overall Mcc value turns out to be 0.51 for this algorithm which shows that there is strong correlation between the predicted tremor and the actual tremor.

TABLE VI

PREDICTION RESULTS FOR EACH PD PATIENT AND OVERALL USING SVM BASED TREMOR PREDICTION ALGORITHM. LEGEND: N = TOTAL # OF TRIALS, A = ACCURACY IN %, S = SENSITIVITY IN %, FA = FALSE ALARM RATE IN %.

PAT #	**N**	**NTD**	**TP**	**TN**	**FP**	**FN**	**A (%)**	**S (%)**	**FA (%)**	**Mcc**	R_{pd}	R_{dt}	R_{pt}
PD1	16	2	12	2	2	0	87.50	100.0	0.00	0.65	85.83	34.05	30.70
PD2	26	1	21	1	3	1	84.62	95.45	0.00	0.28	77.56	35.67	31.40
PD3	18	0	15	0	1	2	88.33	88.24	NA	NC	76.42	15.46	13.52
PD4	32	8	18	8	5	1	81.25	94.74	00.0	0.61	84.80	43.37	40.54
ALL	92	11	66	11	11	4	83.70	94.29	0.00	0.51	NC	NC	NC

2.7.5 Performance comparison of different algorithms

The performance comparison of all machine learning technique based PD tremor prediction algorithms with manual tremor prediction algorithm [6] is shown in Figure 6. The exact comparison between the machine learning technique based tremor prediction algorithms with manual tremor prediction algorithm is not possible as the total time of the recording, (T_{total}) is different is these cases. In machine learning technique based tremor prediction algorithms the total time of the recording is same as the actual time of recording but in case of the manual tremor prediction algorithm the total time

of the recording is less than the actual time of the recording and this is done to increase the NTD trials. The comparison of total number of TP, TN, FP and FN trials for different prediction algorithm is shown in Figure 6. The total number of FN trials is 0 for DT based tremor prediction algorithm and manual tremor prediction algorithm. The number of FN trials is maximum in case of NN followed by SVM. The number of FN trials for TBAG is very less compared to NN, SVM. Therefore in terms of miss prediction of the tremor, the performance of TBAG is better than NN and SVM. In terms of miss tremor prediction criteria, the performance of DT based algorithm is best among all machine learning techniques and its performance is same as the manual prediction algorithm. The number of FP trials is minimum for SVM and maximum for TBAG. The number of FP trials in case of DT algorithm is more than SVM but less than all other algorithms. Therefore, the early tremor prediction is maximum in case of TBAG compared to all other algorithms. The comparison of DT and manual algorithm in terms of early prediction showed that DT performed better than the manual algorithm as the number of FP trials in case of DT is less than the manual algorithm. The total number of TP trials is maximum in case of DT algorithm and total number of TN trials is maximum in case of SVM. As the total time of recording is different in case of machine learning algorithms compared to manual algorithm, therefore the number of TP and TN trials can not be compared separately. To compare the sum of number of TP and number of TN trials, we have plotted the bar chart of A (%) with other performance metrics for different algorithms as shown in Figure 7. The A turned out to be maximum in case of DT compared to all other algorithms. The second highest A (%) is for SVM and the A (%) for NN and TBAG is comparable. The A (%) of manual algorithm is less than the DT algorithm. In term of sensitivity the performance of DT and manual algorithm is same as S (%) is 100 % for both the algorithms. The False

Alarm (FA) (%) is minimum for SVM algorithm i.e.and maximum for manual algorithm. The FA (%) in case of DT algorithm is slightly better than the manual algorithm. In term of Mcc (%) the performance of DT is best among all algorithms including manual algorithm. Overall, the performance of DT based tremor prediction algorithm is best among all prediction algorithms. Its performance is also better than the manual algorithm in all considered performance metrics. Therefore, towards the design of a fully automated closed-loop DBS system, DT based tremor prediction algorithm is suitable in case of PD patients for commercial implementation.

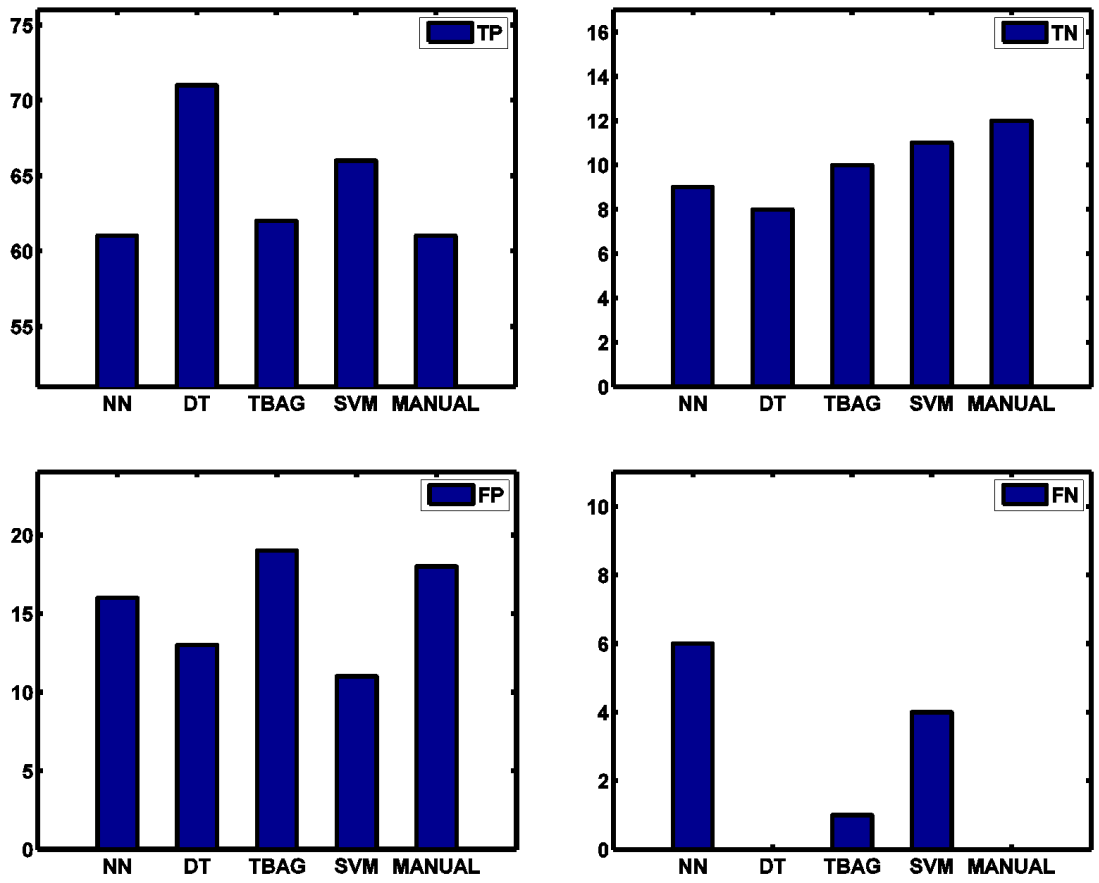

Figure 6. Performance comparison of NN, DT, TBAG and SVM based on Total # of TP, TN, FP and FN trials in all PD patients.

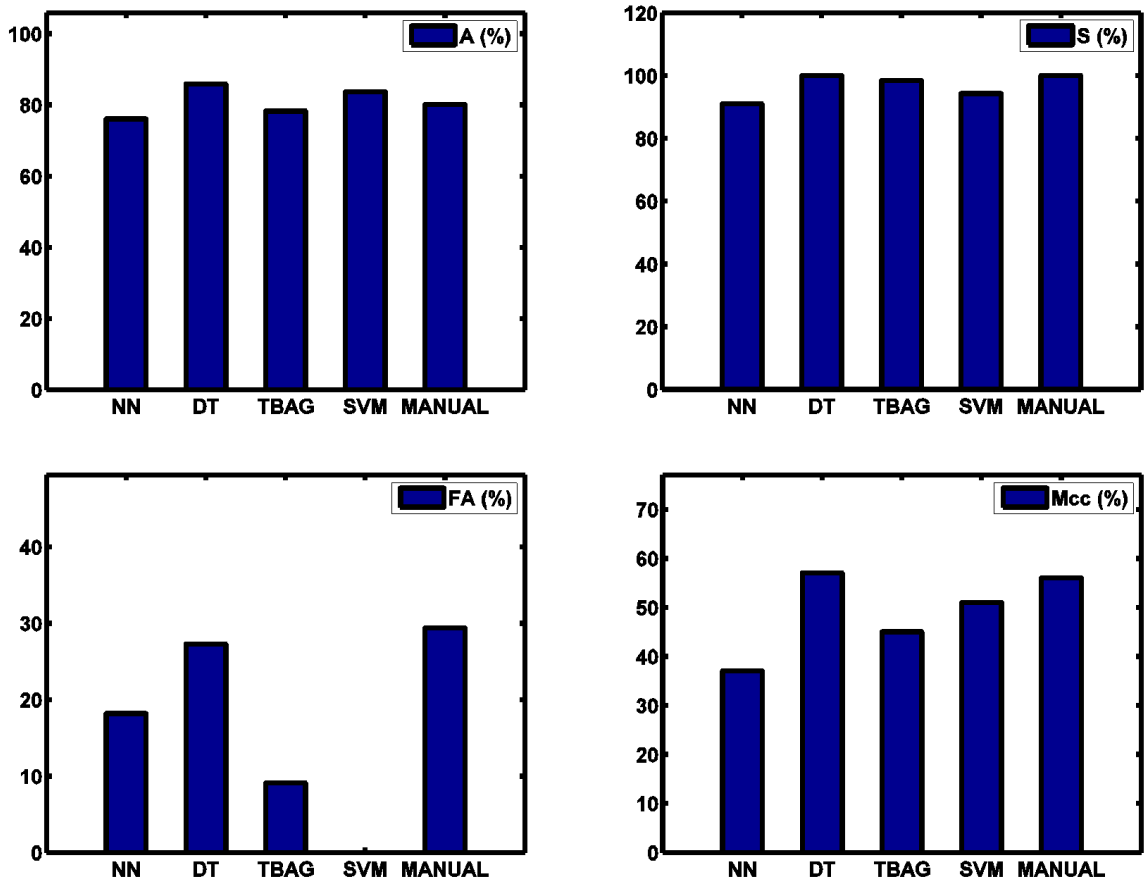

Figure 7. The overall Accuracy (A) %, Sensitivity (S) %, False alarm rate (FA) % and Mcc %. for all 4 PD patient in case of NN, DT, TBAG and SVM.

CHAPTER 3

MACHINE LEARNING TECHNIQUES BASED TREMOR PREDICTION ALGORITHMS IN ESSENTIAL TREMOR PATIENTS

Parts of this chapter appeared [2]: Shukla, P., Basu, I., and Tuninetti, D.: Towards closed-loop deep brain stimulation: Decision tree-based patients state classifier and tremor reappearance predictor. In Engineering in Medicine and Biology Society (EMBC), 2014 Annual International Conference of the IEEE, 2014

[3]: Shukla, P., Basu, I., Graupe, D., Tuninetti, D., Slavin, K. V., Metman, L. V., and Corcos, D. M.: A decision tree classifier for postural and movement conditions in essential tremor patients. In 6th International IEEE Engineering in Medicine and Biology Society (EMBC) Conference on Neural Engineering, accepted, 2013. .

3.1 Background

We already shown that the muscular and kinematic signals, measured non-invasively from the patient's symptomatic extremities by means of surface-electromyogram (sEMG) and acceleration (Acc) sensors, carry predictive information on tremor reappearance and can be successfully used for closed-loop ON-OFF DBS control [6]. In particular, our proposed entropy-based prediction algorithm uses a set of parameters extracted from sEMG and Acc signals during DBS-OFF periods. The tremor prediction of this entropy based algorithm, achieved 100% sensitivity and 85.7% accuracy for all trials. It was

also shown through statistical tests that results from algorithm differ from a random prediction outcome. Since predictor used here require manual training and setting of several parameters [6] therefore, can be deemed good enough for a proof-of-concept for closed-loop DBS based on non-invasively measured signals , but not appropriate for practical implementation.

We took a step forward in developing a fully automated tremor predictor algorithm by using various machine learning techniques such as DT, TBAG and SVM for ET patients. These techniques extract predictive information from the spectral and entropy measure of the sEMG and Acc signals. As the manual thresholding based predictor [6] algorithm for ET patients, is a two step algorithm, wherein first step is classifier stage, which classifies the patient's (posture or movement) conditions when the DBS was turned OFF, and second step is tremor prediction step. Therefore, we designed an automated ET tremor prediction algorithm using machine learning techniques which also comprises of two stages of tremor prediction: first stage is a classifier stage and second is a tremor prediction stage as shown in Figure 8. In automated tremor predictor design, the classifier stage is implemented by using DT which discriminates between movement and postural conditions in ET patients at the time DBS is switched OFF. The condition classifier is followed by tremor predictor stage which predicts the reappearance of the tremor and is implemented using DT and TBAG algorithms. At the outset, two algorithms were developed. In the first algorithm DT is used both as classifier and tremor predictor whereas in the second algorithm DT is classifier and TBAG is used as tremor predictor. Both of these algorithms failed to achieve the sensitivity of 100%, i.e., there were some tremors, that were missed by these algorithms. So we designed an automated tremor predictor for ET without having a classifier stage. Skipping of the classifier stage from tremor prediction algorithm doesn't only avoid the miss tremor prediction due to

the miss classification at the condition classifier stage but also reduces the computational complexity of tremor prediction algorithm. We have implemented three different tremor predictor algorithms based on DT, TBAG and SVM which does not consists of conditions classifier stage.

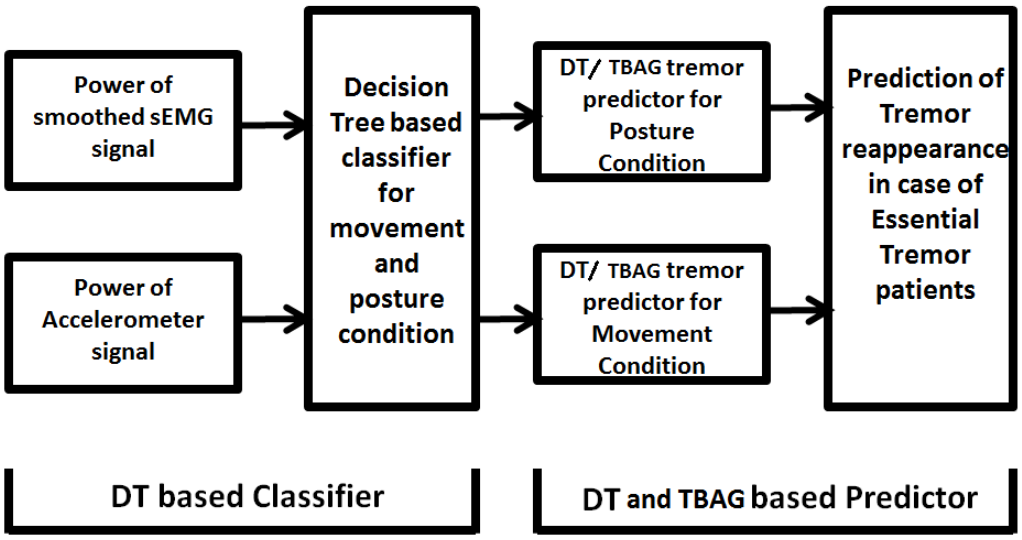

Figure 8. A DT-based classifier (to discriminate between movement and postural conditions) followed by two DT/TBAG-based tremor predictors, one for movement condition and the other for posture condition.

In this chapter we showed the implementation of tremor prediction algorithm in ET patients using five different algorithms based on machine learning techniques. The first algorithm in which, DT condition classifier is followed by DT predictor (DTC-DTP), achieved an overall accuracy of 91.11% and

sensitivity of 97.96% by successfully predicting tremor in 89 trials out of 90 trials recorded from 4 ET patients. The second algorithm is also a two stage tremor predictor algorithm, which consists of a DT classifier stage followed by TBAG predictor stage (DTC-TBAG). It successfully predicted tremor in 88 trials out of 90 trials and achieved an overall accuracy of 87.78% along with 95.56% sensitivity. The other three algorithms do not have a conditions classifier stage. The ET tremor prediction algorithm, which consists only a DT based tremor predictor showed overall accuracy of 90.00% and sensitivity of 100% . It means there is no miss prediction of tremor events. The TABAG based tremor predictor algorithm also achieved an overall sensitivity of 100% by successfully predicting tremor in all 90 tremor trials in case of 4 ET patients and the accuracy for this algorithm was turned out to be 86.67%. Finally, the SVM based tremor predictor showed an overall accuracy 84.44% along with the sensitivity of 95.45% by successful prediction of 88 trials out of 90 trials. The overall summary of all tremor prediction algorithms in case of ET patients is summarized in Table VII

Overall, the performance of DT and TBAG based tremor predictor turned out to be best among all other machine learning algorithms. As the DT algorithm is computationally less complex compare to TBAG, therefore DT based tremor predictor can be the first choice for an automated closed-loop DBS system design without making any further modification to the existing electrodes implanted in the brain.

3.2 Human Subjects

Four patients with ET, who were treated with DBS, participated in this study. Two patients came from the Movement Disorder Clinic at Rush University Medical Center and two from the University of Illinois at Chicago Hospital. Patients' details are listed in Table VIII. The protocol was approved by the IRB of both Institutions and informed consent was given by all patients. In all four patients the

TABLE VII

OVERALL TREMOR PREDICTION SUMMARY IN CASE OF FOUR ET PATIENTS FOR ALL MACHINE LEARNING TECHNIQUES BASED TREMOR PREDICTION ALGORITHMS. LEGEND: N = TOTAL # OF TRIALS, NTD = TOTAL # OF NO TREMOR DETECTED TRIALS, A = ACCURACY IN %, S = SENSITIVITY IN %, FA = FALSE ALARM RATE IN % AND MCC = MATTHEWS CORRELATION COEFFICIENT.

TREMOR PREDICTION ALGORITHM	**N**	**NTD**	**TP**	**TN**	**FP**	**FN**	**A (%)**	**S (%)**	**FA (%)**	**Mcc**
DTC-DTP	90	36	48	34	7	1	91.11	97.96	5.56	0.83
DTC-TBAG	90	36	43	36	9	2	87.78	95.56	00.00	0.76
DT	90	36	51	30	9	0	90.00	100.0	16.67	0.81
TBAG	90	36	43	35	12	0	86.67	100.0	2.78	0.76
SVM	90	36	42	34	12	2	84.44	94.45	5.56	0.71

DBS electrodes (Medtronic DBS, lead model 3389) were located in the ventral intermediate nucleus of the thalamus (VIM). The disease symptoms were controlled by a combination of stimulation and medication.

3.3 Parameter Extraction

3.3.1 Input parameters for conditions classifier

The power of the extensor sEMG and Acc signals is used as an input to the classifier. While, sEMG was recorded from both extensor and flexor muscles, visual inspection showed a higher signal-to-noise

TABLE VIII

DETAILS OF ET PATIENTS

Patient#	age	gender	DBS parameter			DBS active contacts	DBS implant	hand tested
			amplitude (Volts)	frequency (Hz)	pulse width (μs)			
ET1	64	M	2	150	90	2-C+	2002	L
ET2	67	M	1,1.4V(L,R)	130	120	1-C+(L),5-6-C+(R)	2010	L,R
ET3	51	M	2.3	185	60	9-C+	2010	R
ET4	62	F	2	185	90	0-C+	2007	R

ratio in the extensor muscle recordings and therefore we only considered the power of the extensor sEMG and Acc signals recordings in our paradigm. These powers are computed as:

$$X_{P_{sEMG}}(i) = \int_{t\in[t_p(i),t_p(i)+0.5]} x^2_{\text{sEMG}}(t)\,\mathrm{d}t \tag{3.1}$$

$$X_{P_{Acc}}(i) = \int_{t\in[t_p(i),t_p(i)+0.5]} x^2_{\text{Acc}}(t)\,\mathrm{d}t \tag{3.2}$$

where $x_{sEMG}(t)$ and $x_{\text{A}cc}(t)$ are the recorded sEMG and Acc signal, respectively, and $t_p(i) = t_0 + i\Delta$, $i = 0,1,2,3,\ldots,80$, t_0 is the postural/movement condition start time for different trials, and $\Delta = 0.025$ step size for the power sliding window as shown in Figure 9. For the classification of two conditions in ET patients, i.e., movement and posture, is based on the power of sEMG in (Equation 3.1) and on the power of Acc in (Equation 3.2). For a particular trial the input matrix is defined as

$$X(i) = [X_{P_{Acc}}(i), X_{P_{sEMG}}(i)] \tag{3.3}$$

and the corresponding output vector is defined as:

$$Y(i) = y_i \tag{3.4}$$

where $y_i = P$ for posture condition $y_i = M$ for movement condition , $i = 0, 1, \ldots, 80$.

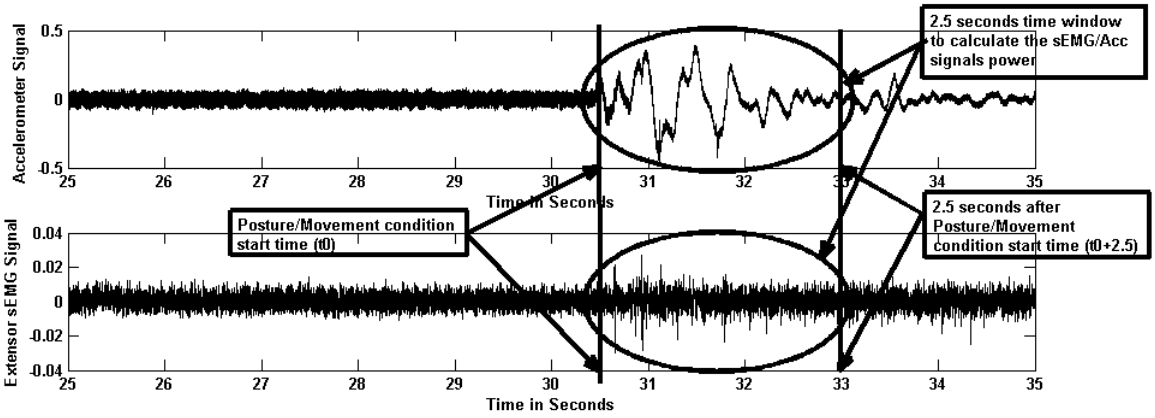

Figure 9. sEMG signal from extensor muscle and Acc signal plotted over a window of 10 seconds. A 2.5 second time window after postural/movement start time is used in power calculation.

3.3.2 Input parameters for tremor predictor algorithms

Our tremor predictor inputs are combination of spectral, entropy and recurrence measures from the *smoothed sEMG* signal obtained by averaging the raw signal over 1s windows and then sliding the window by 0.25s therefore generating a sample every 0.25s. The mean frequency F_{mean} as described

in Equation 2.1, the peak frequency F_{max} and the power at peak frequency P_{max} as in Equation 2.3, the mean power in n-th frequency band $\overline{P}_j$ as given in Equation 2.4, the sample entropy $SpEn(U,m,r)$ in Equation 2.5 and the recurrence rate R as described in Equation 2.6 are used as the input parameters for the tremor predictor algorithm. At time instant $l \in [1:4T]$, where T is an integer that equals the duration of a trial which is multiplied by 4 as we are generating parameter samples every 0.25s, the inputs is defined as:

$$X(i) = \left[F_{mean}(i), F_{max}(i), P_{max}(i), \overline{P_j}(i), SpEn(U,m,r)(i), \mathsf{R}(i)\right] \tag{3.5}$$

and the corresponding output vector is defined as:

$$Y(i) = y_i \tag{3.6}$$

where, $y_i = 0$ for *Non-Tremor* events and $y_i = 1$ for *Tremor* events. We use a sliding window processing of 0.25s; by training the algorithm to transition from *Non-Tremor* to *Tremor* at the time instant where tremor was visually detected, the prediction of tremor for some of the trials turned out to be 'delayed' by 0.5s to 2.5s; for this reason, we train the algorithm to transition from *Non-Tremor* to *Tremor* 2.5s before tremor was visually observed to capture the building up of the tremor. This procedure is depicted in Figure 10. In Figure 10 the six elements of the input vector at a particular time instance are indicated by arrows and the corresponding output is 1 (as this time instance lies in *Tremor* region).

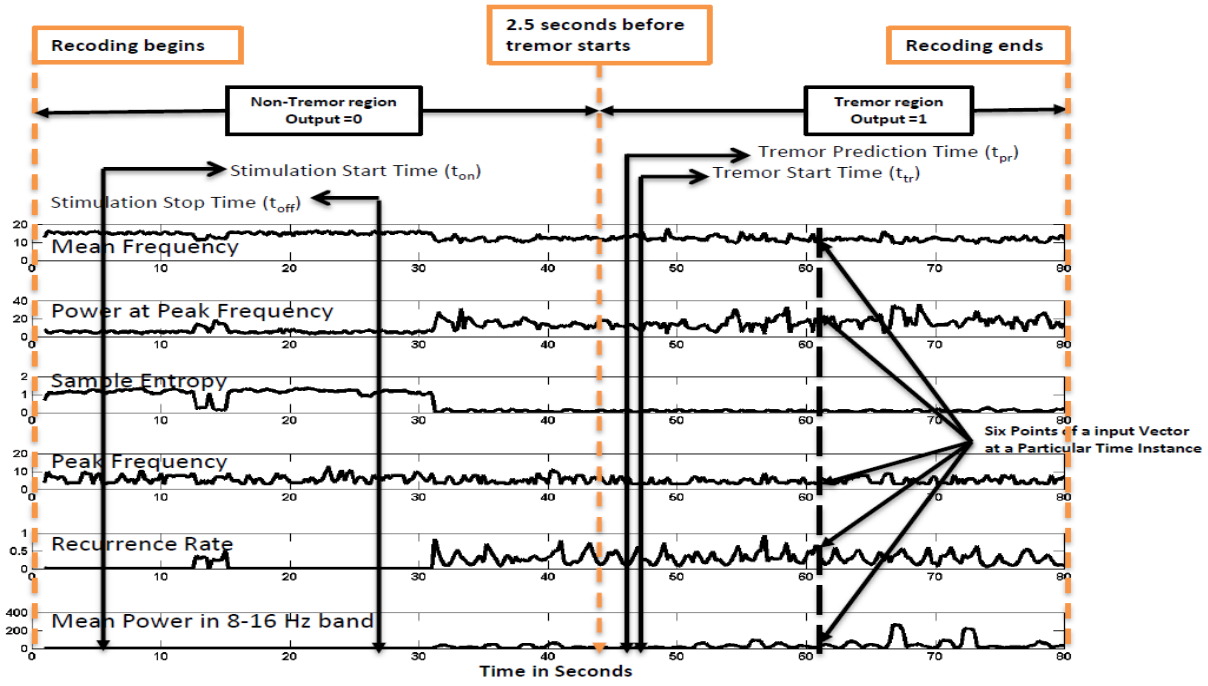

Figure 10. Inputs and output for the DTC-DTP, DTC-TBAGP, DT, TBAG and SVM based predictor in a particular trial used for training. The bold vertical line, set at 2.5 sec before tremor was visually observed, divides the time series of the extracted parameters into Tremor (output equals 1) and No-Tremor regions (output equals 0). A time instance in the 'tremor region' is shown via a thin vertical line: the six elements of the corresponding input vector are indicated by six arrows, which results in an output equal to 1.

3.4 Machine Learning Tremor Prediction Algorithms in ET Patients

In case of four ET patients, we have developed five different machine learning technique based on automated tremor prediction algorithms. These five different automated algorithms were implemented using Decision Tree (DT) as discussed in Section 2.4.2, Tree Bagger (TBAG) as described in Section 2.4.3 and Support Vector Machine (SVM) as discussed in Section 2.4.4. In the following section the performance of individual algorithms will be discussed based on the performance matrix described in Chapter 2 in Section 2.6. Finally, the performance of all algorithms will be compared to select best tremor prediction algorithm for ET patients among all tremor prediction algorithms. We also show the comparison of machine learning algorithms with the manual threshold based tremor prediction algorithm as proposed in [6]. The exact comparison between the machine learning based tremor prediction algorithms can not be performed with the manual algorithm [6], as the total time of recording T_{total} is different in case of manual algorithm with respect to all other machine learning algorithms. In manual threshold based tremor prediction algorithm the T_{total} was chosen to be less than the actual time of recording on the other hand in all machine learning technique based tremor prediction algorithms the T_{total} is considered to be the actual time of recording. The rationale behind choosing the T_{total} less than the actual time of recording to increase the number of NTD trials and to perform some statistics based on number of NTD trials.

3.5 Results and discussion

3.5.1 Tremor prediction results for DT classifier followed by DT tremor predictor algorithm

ET tremor prediction algorithm based on DT condition classifier followed by DT predictor achieved an overall sensitivity of 97.96% for four ET patients by successfully predicting tremor in 89 trials out of

90 trials. The sensitivity is 100% in all ET patients except ET4 where this algorithm missed to predict one tremor event out of 30 tremor events. The individual accuracy for ET2, ET3 and ET4 is more than 90%, as for these 3 ET patients there is only one FP tremor prediction trial. This algorithm has achieved an overall accuracy of 91.11%. The minimum and maximum accuracy are 80.00% and 94.74% in case of ET1 and ET2 (L) patients respectively. In case of ET1 this tremor prediction algorithm showed FA of 50.00% as there were only 2 NTD trials and this algorithm predicted tremor in one of those NTD trials. This algorithm predicted tremor in 2 NTD trials out of 36 NTD trials and therefore achieved an overall FA of 5.56%. The timing R_{pd} parameter is greater than 80% in all ET patients except ET1 (78.28%) which means that the DT classifier followed by DT predictor loses less than 20% of the actual delay period due to early prediction. In case of ET2 (L) and ET4 turned out to $\sim$ 95% which means loss due to early tremor prediction is very less in these two cases. This algorithm has also achieved an overall Mcc value of 0.83 which means the predicted classification results are strongly correlated with actual classification results.

3.5.2 Tremor prediction results for DT classifier followed by TBAG tremor predictor algorithm

The another two stage ET tremor prediction algorithm based on DT classifier followed by TBAG predictor successfully predicted tremor in 88 trials out of 90 trials in case of four ET patients and achieved an overall sensitivity of 95.56%. For both ET3 and ET4 patient this algorithm failed to predict tremor in one of the trials. The overall FA for this tremor prediction algorithm is 0.00% as there was no miss tremor predicted event for all 36 NTD trials. This algorithm has 9 FP trials and therefore achieved an overall accuracy of 87.78%. The minimum accuracy is turned out to be 60% in case of ET2 (R) patient where this algorithm showed 4 FP trials out of 10 trials. In all other cases accuracy is

TABLE IX

PREDICTION RESULTS FOR EACH ET PATIENT AND OVERALL USING DT CLASSIFIER FOLLOWED BY DT TREMOR PREDICTOR LEGEND: N = TOTAL # OF TRIALS, A = ACCURACY IN %, S = SENSITIVITY IN %, FA = FALSE ALARM RATE IN %.

PAT #	**N**	**NTD**	**TP**	**TN**	**FP**	**FN**	**A** (%)	**S** (%)	**FA** (%)	**Mcc**	R_{pd} (%)	R_{dt} (%)	R_{pt} (%)
ET1	15	2	11	1	3	0	80.00	100.0	50.00	0.44	78.28	43.42	37.53
ET2 (R)	10	2	7	2	1	0	90.00	100.0	00.00	0.76	81.74	40.12	35.38
ET2 (L)	19	11	7	11	1	0	94.74	100.0	00.00	0.90	96.79	53.67	52.55
ET3	16	5	11	4	1	0	93.75	100.0	20.00	0.86	89.96	46.31	43.69
ET4	30	16	12	16	1	1	93.33	92.31	00.00	0.86	94.70	57.73	57.31
ALL	90	36	48	34	7	1	91.11	97.96	5.56	0.83	NC	NC	NC

$>85\%$. This algorithm showed R_{pd} value $>85\%$ in all cases except ET2 (R) where it achieved only R_{pd} value of 64.57% therefore this ET tremor prediction algorithm losses less than 15% of the actual tremor delay period due to early prediction. The R_{pd} is low for ET2 (R) as there were many FP trials. In case of ET2 (L) and ET4 this algorithm has achieved R_{pd} value of 98.49% and 92.16% respectively. The overall Mcc value for this algorithm is 0.76 based on this value we can conclude that there is strong correlation between the predicted tremor classification results and the actual tremor classification results.

3.5.3 Tremor prediction results for DT tremor predictor algorithm

To reduce the complexity of the tremor prediction algorithm we also implemented single stage tremor prediction algorithms based on DT, TBAG and SVM machine learning techniques. In this section we discuss the result of single stage tremor predictor algorithm based on DT. This algorithm successfully predicted tremor in all 90 trials for all four ET patients and therefore achieved an overall sensitivity of

TABLE X

PREDICTION RESULTS FOR EACH ET PATIENT AND OVERALL USING DT CLASSIFIER FOLLOWED BY TBAG TREMOR PREDICTOR LEGEND: N = TOTAL # OF TRIALS, A = ACCURACY IN %, S = SENSITIVITY IN %, FA = FALSE ALARM RATE IN %.

PAT #	**N**	**NTD**	**TP**	**TN**	**FP**	**FN**	**A** (%)	**S** (%)	**FA** (%)	**Mcc**	R_{pd} (%)	R_{dt} (%)	R_{pt} (%)
ET1	15	2	12	2	1	0	93.33	100.0	00.00	0.78	88.58	43.42	40.47
ET2 (R)	10	2	4	2	4	0	60.00	100.0	00.00	0.41	64.57	40.12	30.19
ET2 (L)	19	11	7	11	1	0	94.74	100.0	00.00	0.90	98.49	53.37	52.99
ET3	16	5	9	5	1	1	87.50	100.0	00.00	0.73	86.49	46.31	44.55
ET4	30	16	11	16	2	1	90.00	91.67	00.00	0.80	92.16	57.73	56.64
ALL	90	36	43	36	9	2	87.78	95.56	00.00	0.76	NC	NC	NC

100.00%. The overall accuracy is turned out to be 90.00% which shows that this DT based single stage tremor prediction algorithm correctly predicts tremor in 90.00% of total ET trials. In our analysis correct tremor prediction means that the tremor was not predicted too early in case of the TD trials and no tremor was predicted in NTD trials. As there were only 9 FP trials and no FN trials therefore this algorithm has achieved an overall accuracy of 90.0%. The overall FA of this tremor algorithm is 16.67% as this algorithm predicted tremor in 6 NTD trials out of 36 NTD trials. The FA for ET1 is 50% as this algorithm predicted tremor in one of the 2 NTD trials and similarly in case of ET3 it predicted tremor in 2 NTD trials out of 5 NTD trials. The R_{pd} value for ET1 and ET2 (R) is 68.65% and 79.50% respectively. For ET2 (L), ET3 and ET4 R_{pd} is $> 90\%$ therefor the loss of tremor prediction delay in all these cases is $<10\%$. The overall Mcc value is turned out to be 0.76 for this algorithm which shows that there is strong correlation between the predicted tremor and the actual tremor.

TABLE XI

PREDICTION RESULTS FOR EACH ET PATIENT AND OVERALL USING DT BASED TREMOR PREDICTION ALGORITHM. LEGEND: N = TOTAL # OF TRIALS, A = ACCURACY IN %, S = SENSITIVITY IN %, FA = FALSE ALARM RATE IN %.

PAT #	**N**	**NTD**	**TP**	**TN**	**FP**	**FN**	**A** (%)	**S** (%)	**FA** (%)	**Mcc**	R_{pd} (%)	R_{dt} (%)	R_{pt} (%)
ET1	15	2	12	1	2	0	86.67	100.0	50.00	0.53	68.65	43.42	34.51
ET2 (R)	10	2	6	2	2	0	80.00	100.0	00.00	0.61	79.50	40.12	34.75
ET2 (L)	19	11	7	10	2	0	89.47	100.0	09.10	0.81	97.52	53.37	52.74
ET3	16	5	13	3	0	0	100.00	100.0	40.00	1.00	90.58	46.31	43.86
ET4	30	16	13	14	3	0	90.00	100.0	12.50	0.82	91.32	57.73	55.50
ALL	90	36	51	30	9	0	90.00	100.0	16.67	0.81	NC	NC	NC

3.5.4 Tremor prediction results for TBAG tremor predictor algorithm

The TBAG based single stage ET tremor prediction algorithm achieved an overall sensitivity of 100.0% by correctly predicting tremor in all 90 trials in case of all number ET patients. Out of total number of 90 trials 12 trials were turned out to be FP and therefore this algorithm has achieved an overall accuracy of 86.67%. The minimum accuracy is obtained for ET2 (R) as there were 4 FP trials out of 10 trials. For ET1 and ET3 the accuracy is 93.33% and 93.75% respectively. The A is quite high which is desirable. Out of 36 NTD trials TBAG based ET tremor prediction algorithm predicts no tremor in case of 35 trials and achieved an overall FA of 2.78% which is quite low as desirable. This low FA is reflected in high R_{pd} values. The R_{pd} >90% in all cases except ET2 (R) (69.78%) which means that the predictor loses less than 10% of the actual delay period due to early prediction. The overall Mcc value

for this algorithm is 0.76 which shows strong correlation between the predicted and actual classification for all 4 ET patients.

TABLE XII

PREDICTION RESULTS FOR EACH ET PATIENT AND OVERALL USING TBAG BASED TREMOR PREDICTION ALGORITHM. LEGEND: N = TOTAL # OF TRIALS, A = ACCURACY IN %, S = SENSITIVITY IN %, FA = FALSE ALARM RATE IN %.

PAT #	**N**	**NTD**	**TP**	**TN**	**FP**	**FN**	**A** (%)	**S** (%)	**FA** (%)	**Mcc**	R_{pd} (%)	R_{dt} (%)	R_{pt} (%)
ET1	15	2	13	1	1	0	93.33	100.0	50.00	0.68	90.67	43.42	41.03
ET2 (R)	10	2	4	2	4	0	60.00	100.0	00.00	0.41	69.78	40.12	31.86
ET2 (L)	19	11	6	11	2	0	89.47	100.0	00.00	0.84	97.10	53.37	52.63
ET3	16	5	10	5	1	0	93.75	100.0	00.00	0.87	94.82	46.31	44.99
ET4	30	16	10	16	4	0	86.67	100.0	00.00	0.76	92.95	57.73	55.93
ALL	90	36	43	35	12	0	86.67	100.0	2.78	0.76	NC	NC	NC

3.5.5 Tremor prediction results for SVM tremor predictor algorithm

The SVM based ET tremor predictor missed to predict 2 tremor events out of 90 trials in case of all 4 ET patients and achieved an overall sensitivity of 94.45%. Both the miss tremor prediction events happened for ET2, 1 for ET2 (R) and 1 for ET2 (L). It has achieved S of 100.0% in all ET patients except for ET2 (R) and ET2 (L) where it achieved sensitivity of 85.71% and 83.33% respectively. The maximum accuracy is turn out to 100.0% and minimum obtained accuracy by this algorithm is 70.0% in case of ET2 (R). For ET2 (L), ET3 and ET4 the accuracy is 84.21%, 87.50% and 80.00% respectively.

The A is an important criterion for the performance of tremor prediction algorithm which is quite high for this algorithm but there are 2 trials where this algorithm failed to predict tremor events. Out of 36 NTD trials this algorithm predicts no tremor in case of 34 trials and achieved an overall FA of 5.56%. This algorithm predicted tremor for 1 NTD trial of ET1 and 1 NTD of ET2 (R). The overall Mcc value for this algorithm is 0.71 which shows strong correlation between the predicted and actual classification for all 4 ET patients. The R_{pd} is very high for all 4 ET. The maximum R_{pd} achieved by this algorithm is 95.78% for ET2 (L) and minimum obtained R_{pd} value is 76.98% for ET2 (R). The tremor predictor algorithm loses less of the actual delay period due to early prediction.

TABLE XIII

PREDICTION RESULTS FOR EACH ET PATIENT AND OVERALL USING SVM BASED TREMOR PREDICTION ALGORITHM. LEGEND: N = TOTAL # OF TRIALS, A = ACCURACY IN %, S = SENSITIVITY IN %, FA = FALSE ALARM RATE IN %.

PAT #	**N**	**NTD**	**TP**	**TN**	**FP**	**FN**	**A** (%)	**S** (%)	**FA** (%)	**Mcc**	R_{pd} (%)	R_{dt} (%)	R_{pt} (%)
ET1	15	2	14	1	0	0	100.0	100.00	50.00	1.00	80.22	43.42	38.11
ET2 (R)	10	2	6	1	2	1	70.00	85.71	50.00	0.31	76.98	40.12	37.22
ET2 (L)	19	11	5	11	2	1	84.21	83.33	00.00	0.68	95.78	53.37	53.22
ET3	16	5	9	5	2	0	87.50	100.0	00.00	0.76	93.84	46.31	44.73
ET4	30	16	8	16	6	0	80.00	100.0	00.00	0.64	88.49	57.73	54.72
ALL	90	36	42	34	12	2	84.44	94.45	5.56	0.71	NC	NC	NC

3.5.6 Performance comparison for all tremor prediction algorithms

The performance comparison of all ET tremor prediction algorithms based on TP, TN, FP and FN criterion is shown in Figure 11. The exact comparison between the machine learning technique based tremor prediction algorithms with manual tremor prediction algorithm is not possible as the total time of the recording, T_{total} is different is these cases. In case of all five machine learning technique based tremor prediction algorithms the total time of the recording is same as the actual time of recording but in case of the manual tremor prediction algorithm the total time of the recording is less than the actual time of the recording and this is done to increase the NTD trials. Based on Figure 7, the total number of FN trials is 0 for single stage DT based tremor predictor algorithm and single stage TBAG tremor predictor algorithm. Also, for the manual threshold based tremor prediction algorithm the total number of FN trials is turned out to be 0. The SVM based single stage tremor prediction algorithm and two stage tremor predictor based on DT classifier followed by TBAG predictor (DTC-TBAGP) obtained 2 FN trials. The DT classifier followed by DT predictor (DTC-DTP) algorithm has only 1 FN trial. The total number of FN is maximum in case of DTC-TBAGP and SVM algorithms and minimum is case of single stage DT and TBAG based tremor prediction algorithms. Using the FN performance criterion we can conclude that DT and TBAG based single stage tremor predictor performed better than DTC-DTP, DTC-TBAGP and SVM algorithms. Finally, based on FN criteria the performance of DT and TBAG is same as the manual threshold based tremor prediction algorithm. The DTC-DTP algorithm showed the minimum number of FP trials among all prediction algorithms. Among all machine learning technique based algorithms the number of FP trials is maximum is case of TBAG and SVM algorithms but is less than the total number of FP obtained by manual algorithm. Therefore, the early tremor prediction is

maximum in case of manual algorithm compare to all other algorithms. As the total time of recording, T_{total} is different in case of machine learning technique based algorithms compare to manual threshold based algorithm therefore we will not make a comparison of total number of TP and total number of TN trials in case of machine learning technique based algorithms with manual threshold based algorithm. Among all machine learning technique based tremor prediction algorithms the single stage DT based tremor predictor algorithm achieved maximum number of TP trials and SVM based single stage tremor predictor algorithm has achieved minimum number of TP trials. The total number of TN is maximum for DTC-TBAGP algorithm and minimum for DT based single stage tremor predictor, therefore we can conclude that for NTD trials the performance of DTC-TBAGP algorithm is best among all machine learning technique based algorithms.

To compare the sum of number of TP and number of TN trials, we have plotted the bar chart of A (%) with other performance metrics such as S (%), FA (%) and Mcc (%) for all machine learning technique based algorithms and manual algorithm in Figure 12.The maximum A (%) is achieved by DTC-DTP algorithm which in turn out to be slightly higher than the single stage DT based tremor prediction algorithm. Similarly, A (%) of DTC-TBAGP is slightly higher than that of single stage TBAG algorithm therefore we can conclude that the two stage prediction algorithms achieved higher A (%) compared to the single stage predictor algorithms. The least accuracy is obtained by SVM based single stage tremor prediction algorithm. The A (%) for manual algorithm is slightly higher than SVM based tremor prediction algorithm but lower than all other algorithms. As A(%) is proportional to the sum of total number of TP and total number of TN trials therefore it is least for SVM based single stage algorithm followed by manual threshold based algorithm. The S (%) bar chart in Figure 12 shows that

single stage DT predictor, single stage TBAG predictor and manual threshold based predictor achieved an overall sensitivity of 100%. The sensitivity is minimum for SVM based tremor prediction algorithm. Among all machine learning techniques based algorithms the minimum FA (%) is achieved by single stage TBAG predictor algorithm and maximum FA (%) is achieved by single stage DT tremor predictor algorithm. The FA (%) for manual algorithm is lower than the single stage DT tremor predictor but higher than all other algorithms. In term of Mcc (%) the performance of DTC-DTP is best among all algorithms including manual algorithm as shown in Figure 12.

Overall the performance of single stage TBAG algorithm is best among all other ET tremor prediction algorithms as it achieved 100% sensitivity with high accuracy and least false alarm rate. The performance of single stage TBAG algorithm is quite comparable to single stage DT algorithm as it has also achieved the sensitivity of 100% with high accuracy. If we compare the performance of single stage TBAG algorithm with single stage DT algorithm we will find that the the sensitivity for both the algorithm is same, the accuracy for single stage DT tremor prediction algorithm is slightly higher than the single stage TBAG tremor prediction algorithm but there is significant difference between the FA of both the algorithm. The FA (%) of single stage DT algorithm is 2.78% with only 1 FP trial and FA (%) of single stage TBAG algorithm is 16.67 with 9 FP trials. The single stage TBAG tremor prediction algorithm is computationally more complex than the single stage DT tremor prediction algorithm. The performance of single stage TBAG tremor prediction algorithm is better than the manual threshold based tremor prediction algorithm in term of A, S, FA and Mcc values. Now, if we compare the performance of single stage DT tremor prediction algorithm with manual algorithm we can conclude that DT based single stage tremor prediction algorithm has performed better than the manual algorithm is term

of A and Mcc. Only the FA in case of single stage DT algorithm is higher than the manual algorithm it may be due to the fact that the single stage DT algorithm does not have conditions classifier. Finally based on the performance of various machine learning technique algorithms we can conclude that a fully automated closed-loop DBS system can be designed based on single stage DT and single stage TBAG tremor prediction algorithms in case of ET patients. As the complexity of TBAG algorithms is higher than the DT algorithm therefore DT based single stage tremor predictor is most suitable for commercial implementation in case of ET patients.

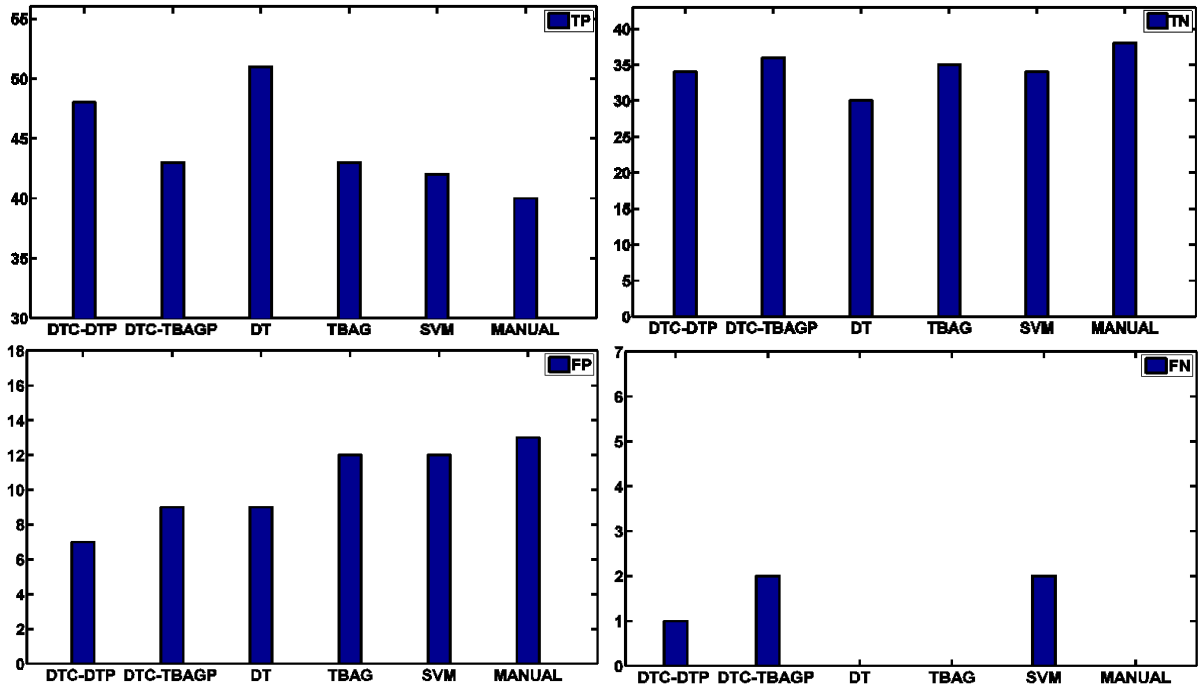

Figure 11. Performance comparison of DTC-DTP (Decision Tree Classifier followed by Decision Tree Predictor), DTC-TBAGP (Decision Tree Classifier followed by Tree Bagger Predictor), DT, TBAG and SVM tremor prediction algorithms based on Total # of TP, TN, FP and FN trials in all PD patients.

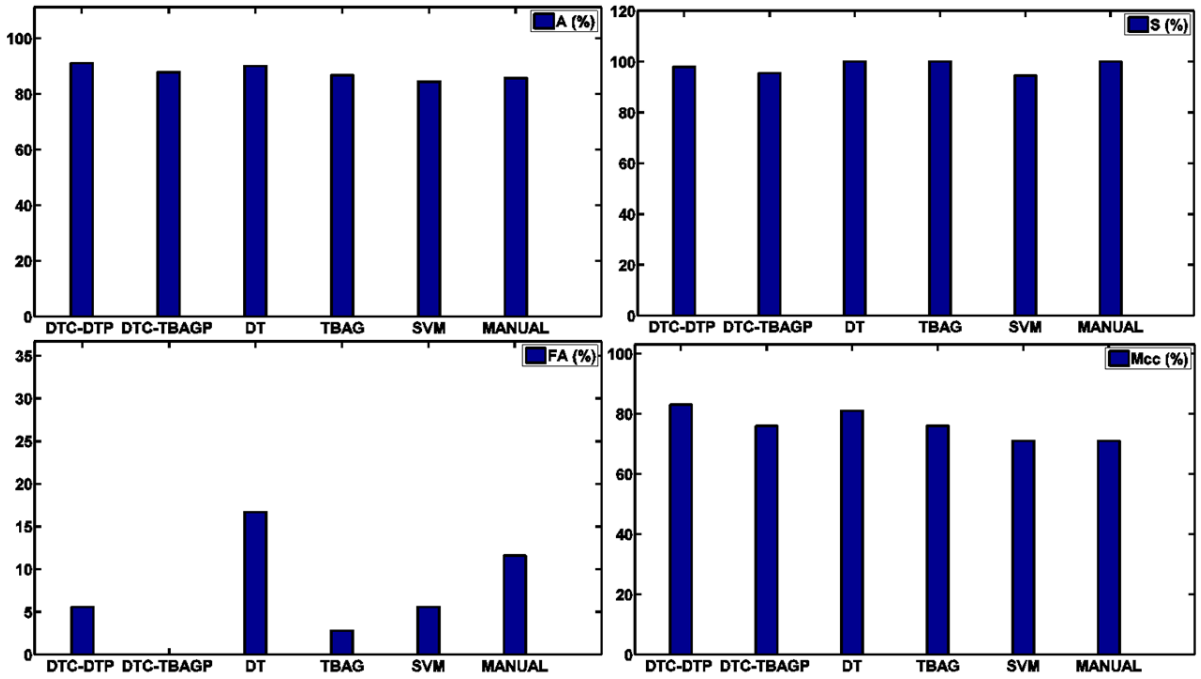

Figure 12. The overall Accuracy (A) %, Sensitivity (S) %, False alarm rate (FA) % and Mcc %. for all 4 ET patient in case of DTC-DTP (Decision Tree Classifier followed by Decision Tree Predictor), DTC-TBAGP (Decision Tree Classifier followed by Tree Bagger Predictor), DT, TBAG and SVM

CHAPTER 4

STOCHASTIC MODELING OF NEURONAL FIRING ACTIVITY IN THE THALAMUS OF ESSENTIAL TREMOR AND THE SUBTHALAMIC NUCLEUS OF PARKINSON'S DISEASE PATIENTS.

A part of this chapter appeared [4]: Shukla, P., Basu, I., Graupe, D., Tuninetti, D., and Slavin, K. V.: On modeling the neuronal activity in movement disorder patients by using the orntein uhlenbeck process. In Engineering in Medicine and Biology Society (EMBC), 2014 Annual International Conference of the IEEE, 2014.

[5]: Shukla, P., Basu, I., Tuninetti, D., Graupe, D., and Slavin, K.: Stochastic modeling of neuronal activity in the thalamus of essential tremor and the subthalamic nucleus of parkinsons disease patients. Biological Cybernetics, submitted.

4.1 Background

Mathematical modeling of neuronal activity of GPi/STN (in PD) and VIM (in ET) can provide some understanding of the underlying mechanism of DBS and the pathophysiology of PD and ET. The time variations in extracted parameters of the predictive mathematical model for neuronal activity of GPi/STN and VIM can be used to predict the reappearance of the disease symptoms in case of PD and ET patients when the DBS stimulation is turned off. Moreover, the model parameters can be used to predict the effects of the DBS parameters and therefore can be used in optimizing DBS parameters [10, 11, 77]. The next generation closed-loop, adaptive DBS system can be designed based on good

predictive mathematical model which captures the system dynamics of GPi/STN and VIM in case of PD and ET patients respectively. Mathematical modeling of neuronal activity in GPi/STN and VIM can be performed by either deterministic or stochastic neuronal models. The deterministic neuronal modeling technique requires the detailed interaction among all the neurons at microscopic level, which makes it parameter extensive and also parameter specific [78]. On the other hand, macroscopic stochastic modeling of neuronal activity does not require the microscopic detailed knowledge of all possible interactions between neurons and thus needs less parameters for modeling [79].

In this work, our main goal is to derive macroscopic stochastic models for the neuronal spiking activity in the STN and the VIM, based on actual patient data obtained during micro-electrode recording obtained during DBS surgery. Here, we will use the Ornstein Uhlenbeck Process (OUP) whose parameters are extracted using the Fortet Integral Equation (FIE) as described in [14, 15] to capture the dynamics of the neuronal spiking activities in the STN of PD patients and in the VIM of ET patients. Furthermore, we aim to statistically compare and evaluate the performance of OUP-FIE method with other stochastic process such as the Poisson Process (PP), the Brownian Motion (BM) and the OUP whose parameters are extracted using moments method as described in [16] which were previously discussed, but in the context of limited data sets [17]. Such mathematical modeling of micro-electrode recordings may provide understanding of neuronal activity in these parts of the brain [20]. This knowledge can potentially be helpful when designing improved closed-loop control of DBS and predicting its behavior.

Neurons communicate with one another through electrical impulses that come in the form of action potentials generated when the neuronal membrane voltage exceeds a certain threshold. Various

stochastic processes have been proposed to model the randomness of the inter-spike interval (ISI), the time interval between the two consecutive neuronal firings. One of the earliest studies used the Poisson Process (PP) [80, 81] which is a simple stochastic process that counts the number of events and the time when these events occur in a given interval of time. The inter-arrival time in the PP has a negative exponential distribution described by a single parameter, the average number of events per unit time. Unfortunately, the PP does not capture the mechanism of the spike generation [82]. Various stochastic processes based on the integrate-and-fire model have been proposed to capture the mechanism behind the spike generation [83, 84]. The Brownian Motion (BM) with positive drift which has the Inverse Gaussian (IG) distribution as the underlying distribution [82] was the first stochastic process applied to the leak-less integrate-and-fire neuronal model. The BM provides a closed form solution to the ISI distribution. Unfortunately, BM does not model the exponential decay between two subsequent neuronal spikes. Other approaches to model neuronal spiking include point processes [85, 86]. These methods however require a large number of parameters for modeling the ISI [87]. To avoid the complexities and shortcomings of previous methods, in the present work we propose to use the Ornstein-Uhlenbeck Process (OUP) to model the neuronal activity [88].

The OUP is a modified Wiener Process, derived via a leaky integration assumption that can generate irregular neuronal spike activity [89, 90]. This process accounts for the spike generation mechanism and the change in membrane potential between two firing events, which were ignored in oversimplified stochastic processes such as PP and BM [80]. OUP only needs two parameters, together with three free parameters, which reduces the computational complexity compared to generalized point processes. In [17] and [18], we used the OUP to model the spike activity recorded from the STN of a PD patient

and from the VIM of an ET patient, respectively. Although the results were promising, the statistical significance of the proposed method remained unclear due to a limited data set. Moreover, in our previous studies [17, 18], the two OUP parameters were estimated based on the first two moments of the first passage time (FPT) distribution, the time distribution when the neuron membrane potential exceeds a certain threshold starting from some initial resting potential [16], and hence does not take the entire distribution into consideration.

This segment of this thesis includes the following: We present data from a large number of patients; specifically, we used 19 VIM recordings from ET patients and 10 STN recordings from PD patients. We estimate the OUP parameters from the measured ISI distribution by using the minimization of maximum Kolmogorov-Smirnov statistical error of the FPT distribution function using the FIE [14, 15]. By using a directional Wilcoxon signed rank test [19], we compare the results obtained from the OUP whose parameters were obtained using FIE method with the OUP in which the model parameters were extracted using the moments method based on the Ricciardi's approach [16] as in [17, 18]. Finally, we show that the model parameter estimated based on the FIE method gives overall better results compared to the moment method, while both OUP-based models provide a better fit for the measured ISI than the simplistic stochastic models like PP and BM.

This chapter is organized as follows: Section 4.2 describes the data set used for modeling the ISI distribution followed by the introduction of OUP and the parameter estimation in the FPT problem. Section 4.3 outlines the mathematical foundations of the four models considered in the paper, namely OUP with its Moment-based parameter identification method, OUP with FIE parameter identification, the PP and BM models. Section 4 presents the modeling results of the ISI distributions by using the

various models. It also includes the statistical analysis performed on the results to prove its statistical significance. Finally, conclusions of the present work are highlighted in Section 4.5.

4.2 Data Set

We obtained electrophysiological datasets from the University of Illinois at Chicago (UIC) and the Rush University in Chicago, with respective IRB approvals. The data were recorded pre-stimulation, during stimulation and post stimulation at the time of DBS surgery for ET patients (target VIM) and PD patients (target STN). During the DBS-implant procedure, micro-electrode recordings (MER) were routinely performed by the DBS team to precisely locate the target for DBS lead placement by assessing neuronal spiking activity at different depths along the pre-calculated trajectory that leads to the intended target. In both institutions, MER was performed using platinum-iridium tipped microelectrodes (microTargeting, FHC Inc, Bowdoinham, ME) connected to either Guideline 3000A system (Axon Instruments, Union City, CA) in Rush University, or NeuroNav and MicroGuide MER systems (Alpha Omega Engineering, Nazereth-llit, Israel) in UIC. With the Guideline system, the data were sampled at 20 KHz [91] and recorded without any test stimulation. With the NeuroNav/MicroGuide system, the data were sampled at 25 KHz and the dataset included MER before and during intraoperative stimulation at 130 Hz and 160 Hz [92, 93].

MER is used to analyze the high-frequency activity of a single neuron in the form of electrical potential differences across the cell membrane of the neuron. With the extracellular recording approach used in clinical practice, there are unavoidable sources of electrical noise such as background noise due to cellular activity of neighboring neurons and measurement noise. Another source of noise comes in the form of stimulus artifact that is present in MER data when a train of high-frequency DBS pulses is

applied through the macro contact of the microelectrode assembly. These stimulus artifacts are removed from the signal by subtracting the artifact template from the recorded signal to recover the neuronal activity; however, since the stimulus artifacts are large enough to saturate the signal amplification, it is not possible to determine any spiking activity embedded inside the artifact. Data recorded before and after stimulus artifact appear similar. The stimulus artifact look similar to pre- and post-stimulation recordings. Finally, the timestamps of spike occurrences were detected by setting a threshold. The physician performing the MER determined the threshold based on visual inspection of the recorded spikes as shown in Figure 13. The difference between the two consecutive timestamps is the ISI that is required for parameter extraction for the OUP, IG and PP.

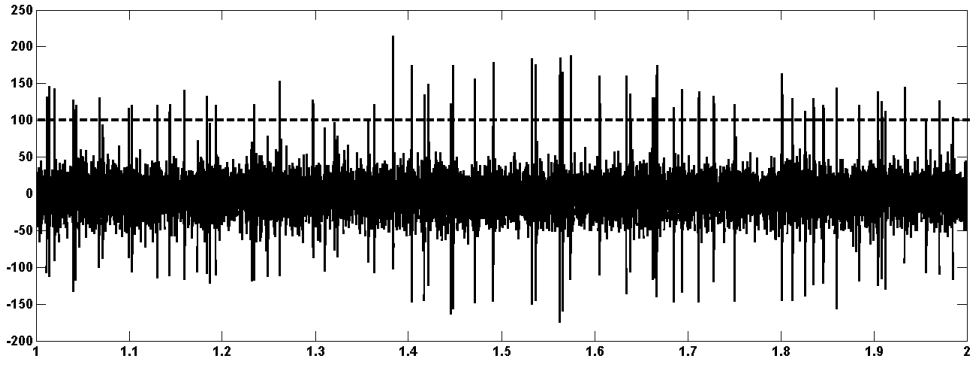

Figure 13. Sample of recorded data set over a window of 1 sec with spike thresholding. Dotted line = Threshold.

4.3 The First Passage Time problem using the OUP model

The neurons generate electrical impulses called action potentials or spikes when the membrane voltage exceeds a certain threshold to communicate with each other. After the generation of an action potential, the membrane potential resets to the resting potential and, for modeling purpose, this value is set to be zero in our analysis. The spike timestamps form a renewal random process, related to the First Passage Time problem (FPT). In the rest of the section, we first discuss the OUP model, followed by a discussion on the FPT problem, and finally the OUP-FPT parameter extraction by using the Ricciardi's moment method and FIE method.

4.3.1 The Ornstein Uhlenbeck Process (OUP)

The OUP is a modified Wiener Process X_t, which can be thought as the continuous time analogue of the discrete time AR(1) process. It is based on the Langevin standard differential equation (SDE) [94,95] that can be solved by using Ito calculus [88,96] to give

$$X_t = \mu\tau + (x_0 - \mu\tau)e^{-t/\tau} + \sigma \int_0^t e^{-(t-s)/\tau} dW_s \tag{4.1}$$

where $\tau > 0$ is a time constant, $\mu\tau > 0$ is equilibrium mean value, $\sigma > 0$ is diffusion coefficient or the degree of volatility around the mean, W_t is a standard Wiener Process, and x_0 the initial condition of the process. The probability density function of X_t in (Equation 4.1) is given by [17]

$$f_{OU}(x,t;x_0) = \sqrt{\frac{1}{\pi[1-e^{-2t/\tau}]\sigma^2\tau}} \cdot \exp\left\{ \frac{-[(x-\mu\tau)-(x_0-\mu\tau)e^{-t/\tau}]^2}{[1-e^{-2t/\tau}]\sigma^2\tau} \right\}. \tag{4.2}$$

Physiologically, μ and τ represent the input to the model neuron in terms of excitatory and inhibitory Possion's trains of impulses. For a more detailed mathematical description, we refer the reader to [17] and references therein.

4.3.2 The FPT Problem and OUP Parameter Extraction

An input impulse to a neuron generates a spike only when its membrane potential X_t exceeds a threshold y_0 (assumed constant) and then it resets to its resting potential x_0. Therefore neuron's activity between two consecutive neuronal firing can be described as FPT problem of OUP [97]. The OUP-FPT random variable T is defined as the time t after time 0 at which X_t first hits a constant threshold, y_0 starting from the initial value $x_0 < y_0$. Mathematically, T is defined as

$$T = \inf\{t \geq 0 : X_t \geq y_0,\ X_t|_{t=0} = x_0 < y_0\}. \tag{4.3}$$

The probability density function of T, formally defined as

$$f_T(t;x_0,y_0) = \frac{\partial}{\partial t}\mathbb{P}[T \leq t], \tag{4.4}$$

is not known in closed form, but its moment generating function is [16]. Based on the moment generating function, all the moments of T can be calculated as described in [17, 97]. The FPT density function in (Equation 4.4) is defined in terms of five parameters: μ, σ, τ, x_0 and y_0 of which the last three parameters (membrane time constant τ, membrane resting potential x_0 and constant threshold voltage y_0) are intrinsic parameters of the neurons and can take biologically plausible values. The first two parame-

ters (equilibrium mean value μ and degree of volatility around the mean σ) are input parameters of the model responsible for the neuronal activity and can be extracted from the ISI distribution.

In this work, the OUP parameter estimation is performed based on two methods: (1) the Ricciardi moment method, where the first two moments of the FPT are equated to the first two moments estimated from the data [17], and (2) the Fortet Integral Equation, where two different expressions of the probability density function for the dimensionless form of OUP are equated.

4.3.2.1 The Ricciardi's Moment Method (RMM).

Several methods are known to obtain numerically the approximate moment generating function of the OUP [17, 97]. In this work we use the explicit expression for the first two moments

$$\tau^2 M_n(\eta|\xi) = m_n(\eta|\xi) = \mathbb{E}[T^n]$$

as described in [16] given by

$$M_1(\eta|\xi) = \phi_1(\eta) - \phi_2(\xi) \tag{4.5a}$$

$$M_2(\eta|\xi) = 2\phi_1^2(\eta) - \phi_2(\eta) - 2\phi_1(\eta)\phi_1(\xi) + \phi_2(\xi) \tag{4.5b}$$

$$\xi = \sqrt{\frac{2}{\sigma^2\tau}}(x_0 - \mu\tau), \tag{4.5c}$$

$$\eta = \sqrt{\frac{2}{\sigma^2\tau}}(y_0 - \mu\tau) \tag{4.5d}$$

where $\eta \geq \xi$ and where the $\phi_k(z)$, $k = 1,2$ are given by

$$\phi_k(z) = \frac{k}{2^k} \sum_{n=1}^{\infty} \frac{(\sqrt{2}z)^n}{n!} \Gamma\left(\frac{n}{2}\right) \rho_n^{(k)} \tag{4.5e}$$

$$\rho_n^{(1)} = 1, \tag{4.5f}$$

$$\rho_n^{(2)} = \psi(n/2) - \psi(1) \tag{4.5g}$$

Here $\Gamma(y)$ and $\psi(y)$ are the gamma and digamma functions, respectively [16]. To obtain the estimates of $\hat{\mu}$ and $\hat{\sigma}$, we first solve for ξ in (Equation 4.5c) and η in (Equation 4.5d) from

$$\tau M_1(\eta|\xi) = m_1 \tag{4.6a}$$

$$\tau^2 M_2(\eta|\xi) = m_2 \tag{4.6b}$$

where m_1 and m_2 are the first two moments obtained from the recorded FPT distribution, and then we inverse the relationship in (Equation 4.5c) and (Equation 4.5d) to obtain [98]

$$\hat{\mu} = \frac{1}{\tau} \frac{\hat{\eta} x_0 - \hat{\xi} y_0}{\hat{\eta} - \hat{\xi}} \tag{4.7a}$$

$$\hat{\sigma} = \sqrt{\frac{2}{\tau}} \frac{y_0 - x_0}{\hat{\eta} - \hat{\xi}} \tag{4.7b}$$

where τ, x_0 and y_0 are neuronal membrane potential, resting potential and firing threshold respectively.

4.3.2.2 The Fourtet Integral Equation (FIE) Method

In this method we considered the dimensionless form of the OUP-FPT problem to estimate the parameters μ and σ of the model. The corresponding probability for the dimensionless OUP-FPT problem, in the form of standard normal distribution function $\Phi(\cdot)$ is given by [15]:

$$P[Y_s > 1] = \Phi\left(\frac{\alpha(1-e^{-s})-1}{\beta\sqrt{1-e^{-2s}}}\right) \tag{4.8}$$

where Y_s, α, β and s are defined as [15]:

$$Y_s = \frac{X_{s\tau}}{y_0} \tag{4.9a}$$

$$\alpha = \frac{\mu\tau}{y_0} \tag{4.9b}$$

$$\beta = \frac{\sigma}{y_0}\sqrt{\frac{\tau}{2}} \tag{4.9c}$$

$$s = \frac{t}{\tau} \tag{4.9d}$$

This probability can also be calculated using transition integral equation [15].

$$P[Y_s > 1] = \int_0^s f(u)\Phi\left(\frac{\alpha-1}{\beta}\frac{1-e^{-(s-u)}}{\sqrt{1-e^{-2(s-u)}}}\right)du \tag{4.10}$$

where $f_{ou}(x, s\tau; x_0)$ is probability density function of X_t for $s = t/\tau$. The integral equation obtained after equating the right hand side of (Equation 4.8) and (Equation 4.10) is [15]:

$$\Phi\left(\frac{\alpha(1-e^{-s})-1}{\sqrt{1-e^{-2s}}\beta}\right)=\int_0^s f(u)\Phi\left(\frac{\alpha-1}{\beta}\frac{1-e^{-(s-u)}}{\sqrt{1-e^{-(s-u)}}}\right)du \tag{4.11}$$

The estimate $\hat{\alpha}$, $\hat{\beta}$ of the parameters α, β is based on the minimization of maximum Kolmogorov-Smirnov statistical error calculated for the integral equation (Equation 4.11) [15]:

$$(\hat{\alpha},\hat{\beta})=\arg\min_{\alpha,\beta}\max_{s\in\mathbb{R}_+}|RHS_{est}(s)-LHS(s)| \tag{4.12}$$

where, RHS and LHS are left and the right hand side of the equation (Equation 4.11), and consists of ordered independent normalized FPT events t/τ, such that $s_1 \leq s_2 \leq s_3 \leq s_4 \leq.....\leq s_N$. Based on these ordered samples of s, the $LHS(s)$ can easily be calculated as described in (Equation 4.11) but to solve for $RHS_{est}(s)$ we used the approximate solution [15] for the integral equation:

$$RHS_{est}(s)\approx\sum_{i=1}^{\max\{n:s_n\leq s\}}\Phi\left(\frac{\alpha-1}{\beta}\sqrt{\frac{1-e^{-(s-s_i)}}{1+e^{-(s-s_i)}}}\right) \tag{4.13}$$

The estimates of the parameters $\hat{\mu}$ and $\hat{\sigma}$ of dimensionless OUP is obtained by inverting the relationship in (Equation 4.9b), (Equation 4.9c) to obtain [15]:

$$\hat{\mu}_{fie}=\frac{\hat{\alpha}y_0}{\tau} \tag{4.14a}$$

$$\hat{\sigma}_{fie}=\frac{\hat{\beta}y_0}{\sqrt{2\tau}} \tag{4.14b}$$

4.3.3 Other Commonly Used Stochastic Processes

The ISI distribution has also been modeled as a negative exponential distribution, arising from a PP, or an inverse Gaussian (IG) distribution, resulting from BM with positive drift [80, 81]. We compare the performance of the proposed OUP model with those of the PP and BM.

4.3.3.1 The Poisson Process (PP).

When the spiking activity is modeled as a PP, the resulting ISI has a Negative Exponential (NE) distribution.

$$f_{PP}(x;\mu_{pp}) = \frac{1}{\mu_{pp}} e^{-x/\mu_{pp}}\ 1_{[x\geq 0]} \tag{4.15}$$

where μ_{pp} is the mean value of the ISI [17]. μ_{pp} is a parameter of the distribution, which happens to be its expected value too. In the following, $\hat{\mu}_{pp}$ will denote the the maximum likelihood (ML) estimate of μ_{pp}, which can be calculated as the sample mean of the measured ISI in (Equation 4.15).

4.3.3.2 The Brownian Motion (BM).

When the spiking activity is modeled as a BM with positive drift, the resulting ISI has an inverse Gaussian (IG) distribution.

$$f_{BM}(x;\mu_{bm},\lambda_{bm}) = \sqrt{\frac{\lambda_{bm}}{2\pi x^3}}\ \exp\left\{\frac{-\lambda_{bm}(x-\mu_{bm})^2}{2(\mu_{bm})^2 x}\right\} 1_{[x\geq 0]} \tag{4.16}$$

where μ_{bm} is the mean and $\frac{{\mu_{bm}}^3}{\lambda_{bm}}$ the variance of the ISI [17]. In the following, $\hat{\mu}_{bm}$ and $\hat{\lambda}_{bm}$ will denote the the maximum likelihood (ML) estimate of parameters of the distribution in (Equation 4.16).

4.4 Result

In this work the stochastic modeling of neuronal activity of STN in PD patients and VIM in ET patients is performed based on neuronal spiking activities recorded during DBS implantation surgery. For the stochastic modeling, we first calculated the ISI's (difference between two consecutive spike timestamps) from the recorded neuronal spikes and then based on calculated ISI's we obtained the empirical ISI probability distribution in which the bin width is calculated based on the Freedman Diaconis rule [99] as

$$h = \frac{\mathsf{IQR}(x)}{(n)^{1/3}} \tag{4.17}$$

Where h is the bin width, $\mathsf{IQR}(x)$ stands for inter-quartile range of the data x (in this case ISIs) and n is the number of data samples. This empirical ISI probability distribution is referred to as *measured ISI distribution* in the rest of the discussion of this article.

4.4.1 Numerical Estimation of OUP parameters and ISI simulation

For the numerical estimation of OUP parameters $\hat{\mu}$, $\hat{\sigma}$ in (Equation 4.7), (Equation 4.14), we assume the resting membrane potential to be $x_0 = 0$ (a non zero value for x_0 can be incorporated in the long-term mean value that depends on μ and τ) and the firing threshold $y_0 = 15\text{m}V$ (where 15 mV is the difference between the neuron firing threshold and the neuron resting potential). As the physiological value of the membrane time constant τ has been varied from 1 to 20ms [88], in our analysis τ ranges from 1 to 25ms in time steps of 0.2ms. Finally, we obtain sets of estimated parameters $\hat{\mu}$, $\hat{\sigma}$ in (Equation 4.7) using the RMM as discussed in Section 4.3.2.1 and by using the FIE method as discussed in Section 4.3.2.2. The

box plot of estimated parameters $\hat{\mu}$, $\hat{\sigma}$ for ET and PD is shown in Figure 14. The statistical parameters calculated based on the box plot comparison (Figure 14) with some statistical dispersion parameters of $\hat{\mu}$ and $\hat{\sigma}$ for all ET and PD patients recordings in case of FIE and RMM are summarized in Table XIV.

Based on these estimated sets of parameters, we then proceed to simulate the ISI distributions by numerically solving an integral equation as in [100] with $x_0 = 0$, $y_0 = 15\text{m}V$, and τ ranging from 1 to 25ms in time steps of 0.2ms. For each measured ISI distribution there are 121 simulated ISI distributions corresponding to each value of τ. To quantify the goodness of the fit of the numerically simulated ISI distribution with its measured ISI and to select the best set of parameters among all estimated sets of parameters (corresponding to each value of τ) for a particular measured ISI distribution, we use the Integral Square Error (ISE) as a performance measure [17]. The ISE is calculated as the sum of the squared error between the measured ISI distribution and the numerically simulated ISI distribution at each bin. The ISE does not require any prior knowledge about the underlying distribution that governs the empirical ISI distribution. The value of τ was chosen as the one that minimizes the ISE for OUP.

4.4.2 Performance Comparison

The ISE summary results for ET and PD patients are reported in Table XV and Table XVI, respectively, and discussed next. The Tables also report the ISE results for the PP and the BM. The visual performance comparison of the different stochastic models is shown in 15(a) and 15(b) which is based on Table XV and Table XVI.

Recordings from ET patients in 15(a), show that the FIE method produces the lowest ISE values in all recordings. The BM shows very large ISE values compared to other stochastic processes for the recordings 2, 5, 6, 8, 9, 14 and 15; similarly, the PP shows large ISE values for the recordings 12 and

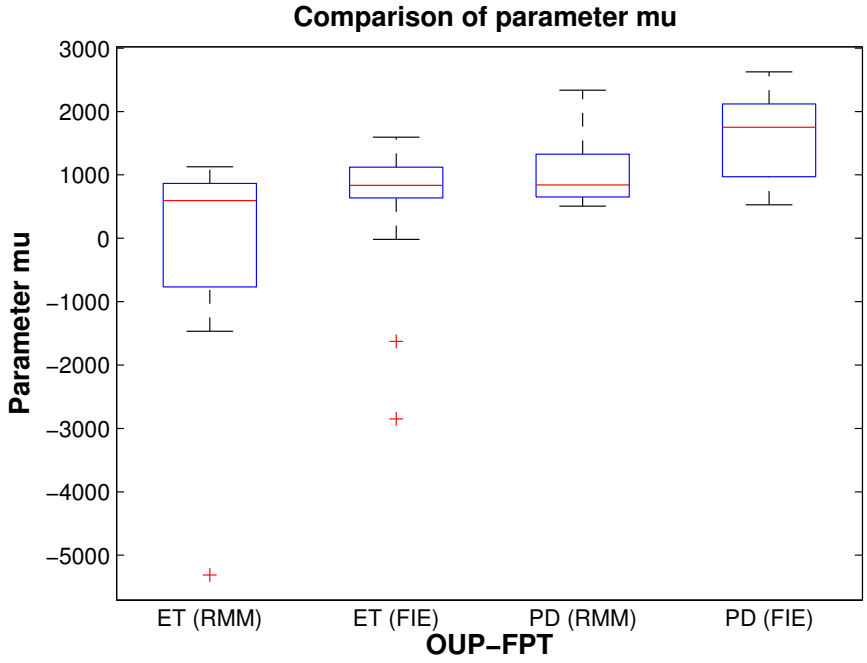

(a) Box Plot comparison of parameter μ for all ET and PD patients recordings in case of FIE and RMM.

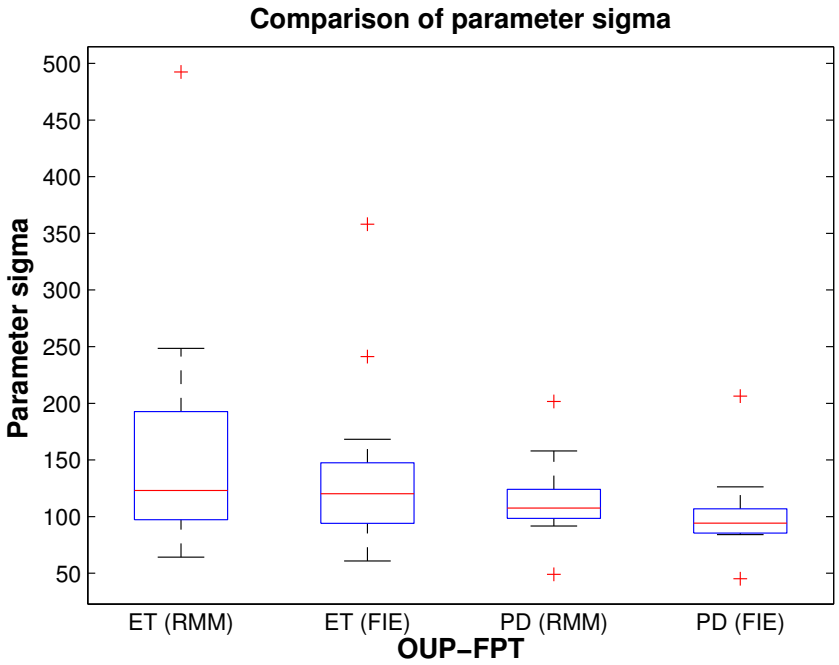

(b) Box Plot comparison of parameter σ for all ET and PD patients recordings in case of FIE and RMM.

Figure 14. Parameter Comparison.

TABLE XIV

STATISTICAL PARAMETERS CALCULATED BASED ON THE BOX PLOT COMPARISON (FIG. 7) AND THE STATISTICAL DISPERSION PARAMETERS OF $\hat{\mu}$ AND $\hat{\sigma}$ FOR ALL ET AND PD PATIENTS RECORDINGS IN CASE OF FIE AND RMM.

Patient	Parameter	OUP-FPT	First Quartile (Q1) $*10^3$	Second Quartile (Q2) $*10^3$	Third Quartile (Q3) $*10^3$	Standard Deviation $*10^3$	Inter Quartile Range (IQR) $*10^3$	Median Absolute Deviation (MAD) $*10^3$
ET	$\hat{\mu}$	RMM	-0.7690	0.5959	0.8649	1.5310	1.6339	0.4290
		FIE	0.6352	0.8365	1.1210	1.0781	0.4858	0.2287
	$\hat{\sigma}$	RMM	0.0973	0.1230	0.1927	0.0983	0.0954	0.0299
		FIE	0.0941	0.1202	0.1476	0.0693	0.0535	0.0272
PD	$\hat{\mu}$	RMM	0.6516	0.8418	1.3255	0.5657	0.6739	0.2568
		FIE	0.9721	1.7524	2.1196	0.7102	1.1475	0.4365
	$\hat{\sigma}$	RMM	0.0985	0.1075	0.1240	0.0407	0.0255	0.0124
		FIE	0.0855	0.0943	0.1069	0.0417	0.0214	0.0095

13. The performance of the RMM is better than the BM and PP in all recordings except recording 3, for which the ISE is comparable to the least ISE value obtained from the BM. 15(a) shows that the lowest ISE value is obtained from the FIE method for recording 19 and the maximum ISE value is obtained from BM for recording 8. Amongst all the processes, the ISE values are the lowest for the FIE method, indicating that it provides the best curve fit to the measured ISI distributions. In another case where the parameters were extracted based on the first two FPT moments, OUP in general performs better than PP and BM as shown in 15(a). Based on 15(a) we also found that the overall performance of PP is better than BM.

TABLE XV

ET PATIENT SUMMARY. *ISE*

Recording Set#	**Patient#** (Set#)	**Hospital** Name	**RMM** $*10^{-3}$	**FIE** $*10^{-3}$	**BM** $*10^{-3}$	**PP** $*10^{-3}$
1	**ET1(1)**	**UIC**	0.0499	0.0192	0.1757	0.0818
2	**ET1(2)**	**UIC**	0.2960	0.2360	3.1150	0.6910
3	**ET2(1)**	**UIC**	1.1000	0.4410	1.3000	0.8840
4	**ET2(2)**	**UIC**	0.0779	0.0209	0.0335	0.3495
5	**ET2(3)**	**UIC**	0.1603	0.1507	2.5556	0.2126
6	**ET2(4)**	**UIC**	0.2570	0.1140	3.3170	0.0770
7	**ET2(5)**	**UIC**	0.4499	0.3370	0.3770	0.5325
8	**ET2(6)**	**UIC**	0.3124	0.1796	4.4999	0.1796
9	**ET2(7)**	**UIC**	0.4780	0.3392	5.8530	0.5801
10	**ET2(8)**	**UIC**	0.2895	0.2818	0.3002	0.7154
11	**ET2(9)**	**UIC**	0.7786	0.3282	1.6367	0.3811
12	**ET3(1)**	**UIC**	0.0515	0.0467	0.0971	0.8111
13	**ET3(2)**	**UIC**	0.1005	0.0943	0.1160	2.1311
14	**ET3(3)**	**UIC**	0.1759	0.1585	2.1483	0.3461
15	**ET3(4)**	**UIC**	0.1235	0.0736	4.0516	1.0488
16	**ET4(1)**	**RUSH**	0.0793	0.0637	0.0621	0.3897
17	**ET4(2)**	**RUSH**	0.0902	0.0533	0.0544	0.5009
18	**ET5(1)**	**UIC**	0.3075	0.2030	1.0319	1.0128
19	**ET5(2)**	**UIC**	0.0505	0.0101	0.4729	0.1254

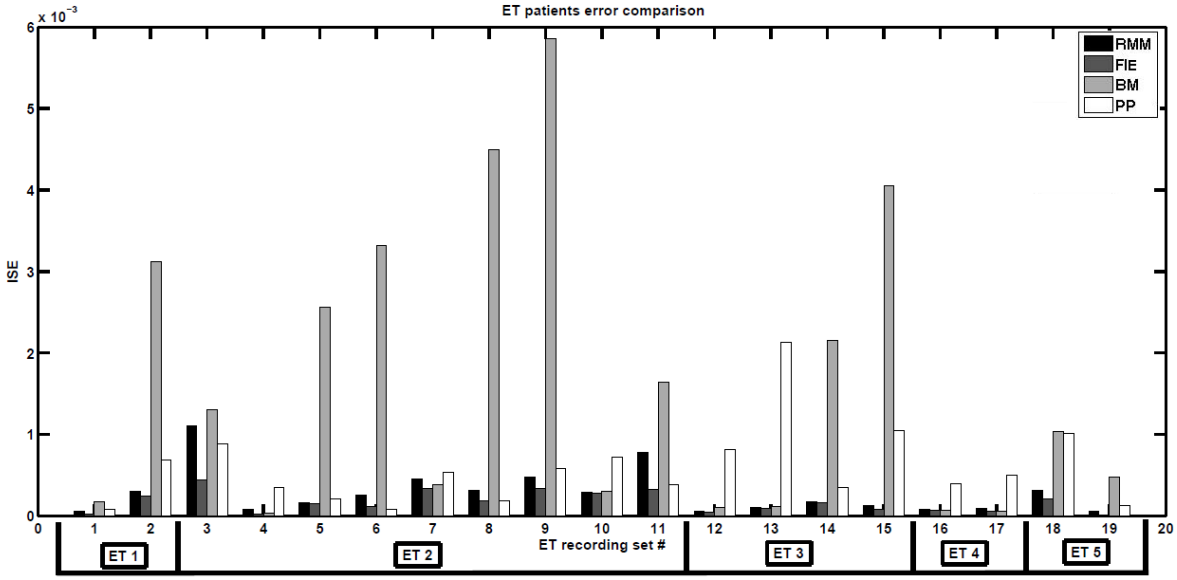

(a) Histogram Plot of ISE for all ET patients recordings.

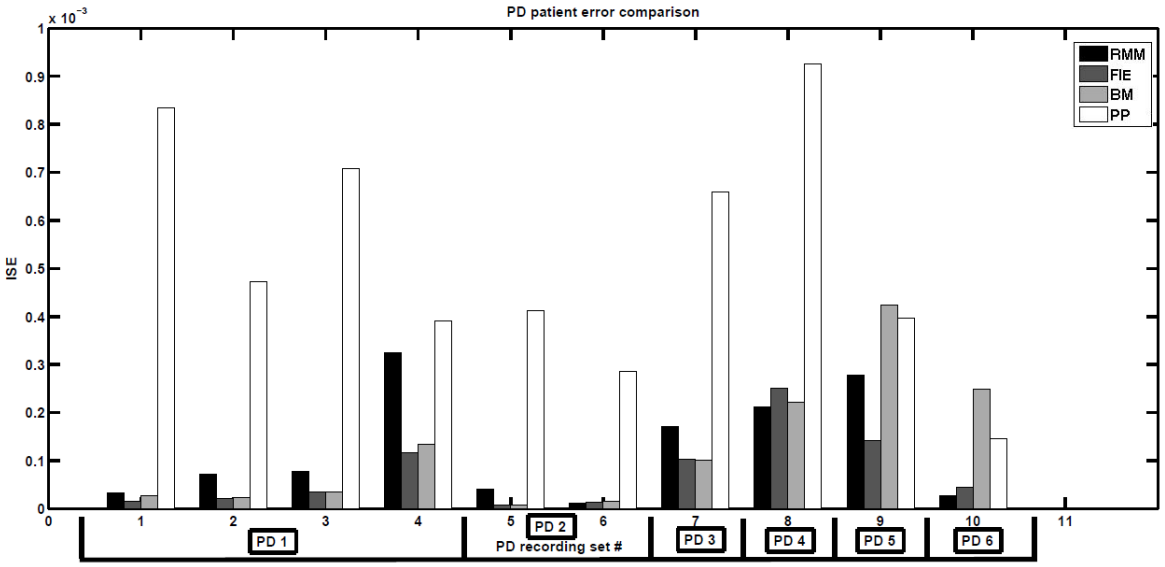

(b) Histogram Plot of ISE for all PD patients recordings.

Figure 15. Histogram Plot for Performance Comparison.

TABLE XVI

PD PATIENT SUMMARY. *ISE*

Recording Set#	**Patient#** (Set#)	**Hospital** Name	**RMM** $*10^{-3}$	**FIE** $*10^{-3}$	**BM** $*10^{-3}$	**PP** $*10^{-3}$
1	**PD1(1)**	**RUSH**	0.0326	0.0162	0.0277	0.8338
2	**PD1(2)**	**RUSH**	0.0710	0.0205	0.0228	0.4734
3	**PD1(3)**	**RUSH**	0.0773	0.0350	0.0356	0.7082
4	**PD1(4)**	**RUSH**	0.3250	0.1166	0.1344	0.3898
5	**PD2(1)**	**RUSH**	0.0410	0.0076	0.0080	0.4121
6	**PD2(2)**	**RUSH**	0.0116	0.0126	0.0148	0.2863
7	**PD3(1)**	**RUSH**	0.1716	0.1023	0.1016	0.6598
8	**PD4(1)**	**UIC**	0.2127	0.2505	0.2220	0.9263
9	**PD5(1)**	**UIC**	0.2789	0.1410	0.4245	0.3956
10	**PD6(1)**	**RUSH**	0.0263	0.0441	0.2487	0.1455

The histogram of ISE values for all processes and for all PD patients is shown in 15(b). The ISE values obtained with the FIE method are lower than all the ISE values obtained with other processes in all recordings, except for recording 8 in which the lowest ISE value is obtained with the RMM. ISE values obtained from all processes were lower in PD than ET patients as the vertical axis scale in 15(b) is smaller compared to that in 15(a). 15(b) shows that the maximum ISE values are obtained with the PP in all recordings except numbers 9 and 10 in which the maximum ISE value is obtained with the BM. The ISE values obtained with the BM are smaller than the ISE values obtained from the RMM in all recordings except numbers 5 and 8 in which is the ISE values are comparable to those obtained from the RMM, and recording number 9 and 10 in which the ISE values are greater than those obtained from the RMM. Therefore, in PD, the performance of OUP with parameter extraction based on FIE, is superior

to all other stochastic process as shown in 15(b). Based on the histogram plot for all ISE values (15(b)) in case of PD patients, the BM provides a better curve fit to the measured ISI distribution than the RMM and PP.

4.4.3 Statistical Analysis

The descriptive statistical analysis of the performance of the different stochastic processes is based on the box plot of ISE values as shown in 16(a) and 16(b) for ET and PD patients, respectively. For the box plot analysis, we have calculated the first quartile Q_1, the second quartile Q_2 and the third quartile Q_3. The statistical parameters for dispersion are inter-quartile range, standard deviation and median absolute deviation [19]. To avoid the effect of outliers on the ISE dispersion, we removed the outliers while calculating the standard deviation. The points which are below the $Q_1 - 1.5(Q_3 - Q_1)$ percentile value and above the $Q_3 + 1.5(Q_3 - Q_1)$ percentile value are considered as outliers in our analysis. These extreme high or low values of outliers can skew the direction of results. We also calculated the median absolute deviation (MAD) [19], which is independent of the outliers. The statistical dispersion parameters along with quantitative measures of the box plot of 16(a) and 16(b) are summarized in Table XVII and Table XVIII, for ET and PD patients, respectively.

In 16(a) and 16(b) the center line of the box represents the median value (i.e., second quartile or Q_2 or 50^{th} percentile), the lower horizontal line of the box represents Q_1, or 25^{th} percentile, while the upper horizontal line of the box represents the third quantile Q_3, or 75^{th} percentile. The lower whisker represents $Q_1 - 1.5(Q_3 - Q_1)$ percentile value, the upper whisker represents $Q_3 + 1.5(Q_3 - Q_1)$ percentile value and the plus sign above the whisker denotes the outliers.

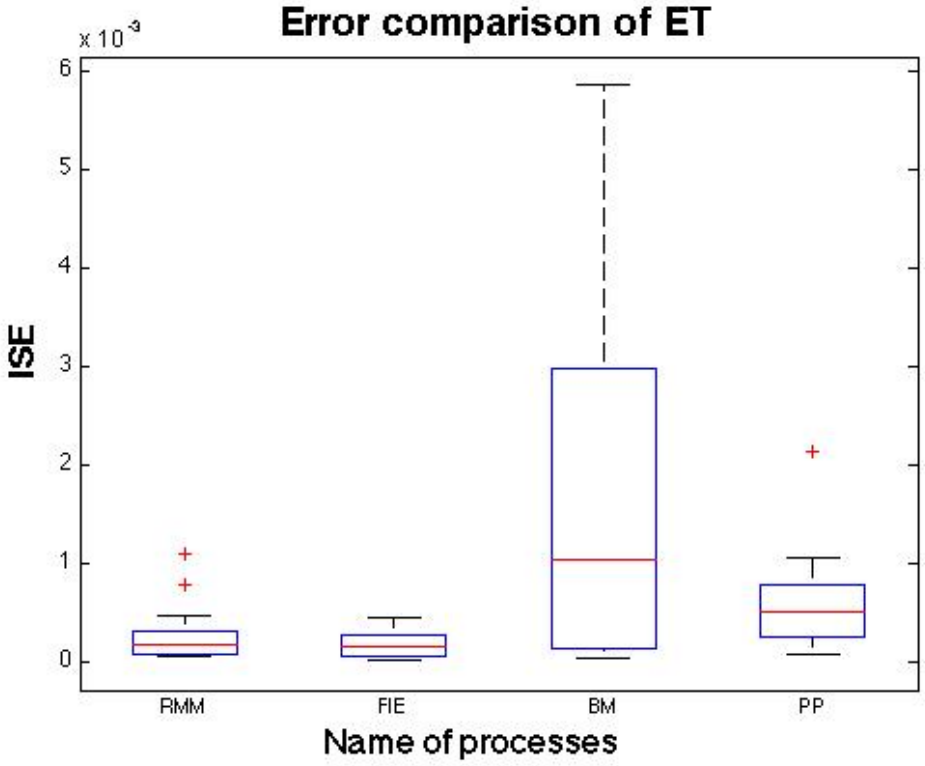

(a) Box Plot comparison for the performance evaluation for all ET patients recordings.

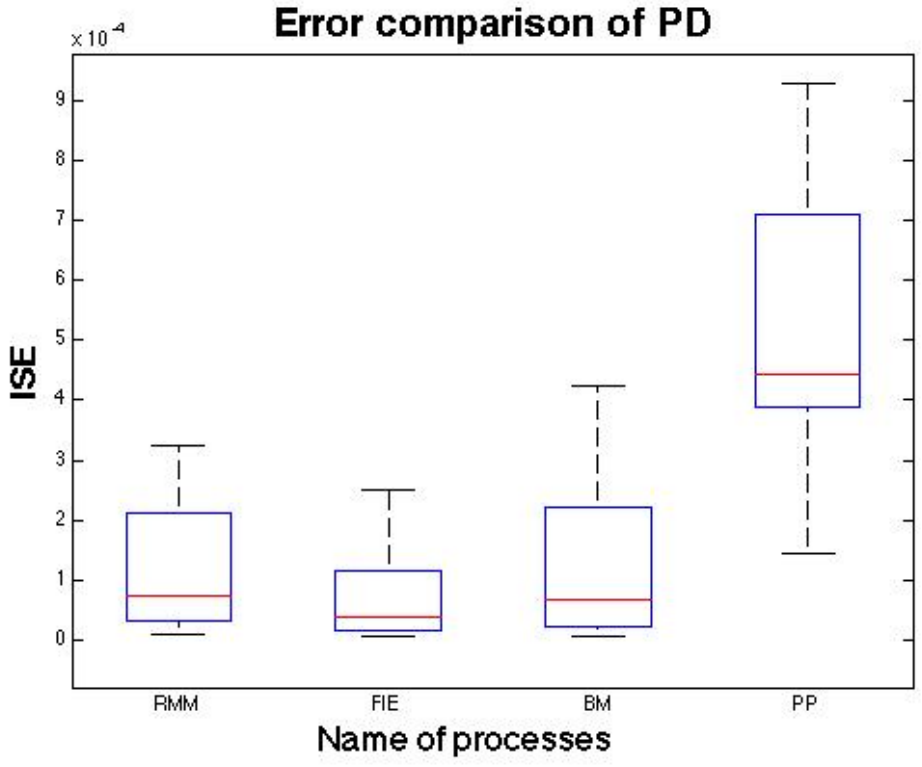

(b) Box Plot comparison for the performance evaluation for all PD patients recordings.

Figure 16. Box Plot for Performance Comparison.

TABLE XVII

STATISTICAL PARAMETERS CALCULATED BASED ON THE BAR CHART COMPARISON (FIG.16A) AND THE STATISTICAL DISPERSION OF ISE VALUES FOR RMM, FIE METHOD, PP AND WP.

Name of process	Median $*10^{-3}$	First Quartile (Q_1) $*10^{-3}$	Third Quartile (Q_3) $*10^{-3}$	Inter-Quartile Range (IQR) $*10^{-3}$	# of Out-liers	Standard Deviation [Without Outliers] $*10^{-3}$	Median Absolute Deviation (MAD) $*10^{-3}$
RMM	0.1759	0.0820	0.3112	0.2292	2	0.1393	0.1201
FIE	0.1507	0.0559	0.2704	0.2145	None	0.1295	0.0974
BM	1.0319	0.1309	2.9752	2.8443	None	1.7873	0.9698
PP	0.5009	0.2460	0.7872	0.5412	1	0.3116	0.2883

TABLE XVIII

STATISTICAL PARAMETERS CALCULATED BASED ON THE BAR CHART COMPARISON(FIG.16B) AND THE STATISTICAL DISPERSION OF ISE VALUES FOR RMM, FIE METHOD, PP AND WP.

Name of process	Median $*10^{-3}$	First Quartile (Q_1) $*10^{-3}$	Third Quartile (Q_3) $*10^{-3}$	Inter-Quartile Range (IQR) $*10^{-3}$	# of Out-liers	Standard Deviation [Without Outliers] $*10^{-3}$	Median Absolute Deviation (MAD) $*10^{-3}$
RMM	0.0742	0.0326	0.2128	0.1802	None	0.1140	0.0552
FIE	0.0396	0.0163	0.1166	0.1003	None	0.0782	0.0294
BM	0.0686	0.0228	0.2220	0.1992	None	0.1369	0.0572
PP	0.4428	0.3898	0.7082	0.3184	None	0.2493	0.1867

The qualitative bar chart comparison of the performance of different stochastic processes is shown in 16(a) and the corresponding quantitative statistical parameter based comparison of different stochastic processes is summarized in Table XVII for all ET patients' data sets. The median of ISE values is minimum in case of FIE method and is maximum in case of BM, therefore FIE method provides better curve fit to measured ISI distributions compared to BM. There are two outliers for the RMM and one outlier for PP. The length of two whisker ends is the greatest for BM and the shortest for FIE. Therefore the dispersion of ISE values is highest in case of BM and lowest in case of FIE method. 16(a) shows that the inter quartile range (IQR) of ISE values is the shortest in case of FIE method and the longest in case of BM. From Table XVII, we conclude that the minimum dispersion of ISE values is obtained with the FIE method. The maximum dispersion ISE values for IQR, standard deviation and MAD are obtained with the BM. The ISE dispersion and median values are the lowest with FIE method which indicates that the performance of the FIE method is superior among all processes and provides the best curve fit to the measured ISI distribution. The performance of the RMM is better than that of BM and PP as it has the lowest ISE median value and has the least ISE dispersion compared to PP and BM distribution as shown in 16(a).

In case of PD patients, a similar qualitative box plot comparison is shown in 16(b) and the quantitative comparison based on statistical parameters is summarized in Table XVIII. In PD, the median of ISE values is minimum in case of the FIE method and maximum in case of PP. The minimum dispersion ISE values for IQR, standard deviation and MAD are obtained with the FIE method. The dispersion of ISE values is minimum in case of FIE method and maximum in case of PP. Therefore, among all the modeling processes, the FIE method shows the best performance with the lowest ISE median values

and with the lowest values for the different ISE dispersion parameters. Overall, for PD data sets, the BM gives better curve fit to the empirical ISI distributions compared to the RMM and PP as shown in 16(b). The BM also shows a significant improvement in the performance for PD patients compared to ET patients.

Finally, to determine whether the ISE values of one distribution were significantly higher or lower than another, we performed a directional Wilcoxon rank test [101]. The directional Wilcoxon rank test is a non-parametric statistical test which is used to compare the performance between two processes based on ranking. This test is applied to low sample size problems when the underlying distribution of the sample population is unknown. Four directional Wilcoxon rank tests were conducted for both ET and PD patients to statistically compare the performance of different stochastic processes: (1) the first test is performed to check whether the ISE values obtained from the FIE method are lower than those obtained from the BM. (2) the second test is performed to check whether the ISE values obtained from the FIE method are lower than those obtained from the PP, (3) the third test checks whether the ISE values obtained from the FIE method are lower than those obtained from the RMM, and (4) the fourth test is performed to check whether the ISE values obtained from the BM are less than those obtained from the PP. The conclusion is made based on the p-value, i.e., if p-value is less than 0.05 then the null hypothesis of equality is rejected. The results corresponding to all tests for both ET and PD patients are summarized in Table XIX.

Test 1 shows that the ISE between the measured ISI distribution and the simulated OUP-FPT distribution using the FIE method is significantly lower than that between the measured ISI distribution and the simulated BM. This establishes the superiority of the OUP-FPT distribution in which the model

TABLE XIX

COMPARISON OF ISE VALUES CORRESPONDING TO DIFFERENT DISTRIBUTIONS BY USING A DIRECTIONAL WILCOXON SIGNED RANK TEST.

Data Set	**Test1**	**Test2**	**Test3**	**Test4**
ET	**FIE <BM**	**FIE <PP**	**FIE <RMM**	**PP <BM**
Results	Yes	Yes	Yes	Yes
p-value	0.0001	0.0001	0.0001	0.0392
PD	**FIE <BM**	**FIE <PP**	**FIE <RMM**	**BM <PP**
Results	Yes	Yes	Yes	Yes
p-value	0.0485	0.0027	0.0314	0.007

parameters were extracted using FIE method over the BM in fitting the measured ISI distributions. Test 2 shows that the ISE between the measured ISI distribution and the simulated OUP-FPT distribution using the FIE method is significantly lower than that between the empirical ISI distribution and the PP. Thus, the OUP-FPT distribution in which the model parameters were extracted using FIE method better fits the measured ISI distributions than the PP. Test 3 shows that the ISE between the measured ISI distribution and the simulated OUP-FPT distribution using the FIE method is significantly lower than that between the measured ISI distribution and the simulated OUP-FPT distribution using RMM, but OUP based on FIE parameter extraction method offers a greater improvement over the OUP based on FPT moment parameter extraction for the PD patients data set compare to the ET patients data set. Test 4 shows that the PP provides a better fit to the measured ISI distribution than the BM in case of ET patients since the ISE corresponding to PP is significantly lower than that corresponding to the BM. In the PD data set, the BM actually provides a better fit than the PP and is also very close to the performance of the OUP-FPT in which parameter extraction was based on FIE method.

Based on results from the four statistical tests, we can conclude that the overall performance of the FIE method is superior amongst all stochastic process, i.e., it provides the best fit to all measured ISI distributions for both PD and ET patients.

4.5 Conclusions

In this work we demonstrated the applicability of OUP to model the neuronal spiking activity in the STN of PD patients and in the VIM of ET patients. The OUP requires less parameters compared to a deterministic model for neuronal activity, therefore it is a computationally efficient method to model neuronal activities. To extract the OUP parameters from the measured ISI distribution, we used the FIE method. We compared the performance of OUP-FIE with OUP-RMM, BM and PP and concluded that in case of PD and ET patients, the OUP-FPT distribution with parameters extracted using the FIE method provides the best fit to all measured ISI distributions.

Comparing the performance of different stochastic processes in case of ET and PD patients, we concluded that all stochastic processes performed better in case of PD patients compared to ET patients and showed significant decrease in ISE values. There is a drastic improvement in the performance of BM in case PD patients as there is approximately one order reduction in ISE values of BM in case of PD patients compared to ET patients. Overall, the OUP-FPT distribution with the model parameters extracted using the FIE method provides the best fit for both PD and ET data sets.

We performed different tests based on directional Wilkoxon rank test to statistically compare the performance of different stochastic process. We concluded that the overall performance of the OUP process with FIE-derived parameters is best amongst all stochastic processes considered, i.e., it provides the best fit to all measured ISI distributions for both PD and ET patients.

CHAPTER 5

CONCLUSION AND FUTURE WORK

5.1 Conclusion

In this work we implemented various machine learning technique based automated tremor prediction algorithms for PD and ET patients. First we implemented feed-forward back-propagation NN in case of PD patients. As we were not able to achieve 100% sensitivity by using NN tremor prediction algorithms therefore we explored other machine learning algorithms such as DT, TBAG and SVM for tremor prediction. Finally, we did the performance comparison of various tremor prediction algorithms is done to choose best among all tremor prediction algorithms. From all the results obtained from different studies performed in this thesis work, we can make the following conclusions:

1. We implemented various machine learning techniques based automated tremor prediction algorithms in case of four PD patients. All the algorithms achieved high accuracy and sensitivity with low false alarm rate, but based on overall performance of DT based tremor prediction algorithm, it turned out to be the best among all algorithms. Therefore, to design a fully automated closed-loop DBS system, DT based tremor prediction algorithm appeared to be the best suitable option in case of PD patients for commercial implementation.

2. In case of four ET patients we implemented five different automated tremor prediction algorithms which are based on DT, TBAG and SVM. Two of them are two stage tremor prediction algorithms in which first stage is a condition classifier stage which classifies between the movement and pos-

tural condition followed by the tremor predictor stage which comprises of two tremor predictors one for each condition. The DT based classifier is used to implement the conditions classifier in case of ET patients. The remaining three are single stage tremor prediction algorithms. All the five tremor prediction algorithms achieved an overall high accuracy and sensitivity. After performance comparison we concluded that either a single stage DT tremor predictor or a single stage TBAG tremor prediction algorithm are suitable for automated closed loop DBS design in case of ET patients.

3. To extract the OUP parameters from the measured ISI distribution we used the FIE method. We compared the performance of OUP-FIE with BM, PP and OUP-MOM using directional Wilkoxon rank test and concluded that overall the OUP-FPT distribution with the model parameters extracted using the FIE method provides the best fit for both PD and ET data sets.

4. We concluded that all stochastic processes performed better in case of PD patients compared to ET patients and showed significant decrease in ISE values. There is also a drastic improvement in the performance of BM in case of PD patients as there is approximately one order reduction in ISE values of BM in case of PD patients compared to ET patients.

5.2 Future Work

The results obtained from various studies show the applicability of the sEMG/Acc signal based automated controlled closed-loop DBS system design using machine learning technique based tremor prediction algorithms in case of PD and ET patients. Based on the findings the future research goals can be as follows:

1. Adaptation of tremor prediction algorithm parameters during online operations
2. Perform the smoothening of sEMG signal by using some other low pass filters such as Chebyshev and Butterworth.
3. Parameter extraction from sEMG and Acc signals using some statistical methods such as Principal Component Analysis (PCA), Factor Analysis (FA) and Component Analysis (ICA).
4. Optimization of parameters or options for various machine learning techniques used in this work.
5. Simulation of sEMG and Acc data set from the recorded sEMG/Acc signals based on the physiological conditions of ET/PD patients.
6. Stochastic modeling of neuronal activities in case of PD and ET patients by using Feller process.

5.2.1 Adaptation of algorithm parameters during online operations

All the machine learning technique based tremor prediction algorithms structures are built off-line during the training phase. The parameters to which the all the algorithms are trained will converge and remain fixed in the testing phase. The parameters of all machine learning techniques based tremor prediction algorithms will not adapt to the patients conditions. Therefore we can further design an adaptive tremor prediction algorithm based on whose parameters will change during online operations.

5.2.2 Smoothening of sEMG signal by using some other low pass filters

The present work was carried out with data recordings of sEMG/Acc from PD and ET patients. The sEMG signals from these recordings were first smoothed out to extract parameters for tremor prediction algorithms. Smoothening is an important step as it filters out the high frequency oscillations and thus extracts the low frequency tremor bursts. In this work smoothening is performed by using moving

average filter. Therefore, the application of other low pass filters such as Chebyshev and Butterworth can be tested in future studies to further improve the process of low pass filtering. The improved process of low pass filtering may improve the performance of automated tremor prediction algorithms in case of PD and ET patients.

5.2.3 Parameter extraction from sEMG and Acc signals using some statistical methods

In this study, the parameters extracted from smoothed sEMG and Acc signals are used for training of various machine learning algorithms for tremor prediction. Our knowledge about the physiology of disease and experience about intrinsic information of signals from sEMG/Acc were the major guiding force for deriving these parameters. In this work, these parameters were extensively used and proved to be excellent for prediction of tremors. Nevertheless, we can explore other statistical methods such as PCA, FA or ICA to extract the optimum number of parameters from filtered signals. This exercise will help us in retaining all useful independent parameters and removing the noise component of it. We can also perform experiments to search for the physical basis of the independent parameters extracted from PCA, FA or ICA. This exercise will give us insight to establish a relation (if any) between the parameters used in present work and the parameters derived from PCA, FA or ICA.

5.2.4 Optimization of parameters or options for various machine learning techniques

Apart from focusing on pre-processing of signals, i.e. filtering and parameter extraction, a rigorous exercise can be undertaken to find out the best combination of parameters or options for various machine learning techniques used in this work. In the present work, Neural Network (NN), Decision Tree Classifier (DTC), Support Vector Machine (SVM) and Tree Bagger is used for tremor prediction. In this work, we implemented feed-forward back-propagation NN for tremor prediction algorithm. The feedforward

NN architecture is one of the simplest type of NN architecture which can extract prediction information from noisy signals. Also, the computatinal speed of this NN is high due to its parallel structure. This NN is not transparent in nature therefore we can further investigate some other transparent NN such as LAMSTAR to improve the tremor prediction performance in case of NN based tremor prediction algorithm. Only DT and TBAG based classifiers are used in present work. DTC is the simplest tree based classifier and Tree Bagger is the simplest ensemble based method for classification. Other advanced ensemble methods such as boosting and random forests algorithms can be used to test its predictive performance. SVM is another machine learning method which is used for tremor prediction. In SVM, only radial basis kernel function with $\sigma = 1.0$ as kernel function and SMO as optimization method is used. We chose SMO as optimization method for SVM tremor prediction algorithm as the convergence time for this optimization method is turns out to be least in our preliminary tremor prediction analysis. A separate study can be carried out to find out the best kernel function and optimization method for tremor prediction. Perceptron and polynomial kernel functions can be tried. For optimization, least square and non-linear optimization methods can also be used to test the impact on final accuracy.

5.2.5 Simulation of sEMG and Acc data set

The major limitation in improving the performance of various automated tremor prediction algorithms in case of PD and ET patients is due to limited data set. This limitation stresses on devising new methods or procedures to simulate a data set that encompasses all the possibilities and realistically presents all the physiological conditions of ET/PD patients recorded through sEMG/Acc.

5.2.6 Stochastic modeling of neuronal activities in PD and ET patients by using Feller process

In Chapter 4, we demonstrated the applicability of the OUP to model the neuronal spiking activities recorded from VIM of thalamus of ET patients and the STN of PD patients during implantation of the DBS electrodes. We can further investigate more complex stochastic process such as Feller process with more dynamic parameters to model the neuronal spiking activities in case of PD and ET patients. Finally, we can compare the performance of the OUP and Feller process in terms of their ISE values. If Feller process provides a better curve fit to measured ISI distribution, we can obtain more accurate stochastic neuronal modeling technique at the cost of the increased complexity of the process.

APPENDICES

For thesis or dissertation works, IEEE does not require formal permission be obtained but does require that you read the Terms, Conditions and Restrictions associated with such use. Those have been pasted below.

Also note that should you later decide to formally publish your work, you are required to obtain a legal, US Copyright License from IEEE. Should this occur, please write to us at pubs-permissions@ieee.org so we can provide for you with the proper instructions. Until such time, best wishes on this exciting part of your educational experience. If we can be of further assistance to you in the future, please do not hesitate to write to us.

Thesis / Dissertation Reuse

The IEEE does not require individuals working on a thesis to obtain a formal reuse license, however, you may print out this statement to be used as a permission grant:

Requirements to be followed when using any portion (e.g., figure, graph, table, or textual material) of an IEEE copyrighted paper in a thesis:

1) In the case of textual material (e.g., using short quotes or referring to the work within these papers) users must give full credit to the original source (author, paper, publication) followed by the IEEE copyright line ©2011 IEEE.

2) In the case of illustrations or tabular material, we require that the copyright line ©[Year of original publication] IEEE appear prominently with each reprinted figure and/or table.

3) If a substantial portion of the original paper is to be used, and if you are not the senior author, also obtain the senior authors approval.

Requirements to be followed when using an entire IEEE copyrighted paper in a thesis:

1) The following IEEE copyright/ credit notice should be placed prominently in the references: ©[year of original publication] IEEE. Reprinted, with permission, from [author names, paper title, IEEE publication title, and month/year of publication]

2) Only the accepted version of an IEEE copyrighted paper can be used when posting the paper or your thesis on-line.

3) In placing the thesis on the author's university website, please display the following message in a prominent place on the website: In reference to IEEE copyrighted material which is used with permission in this thesis, the IEEE does not endorse any of [university/educational entity's name goes here]'s products or services. Internal or personal use of this material is permitted.

If interested in reprinting/republishing IEEE copyrighted material for advertising or promotional purposes or for creating new collective works for resale or redistribution, please go to

http://www.ieee.org/publications_standards/publications/rights/rights_link.html to learn how to obtain a License from RightsLink. If applicable, University Microfilms and/or ProQuest Library, or the Archives of Canada may supply single copies of the dissertation.

Sincerely,

Jacqueline Hansson, Coordinator IEEE Intellectual Property Rights Office 445 Hoes Lane Piscataway, NJ 08855-1331 USA +1 732 562 3828 (phone) +1 732 562 1746(fax) e-mail: j.hansson@ieee.org IEEE Fostering technological innovation and excellence for the benefit of humanity.

©©©©©©©©©©©©©©©©©©©

CITED LITERATURE

1. Shukla, P., Basu, I., Graupe, D., Tuninetti, D., and Slavin, K. V.: A neural network-based design of an on-off adaptive control for deep brain stimulation in movement disorders. In Engineering in Medicine and Biology Society (EMBC), 2012 Annual International Conference of the IEEE, 2012.

2. Shukla, P., Basu, I., and Tuninetti, D.: Towards closed-loop deep brain stimulation: Decision tree-based patient's state classifier and tremor reappearance predictor. In Engineering in Medicine and Biology Society (EMBC), 2014 Annual International Conference of the IEEE, 2014.

3. Shukla, P., Basu, I., Graupe, D., Tuninetti, D., Slavin, K. V., Metman, L. V., and Corcos, D. M.: A decision tree classifier for postural and movement conditions in essential tremor patients. In 6th International IEEE Engineering in Medicine and Biology Society (EMBC) Conference on Neural Engineering, accepted, 2013.

4. Shukla, P., Basu, I., Graupe, D., Tuninetti, D., and Slavin, K. V.: On modeling the neuronal activity in movement disorder patients by using the orntein uhlenbeck process. In Engineering in Medicine and Biology Society (EMBC), 2014 Annual International Conference of the IEEE, 2014.

5. Shukla, P., Basu, I., Tuninetti, D., Graupe, D., and Slavin, K.: Stochastic modeling of neuronal activity in the thalamus of essential tremor and the subthalamic nucleus of parkinson's disease patients. Biological Cybernetics, submitted.

6. Basu, I., Graupe, D., Tuninetti, D., Shukla, P., Slavin, K. V., Metman, L. V., and Corcos, D. M.: Pathological tremor prediction using surface electromyogram and acceleration: potential use in onoff demand driven deep brain stimulator design. Journal of neural engineering., 10:036019, 2013.

7. Volkmann, J., Herzog, J., Kopper, F., and Deuschl, G.: Introduction to the programming of deep brain stimulators. Movement disorders, 17(S3):S181–S187, 2002.

8. Gildenberg, P.: Evolution of neuromodulation. Stereotactic and functional neurosurgery, 83(2-3):71–79, 2005.

9. Bar-Gad, I. and Bergman, H.: Stepping out of the box: information processing in the neural networks of the basal ganglia. Curr Opin Neurobiol, 11:689–95, 2001.

10. Baltuch, G. H. and Stern, M. B.: Deep brain stimulation for Parkinson's disease.. CRC Press, 2007.

11. Feng, X., Greenwald, B., Rabitz, H., Shea-Brown, E., and Kosut, R.: Toward closed-loop optimization of deep brain stimulation for parkinson's disease: concepts and lessons from a computational model. Journal of neural engineering, 4:L14–21, 2007.

12. Lee, J.: A Closed-Loop Deep Brain Stimulation Device With a Logarithmic Pipeline ADC. Doctoral dissertation, University of Michigan, 2008.

13. Schiff, S. J.: Towards model-based control of parkinson's disease. Philos Transact A Math Phys Eng Sci, 368(1918):2269–2308, 2010.

14. Ditlevsen, S. and Lansky, P.: Parameters of stochastic diffusion processes estimated from observations of first hitting-times: application to the leaky integrate-and-fire neuronal model. Phys Rev E, 76, 2007.

15. Ditlevsen, S. and Ditlevsen, O.: Parameter estimation from observations of first-passage times of the Ornstein-Uhlenbeck process and the Feller process . Probabilistic Engineering Mechanics, pages 170–179, 2008.

16. Ricciardi, L. and Sato, S.: First-passage-time density and moments of the Ornstein-Uhlenbeck process. J Appl Probab, 25:43–57, 1988.

17. Basu, I., Graupe, D., Tuninetti, D., and Slavin, K.: Stochastic modeling of the neuronal activity in the subthalamic nucleus and model parameter identification from Parkinson patient data. Biological Cybernetics, 103:273–283, 2010.

18. Basu, I., Tuninetti, D., Graupe, D., and Slavin, K. V.: Stochastic modeling of the neuronal activity in the thalamus of essential tremor patient. In 32nd Annual International Conference of the IEEE Engineering in Medicine and Biology Society. IEEE, pages 1461–1464, 2010.

19. Hoaglin, D. C., Mosteller, F., and Tukey, J. W.: Understanding Robust and Exploratory Data Analysis. Wiley, New York, 1983.

20. Bar-Gad, I. and Bergman, H.: Stepping out of the box: information processing in the neural networks of the basal ganglia. Curr Opin Neurobiol, 11:689–695, 2001.

21. Louis, E. D.: Essential tremor. Springer, Berlin Heidelberg New York., 4:100–110, 2005.

22. Critchley, M.: Observations on essential (heredofamilial) tremor. Brain., 72:113–139, 1949.

23. Busenbark, K. L., Nash, J., Nash, S., Hubble, J. P., and Koller, W. C.: Is essential tremor benign? Neurology., 41(12):1982–1983, 1991.

24. Benito-Leon, J. and Louis, E. D.: Clinical update: diagnosis and treatment of essential tremor. The Lancet, 369:1152–1154, 2007.

25. Louis, E., Ottman, R., and Hauser, W.: How common is the most common adult movement disorder, estimates of the prevalence of essential tremor throughout the world. Movement Disorders: official journal of the Movement Disorder, 13:510, 1998.

26. Deng, H., Le, W., and Jankovic, J.: Genetics of essential tremor. Brain, 130:1456–1464, 1998.

27. Louis, E. and Vonsattle, J.: The emerging neuropathology of essential tremor. Movement disorders:official journal of the Movement Disorder, 23:174, 2008.

28. Zesiewicz, T., Elble, R., Louis, E., Gronseth, G., Ondo, W., Dewey, R., Okun, M. J., Sullivan, K., and Weiner, W.: Evidence-based guideline update: treatment of essential tremor: report of the quality standards subcommittee of the american academy of neurology. Neurology, 77:1752–5, 2011.

29. Shahzadi, S., Tasker, R., and Lozano, A.: Thalamotomy for essential and cerebellar tremor. Stereotactic and Functional Neurosurgery, 65:11–17, 1995.

30. Pahwa, R., Lyons, K., Wilkinson, S., Carpenter, M., Troster, A., Searl, J., Overman, J., Pickering, S., and Koller, W.: Bilateral thalamic stimulation for the treatment of essential tremor. Neurology, 53:1447, 1999.

31. Santaniello, S., Fiengo, G., Glielmo, L., and Grill, W. M.: Closed-loop control of deep brain stimulation: A simulation study. IEEE Transactions on Neural Systems and Rehabilation Engineering., 19:15 – 24, 2011.

32. de Lau, L. and Breteler, M.: Epidemiology of parkinson's disease. Lancet Neurol., 5:525–35, 2006.

33. Jankovic, J. and Tolosa, E.: Parkinsons disease and movement disorders. Lippincott Williams and Wilkins Philadelphia, 2007.

34. Alexander, G. E. and Crutcher, M. D.: Functional architecture of basal ganglia circuits: neural substrates of parallel processing. Trends Neurosci, 13:266–271, 1990.

35. The National Collaborating Centre for Chronic Conditions ed.Symptomatic pharmacological therapy in Parkinsons disease. London: Royal College of Physicians, 2006.

36. Lozano, A. M., Dostrovsky, J., Chen, R., and Ashby, P.: Deep brain stimulation for parkinson's disease: disrupting the disruption. Lancet Neurol, 1(4):225–231, 2002.

37. McIntyre, J. J., Savasta, M., Kerkerian-Le, G. C., and Vitek, J. L.: Uncovering the mechanism(s) of action of deep brain stimulation: activation,inhibition or both. Clin Neurophysiol, 115:1239–1248, 2004.

38. Meissner, W., Leblois, A., Hansel, D., Bioulac, B., Gross, C., Benazzouz, A., and Boraud, T.: Subthalamic high frequency stimulation resets subthalamic firing and reduces abnormal oscillations. Brain, 128(10):2372, 2005.

39. Slavin, K. and Wess, C.: Trigeminal branch stimulation for intractable neuropathic pain: technical note. Neuromodulation, 8(1):7–13, 2005.

40. Volkmann, J., Herzog, J., Kopper, F., and Deuschl, G.: Introduction to the programming of deep brain stimulators. Mov Disord., 17:181–187, 2002.

41. Brown, P., Oliviero, A., Mazzone, P., Insola, A., Tonali, P., and Di Lazzaro, V.: Dopamine dependency of oscillations between subthalamic nucleus and pallidum in Parkinson's disease. Journal of Neuroscience, 21(3):1033 – 1038, 2001.

42. Graupe, D., Basu, I., Tuninetti, D., Vannemreddy, P., and Slavin, K. V.: Adaptively controlling deep brain stimulation in essential tremor patient via surface electromyography. Neurol Res., 32:899–904, 2010.

43. Santaniello, S., Fiengo, G., Glielmo, L., and Grill, W. M.: Closed-loop control of deep brain stimulation: A simulation study. Neural Systems and Rehabilitation Engineering, IEEE Transactions on, 19(1):15–24, 2011.

44. Grahn, P. J., Mallory, G. W., Khurram, O. U., Berry, B. M., Hachmann, J. T., Bieber, A. J., Bennet, K. E., Min, P. H., Chang, S.-y., Lee, K. H., and Lujan, J. L.: A neurochemical closed-loop controller for deep brain stimulation: toward individualized smart neuromodulation therapies. Frontiers in Neuroscience, 8(169), 2014.

45. Leondopulos, S. S. and Micheli-Tzanakou, E.: Advances toward closed-loop deep brain stimulation. Computational Neuroscience, pages 227–253, 2010.

46. Popovych, O. V., Hauptmann, C., and Tass, P. A.: Control of neuronal synchrony by nonlinear delayed feedback. Biological cybernetics, 95(1):69–85, 2006.

47. Tass, P. A.: Phase Resetting in Medicine and Biology: Stochastic Modeling and data Analysis. Springer, Berlin Heidelberg New York., 2006.

48. Hauptmann, C., Roulet, J. C., Niederhauser, J. J., Döll, W., Kirlangic, M. E., Lysyansky, B., Krachkovskyi, V., Bhatti, M. A., Barnikol, U. B., Sasse, L., et al.: External trial deep brain stimulation device for the application of desynchronizing stimulation techniques. Journal of neural engineering, 6:066003, 2009.

49. Basu, I., Tuninetti, D., Graupe, D., and Slavin, K. V.: Adaptive control of deep brain stimulator for essential tremor: entropy-based tremor prediction using surface-emg. In Engineering in Medicine and Biology Society (EMBC), 2011 Annual International Conference of the IEEE, 2011.

50. Srinivasan, V., Eswaran, C., and Sriraam, N.: Approximate entropy-based epileptic eeg detection using artificial neural networks. IEEE Trans Inf Technol Biomed., 11(3):288–295, 2007.

51. Waxman, J. A., Graupe, D., and Carley, D. W.: Automated prediction of apnea and hypopnea,using a lamstar artificial neural network. Am J Respir Crit Care Med., 181(7):727–723, 2010.

52. Sturman, M. M., Vaillancourt, D. E., Metman, L. V., Bakay, R. A., and Corcos, D. M.: Effects of subthalamic nucleus stimulation and medication on resting and postural tremor in parkinson's disease. Brain., 127(pt 9):2131–43, 2004.

53. Richman, J. S. and Moorman, J. R.: Physiological time-series analysis using approximate entropy and sample entropy. Am J Physiol Heart Circ Physiol., 278(6):H2039–49, 2000.

54. Webber Jr, C. L. and Zbilut, J. P.: Recurrence quantification analysis of nonlinear dynamical systems. Tutorials in contemporary nonlinear methods for the behavioral sciences, pages 26–94, 2005.

55. Shannon, C. E.: A mathematical theory of communication. ACM SIGMOBILE Mobile Computing and Communications Review, 5(1):3–55, 2001.

56. Rosso, O. A., Blanco, S., Yordanova, J., Kolev, V., Figliola, A., Schurmann, M., and Basar, E.: Wavelet entropy: a new tool for analysis of short duration brain electrical signals. Journal of neuroscience methods, 105(1):65–75, 2001.

57. Graupe, D.: Principles of Artificial Neural Networks, 2nd Edition,. World Scientific, 2007.

58. Yam, Y. and Chow, T.: Determining initial weights of feedforward neural networks based on least squares method. Neural Processing Letters, 2:13–17, 1995.

59. Yam, Y. and Chow, T.: A new method in determining the initial weights of feedforward neural networks. Neurocomputing, 16:23–32, 1997.

60. Drago, G. and Ridella, S.: Statistically controlled activation weight initialization (scawi). IEEE Trans. Neural Networks, 3:627–631, 1992.

61. Nguyen, D. and Widrow, B.: Improving the learning speed of 2-layer neural neural network by choosing initial values of the adaptive weights. In Proceedings of IEEE International Joint Conference on Neural Networks., 5(4):595–603, 1992.

62. Levenberg, K.: A method for the solution of certain problems in least squares. Quarterly of Applied Mathematics., 5:164–168, 1944.

63. Marquardt, D.: An algorithm for least-squares estimation of nonlinear parameters. SIAM Journal on Applied Mathematics., 11(2):431–441, 1963.

64. Breiman, L., Friedman, J., Olshen, R., and Stone, C.: Classification and Regression Tree. Boca Raton, FL: CRC Press, 1984.

65. Brieman, L.: Heuristics of instability in model selection. In Technical Report. University of California Berkley, 1994.

66. Brieman, L.: Bagging predictors. Machine Learning, 24:123–140, 1996.

67. B.Efron: Bootstrap methods: Another look at jacknkife. The Annals of Statistics, 7:1–26, 1979.

68. Efron, B. and Tibshirani, R.: An Introduction to the Bootstrap. London, Chapman and Hall, 1993.

69. Brieman, L.: Heuristics of instability and stabilization in model selection. The Annals of statistics, 24,6:2350–2383, 1996.

70. Cortes, C. and Vapnik, V.: Support vector networks. Machine Learning, 20:273–297, 1995.

71. Vapnik, V.: The Nature of Statistical Learning Theory. N.Y., Springer, 1995.

72. Platt, J.: Fast training of support vector machines using sequential minimal optimization. In Advances in kernel methods: support vector learning, eds. B. Scholkopf, C. Burges, and A. Smola. MIT Press, 1998.

73. Aronszanj, N.: Theory of reproducing kernels. Trans. Amer. Math. Soc., 686:337–404, 1950.

74. Girosi, F.: An equivalence between sparse approximation and Support Vector Machines., volume A I memo 1606. Princeton NJ, MIT Artificial Intelligence Laboratory, 1997.

75. Wahba, G.: Spline models for observational data. Series in Applied Mathematics SIAM, 59, 1990.

76. Baldi, P., Brunak, S., Chauvin, Y., Andersen, C., and Nielsen, H.: Assessing the accuracy of prediction algorithms for classification: an overview. Bioinformatics, 16(5):412–424, 2000.

77. Tass, P. A.: Phase Resetting in Medicine and Biology: Stochastic Modelling and Data Analysis.. Springer, Berlin, Heidelberg, New York, 2007.

78. Humphries, M., Stewart, R., and Gurney, K.: A physiologically plausible model of action selection and oscillatory activity in the basal ganglia. J of Neuroscience, 26(12):921–942, 2006.

79. Graupe, D.: Time series analysis, identification and adaptive filtering. RE Krieger Publishing, Malabar, 1984.

80. Kuffler, S., Fitzhugh, R., and Barlow, H.: Maintained activity in the cats retina in light and darkness. J Gen Physiol, 40(5):683–702, 1957.

81. Grossman, R. and Viernstein, L.: Discharge patterns of neurons in cochlear nucleus. Science, 134(3472):99–101, 1961.

82. Gerstein, G. and Mandelbrot, B.: Random walk models for the spike activity of a single neuron. J Biophys, 4:41–68, 1964.

83. Lapicque, L.: Recherches quantitatives sur l'excitation electrique des nerfs traitee comme une polarisation. J. Physiol. Pathol. Gen., 9:620–635, 1907.

84. Brunel, N. and Van Rossum, M.: Lapicque's 1907 paper: from frogs to integrate-and-fire. Biol. Cybern., 97(5-6):337–339, 1907.

85. Brown, E. N., Frank, L. M., Tang, D., Quirk, M., and Wilson, M.: A statistical paradigm for neural spike train decoding applied to position prediction from ensemble firing patterns of rat hippocampal place cells. J of Neuroscience., 18(18):7411–7425, 1998.

86. Truccolo, W., Eden, U., Fellows, M., Donoghue, J., and Brown, E.: A point process framework for relating neural spiking activity to spiking history, neural ensemble, and extrinsic covariate effects. J of Neurophysiology, 93:1074–1089, 2005.

87. Sarma, S. V., Cheng, M., Eden, U., Hu, R., Williams, Z., Brown, E., and Eskandar, E.: Modeling neural spiking activity in the sub-thalamic nucleus of parkinson's patients and a healthy primate. In 47th IEEE Conference on Decision and Control, CDC., 2008.

88. Schuss, Z.: Diffusion and stochastic Processes. Springer, New York, 2009.

89. Gerstner, W. and Kistler, W. M.: Spiking Neuron Models: Single Neurons, Populations, Plasticity.. Cambridge University Press, 2002.

90. Tuckwell, H., Wan, F., and Rospars, J.: A spatial stochastic neuronal model with Ornstein-Uhlenbeck input current. Biol. Cybern., 86:137–145, 2002.

91. Toleilis, J. R., Metman, L. V., Pilitis, J. G., Barborica, A., Toleikis, S., and Bakay, R. A.: Effect of intraoperative subthalamic nucleus DBS on human single-unit activity in the ipsilateral and contralateral subthalamic nucleus. Journal of Neurosurgery, 116:1134–1143, 2012.

92. Slavin, K. and Burchiel, K.: Microguide microelectrode recording system. Journal of Neurosurgery, 51:275–278, 2002.

93. Israel, Z. and Burchie, K.: Microelectrode Recording in Movement Disorder Surgery. Thieme, New York, 2004.

94. Uhlenbeck, G. E. and Ornstein, L. S.: On the theory of the brownian motion. Physical Review, 36:830, 1930.

95. Risken, H.: The Fokker-Planck Equation: Methods of Solutions and Applications, 2nd ed.. Springer-Verlag, New York, 1996.

96. Hanson, F.: Applied stochastic processes and control for jump diffusions. Society of Industrial and Applied Mathematics, Philadelphia, 2006.

97. Capocelli, R. M. and Ricciardi, L.: Diffusion approximation and first passage time for a model neuron. Kybernetik, 8:214–223, 1971.

98. Inoue, J., Sato, S., and Ricciardi, L. M.: On the parameter estimation for diffusion model of single neuron's activities. Biological Cybernetics, 73:209–221, 1995.

99. Freedman, D. and Diaconis, P.: On the histogram as a density estimator: L 2 theory. Prob Theory Relat Fields, 57:453–476, 1981.

100. Buonocore, A., Nobile, A., and Ricciardi, L. M.: A new integral equation for the evaluation of rst-passage-time probability densities. Adv Appl Probab., 19:784–800, 1987.

101. Wilcoxon, F.: Individual comparisons by ranking methods. Biometrics Bulletin., 1:80–83, 1945.

VITA

NAME	Pitamber Shukla
EDUCATION	B. Tech, Electronics and Communication Engineering, SASTRA University, Tamil Nadu, India, 2009
	M.S.,Electrical & Computer Engineering, University of Illinois at Chicago, Chicago, Illinois, 2014
RESEARCH	Senior Device Engineer at SanDisk, CA, USA, 2014–present
	Research Assistant in department of Electrical and Computer Engineering, University of Illinois at Chicago, 20011–2013
TEACHING	Adjunct Lecturer in department of Electrical and Computer Engineering, University of Illinois at Chicago, Summer 2013
	Teaching Assistant in department of Electrical and Computer Engineering, University of Illinois at Chicago, 2010–2014
EXPERIENCE	Project Associate at Indian Institute of Technology, Delhi, India, June 2009 – July 2010
SOFTWARE SKILLS	Proficient in C, C++, MATLAB and LabVIEW. Working knowledge of BASH Scripts, Python, SAS, Mathemetica and LaTeX.
MEMBERSHIP	Student member of IEEE engineering in Medicine and Biology society.
PUBLICATIONS	
	Basu, I., Graupe, D., Tuninetti, D., **Shukla, P.**, Slavin, K. V., Metman, L. Verhagen, and Corcos, D. M.: Pathological tremor prediction using surface electromyogram and accelera-tion: potential use in 'ON-OFF' demand driven deep brain stimulator design. Journal of neural engineering, 10:036019, 2013.

Shukla,P., Basu,I., Graupe,D., Tuninetti,D., and Slavin,K.V.: Neural Network-based Design of an Adaptive on-off control for Deep Brain Stimulation in Movement Disorders. 34th IEEE EMBC. 2012.

Shukla, P., Basu, I., Graupe, D., Tuninetti, D., Slavin, K. V., Metman, L. V., and Corcos, D. M.: A decision tree classifier for postural and movement conditions in essential tremor patients. 6th International IEEE EMBC Conference on Neural Engineering, 2013.

Shukla, P., Basu, I., Tuninetti, D.: Towards closed-loop deep brain stimulation: Decision tree-based patient's classifier and tremor reappearance predictor. 36th IEEE EMBC. 2014, accepted.

Shukla, P., Basu, I., Graupe, D., Tuninetti, D., Slavin, K. V.: On modeling the neuronal activity in movement disorder patients by using Ornstein Uhlenbeck Process. 36th IEEE EMBC. 2014, accepted.

Shukla, P., Basu, I., Graupe, D., Tuninetti, D., Slavin, K. V., Metman, L. Verhagen, and Corcos, D. M.: Stochastic modeling of neuronal activity in the thalamus of essential tremor patients and in the subthalamic nucleus of Parkinson's disease patients. (in submission)

Xu, K., Qian, J., **Shukla, P.**, Dutta, M. and Stroscio, M. A.: Graphene-based FET structure: Modeling FET characteristics for an aptamer-based analyte sensor. 15th International Workshop on Computational Electronics (IWCE), 2012.

INVITED TALK

Next Generation Adaptive ON-OFF controlled Deep Brain Stimulation in Movement Disorders: Hosted by Electrical and Computer Engineering department at Illinois Institute of Technology, Nov 2013.

REFERENCES

Prof. Tuninetti, Daniela, email: danielat@uic.edu

Prof. Ansari, Rashid, email: ransari@uic.edu

Dr. Slavin, Konstantin V., email: kslavin@uic.edu